TEKNILLINEN TIEDEKUNTA/FACULTY OF TECHNOLOGY

# MINERALOGY OF THE PALEOPROTEROZOIC RAJA Au-Co PROSPECT, NORTHERN FINLAND

Niilo Taipale

DEGREE PROGRAMME IN GEOSCIENCES
Master´s thesis
December 2018

OULUN YLIOPISTO

TEKNILLINEN TIEDEKUNTA

# MINERALOGY OF THE PALEOPROTEROZOIC RAJA Au-Co PROSPECT, NORTHERN FINLAND

Niilo Taipale

Ohjaaja(t): Jukka-Pekka Ranta, Erkki Vanhanen

GEOTIETEIDEN TUTKIMUSOHJELMA
Pro gradu -tutkielma
Joulukuu 2018

ABSTRACT

**FOR THESIS** University of Oulu Faculty of Technology

| Degree Programme (Bachelor's Thesis, Master's Thesis) | Major Subject (Licentiate Thesis) |
|---|---|
| Degree Programme in Geosciences | Geology and Mineralogy |
| **Author** | **Thesis Supervisor** |
| Niilo Taipale | Jukka-Pekka Ranta |

**Title of Thesis**

Mineralogy of the Paleoproterozoic Raja Au-Co prospect, northern Finland

| Major Subject | Type of Thesis | Submission Date | Number of Pages |
|---|---|---|---|
| Geology and Mineralogy | Master´s thesis | December 2018 | 61 p, 4 appendices |

**Abstract**

The Raja Au-Co prospect is located in the Paleoproterozoic Peräpohja Belt, northern Finland, within an approximately 10 x 10 km gold-enriched area (namely Rompas-Rajapalot) comprised of several gold-cobalt-bearing occurrences. The aim of this study was to describe the mineral assemblages and nature of gold in the Raja Au-Co prospect. Samples were collected from the drill cores representing mineralised and non-mineralised intervals. Silicate-, oxide-, and sulphide phases from polished thin sections were studied under transmitting and reflecting light using petrographic microscope. In addition, chemical compositions of silicates, oxides and sulphides were studied with an electron microprobe analyser (EPMA).

Samples from the mineralised intervals varied from intensely sericite-altered to chlorite-altered metasedimentary rocks. Generally, the mineralised area consists of rocks with albite-quartz matrix with anthophyllite-cordierite assemblages and high aluminum white mica. Only two gold grains were found from the studied samples, one within a chloritised amphibole and one associated with cobaltite. Co-bearing gersdorffite was identified in addition to the previously described Co-mineral phases (cobaltite, Co-pentlandite and linnaeite).

In terms of zoning, micas show compositional differences within and outside of the mineralisation, most notably with their aluminum content being higher in the mineralised rocks, consistent with the intense sericite alteration observed. Amphibole compositions ranges from Ca-amphiboles outside of the mineralisation to Mg-Fe-Mn amphiboles in the mineralised intervals. However, to fully characterise the zoning in the Raja Au-Co prospect, more detailed studies are needed.

Additional Information

# Table of contents

# 1. Introduction

Classification of gold deposits have evolved during the last decades from depth and temperature based (e.g. mesothermal and hypothermal), host-rock based (e.g. turbidite-hosted Au) to more simplified categories, focusing into the processes rather than the final products. This is for example due to the recognition that many giant gold deposits display similarities in crustal to lithospheric settings despite their deposit-scale differences (e.g. Groves et al., 2016). In Precambrian cratonic terranes and in metamorphic areas generally, the most common type of gold deposit is so-called orogenic gold (e.g. Goldfarb et al., 2005). These are gold-only occurences with strict structural control related to major crustal scale structures and formed in collisional to accretional tectonic setting (op.cit.). However, especially in Precambrian terranes, many gold deposits show atypical features that do not fit well or at all, to the traditional classification schemes. Such features include for example atypical metal associations (e.g. Au-Co-U-Cu). Goldfarb et al. (2001) suggested that in intracratonic settings, premetamorphic metal enrichment with circulation of saline fluids within the basement could potentially lead to enrichment of other metals (e.g. Cu, Co, U) prior to gold deposition and would explain the atypical metal association found in many places around the world.

In Finland, the Paleoproterozoic supracrustal belts, including the Central Lapland greenstone belt, Kuusamo belt and Peräpohja belt have proven to be very prospective for gold, and recently for cobalt as well (e.g. Vanhanen et al., 2015; Eilu, 2015; Cook and Hudson, 2018). However, in addition to the more traditional gold deposits found (e.g. orogenic Suurikuusikko Au), many of the occurrences show commonly atypical metal associations (e.g. Au-Co-U or Au-Cu) and very intense alteration of the host rocks. Features of these atypical deposits have been described by many authors during recent years (e.g. Vanhanen, 2001; Vanhanen et al., 2015; Eilu, 2015; Molnár et al., 2016; Ranta et al., 2018) and readers are encouraged to familiarise themselves with those studies.

The mineral exploration completed during the last ten years, mainly by Mawson Oy, have identified multiple gold-rich occurrences from the northern part of Paleoproterozoic supracrustal Peräpohja belt, in the municipalities of Ylitornio and Rovaniemi (Fig. 1). The so-called Rompas-Rajapalot (Fig. 2) area (e.g. Vanhanen et al., 2015; Molnár et al., 2016; Ranta et al., 2018) hosts multiple gold rich occurrences in ~100 $km^2$ area (Fig. 3).

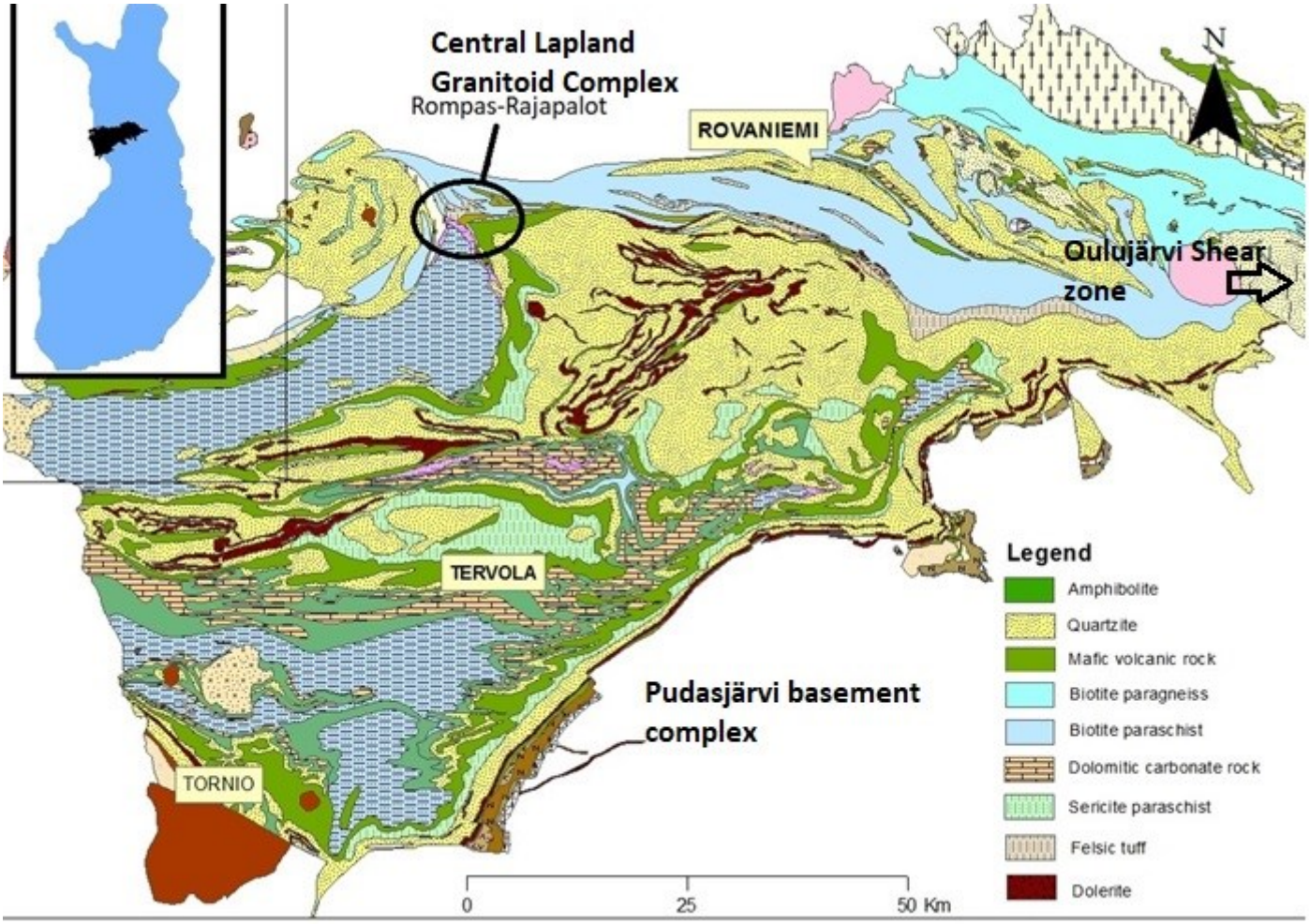


Figure 1. Regional geological map of the Peräpohja belt. modified after the DigiKP version 2.1. (”Digital map database of bedrock geology of Finland” [electronic resource], Geological survey of Finland; referred on 08.10.2018)

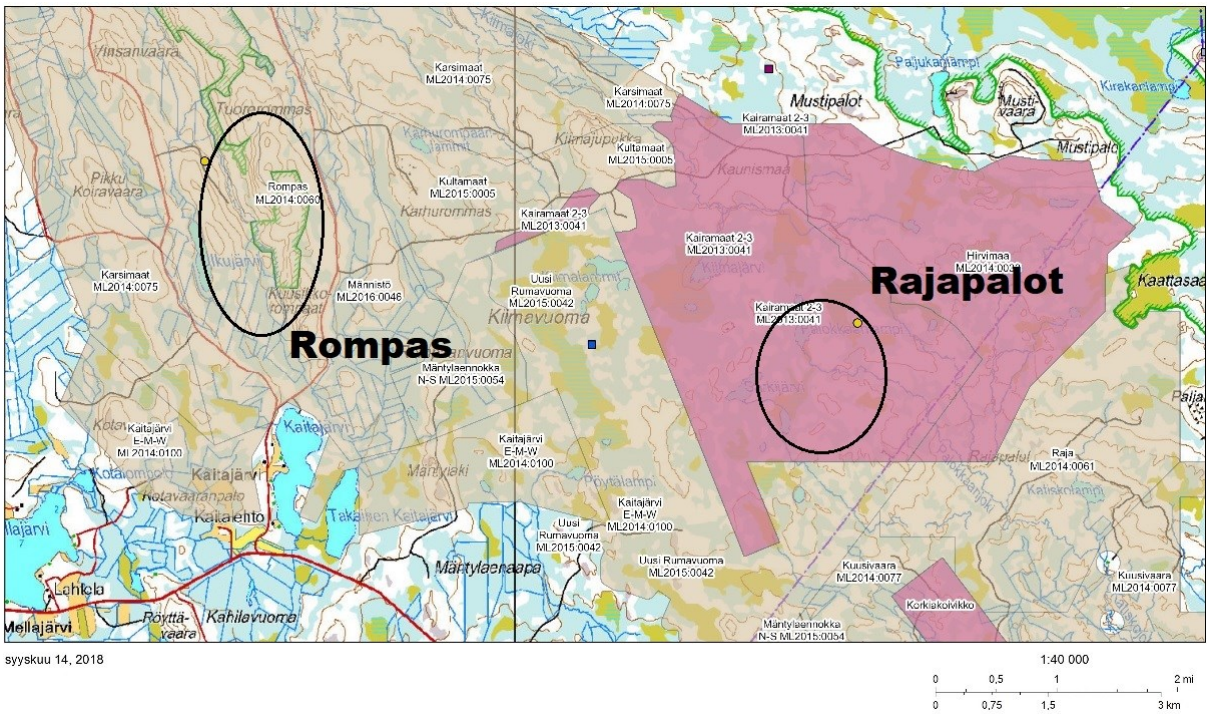


Figure 2. Topographic map showing Rompas and Rajapalot project areas as black circulated ellipsoids. Brown and red coloured areas show Mawson Oy claim area. Figure modified after MDaE ("Digital map database of mineral deposits and mines of Finland [electronic resource], Geological survey of Finland; referred on 14.9.2018)

The mineralised rocks range from nuggety Au-U, quartz-carbonate-calcsilicalte -vein related style in Rompas to disseminated sulphide-associated gold-cobalt in Rajapalot (Fig. 2).

The Rajapalot area holds several gold rich occurrences and currently known targets are shown in Figure 3. Rajapalot became the primary target, over Rompas, upon the discovery of the Palokas, Rumajärvi and Joki occurrences. Since the discovery of the Palokas prospect in 2012, the number of prospects in the area have gone up to six, namely Palokas, South Palokas, The Hut, Rumajärvi, Terry's Hammer and Raja (Fig. 3). Based on the structural geology work done by the Mawson Oy, Au-Co rich occurrences are located in a kilometre scale fold hinge and is hosted by isoclinally folded rocks (Cook and Hudson, 2018)

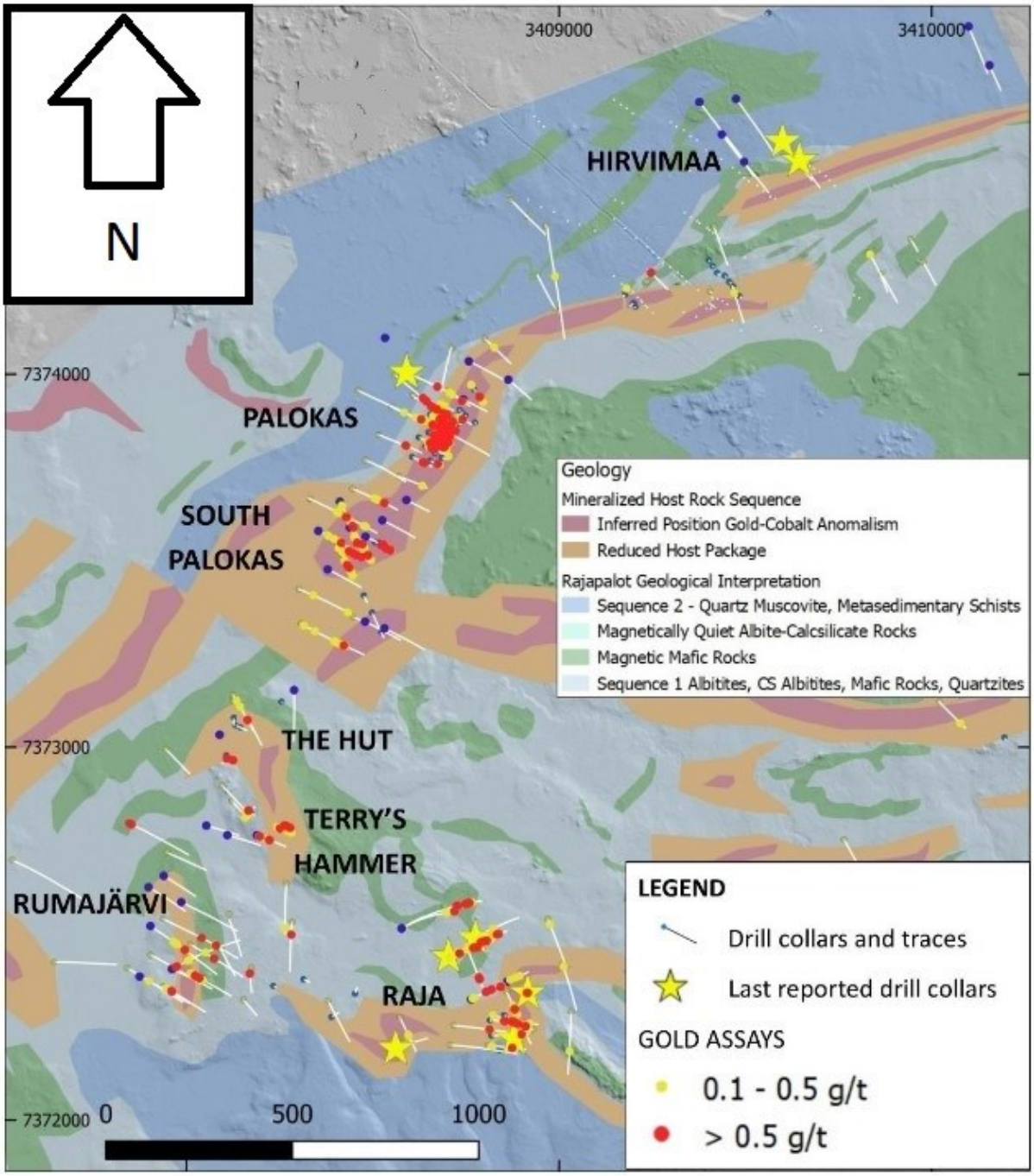


Figure 3. Geological map of the Rajapalot area showing currently known gold-cobalt occurrences. Drill hole collars are shown in blue dots with white traces. Red and yellow points indicates gold content. Figure taken from Cook and Hudson (2018)

The Raja prospect (Fig. 4) was found during the 2016-17 winter diamond drill program (Mawson press release May 02, 2017). Drilling indicates a coherent plunging mineralised body with substantial gold (and cobalt) enrichment (Fig 4.) This thesis concentrates on describing the mineralogy, alteration and typical features of the Raja prospect.

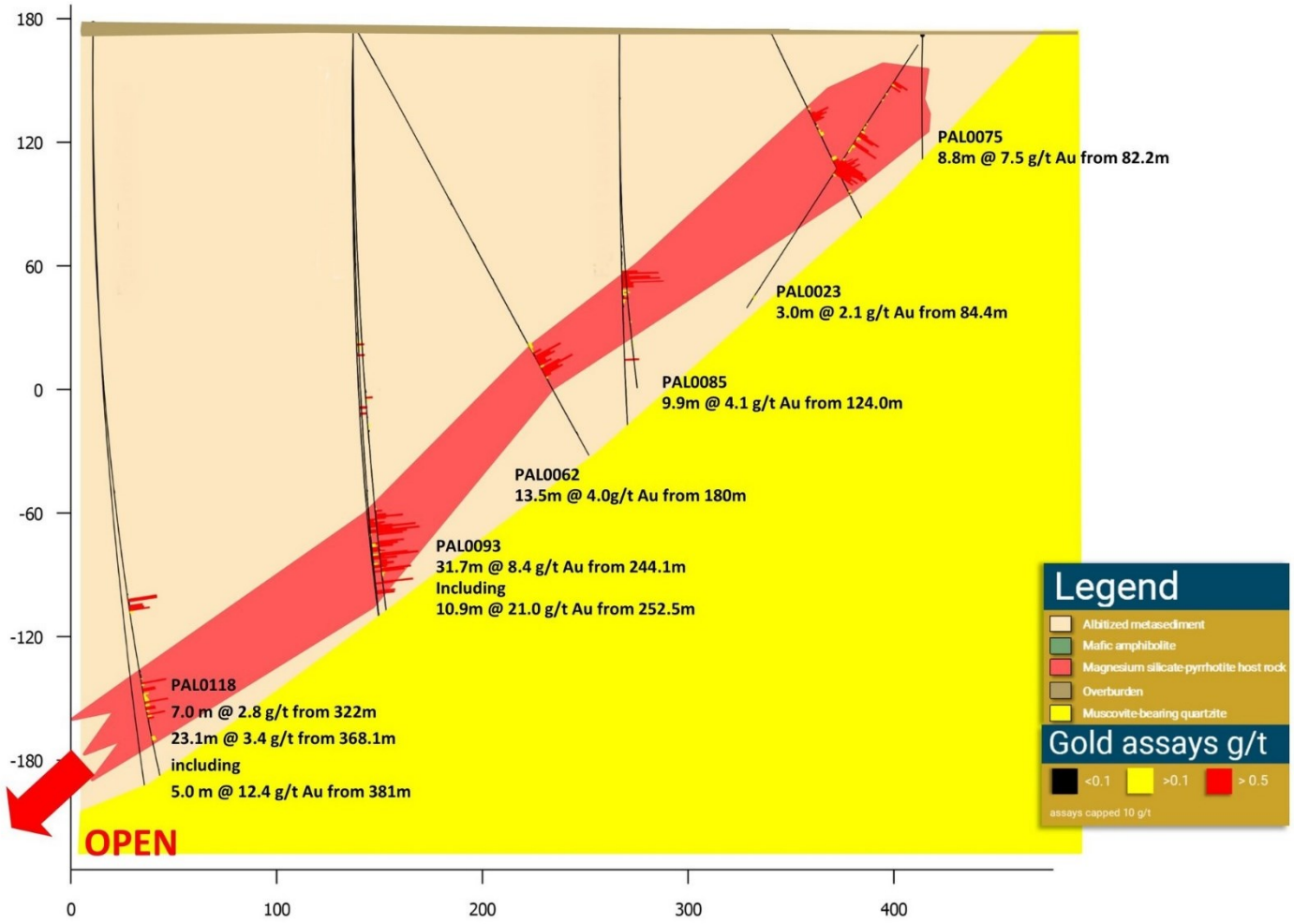


Figure 4. Simplified long section of Raja mineralised body. Figure from Mawson Resources press release (22.03.2018)

# 2. Regional geology of the Peräpohja belt

The Peräpohja belt (PB) is found in the northwestern Finland (Fig. 1) and represents one of the Paleoproterozoic supracrustal formations (Karelian Supergroup; Luukas et al., 2017), deposited on the rifting Archean basement between ca. 2.4-1.9 Ga (e.g. Kyläkoski et al. 2012; Ranta et al., 2015). It lays partially on remnants of some ~2.44 Ga old mafic-ultramafic layered intrusions, which are now found as fragmented belt along the SE border of the Peräpohja belt (see Iljina and Hanski, 2005 and references therein). The Peräpohja belt is bounded by the Archean Pudasjärvi basement complex in the south and by Central Lapland granitoid

complex in the north. In the west, it is separated from the Kalix belt by the Pajala shear zone (e.g. Lahtinen et al., 2015b) and in the east, separated from the Kuusamo belt by the Hirvaskoski shear zone (Laajoki, 2005). The belt is a 170-km-long, 80-km-wide roughly "arrowhead" shaped formation that is around 5 km thick (e.g. Kyläkoski et al, 2012).

The rocks of the Peräpohja belt were deformed and metamorphosed under greenschist to amphibolite facies during Svecofennian composite orogenies between ca. 1.9 – 1.8 Ga (e.g. Lahtinen et al., 2015b; Molnár et al, 2017). Thus, all the original volcanic and sedimentary rocks are now diverse metamorphic rocks, which, especially close to the borders of the Central Lapland granitoid complex and Kemijärvi complexes and within the Oulujärvi shear zone, are migmatised and intruded by Svecofennian plutonic rocks. In the northern and eastern margins of the Peräpohja belt, the metamorphic grade locally reaches upper-amphibolite facies and the supracrustal rocks pass into paragneisses and migmatites (e.g. Ranta et al., 2015). In the southern part of the belt, the metamorphic grade is generally lower-greenschist facies (Laajoki, 2005). Lahtinen et al. (2015b) proposed an updated structural model for Peräpohja belt. According to them, at least five distinct deformational events can be recognised:

D1 - well developed bedding-parallel cleavage (S0/S1). S1 is steeply dipping, roughly EW striking. F1 folds are open to closed, locally symmetric, with the fold axes steeply plunging toward the west.

D2 - The S2 foliation is characterised by a pervasive, generally EW striking and steeply to vertically-dipping foliation. It is associated with F2 folds that have open to closed interlimb angles (∼30◦–110◦). S2 clearly overprints S0/S1 or is subparallel to it in high strain zones of D2.

D3 - The S3 foliation is generally NNW-SSE striking with WNW-ESE trends mixed in. S3 is an NNW-SSE striking steeply-dipping spaced foliation, whereas the L2-3 intersection lineation is moderately to steeply plunging toward the NNW. D3 refolds the F1 folds.

D4 - structures are generally NNE-SSW trending throughout whole Peräpohja region and are associated with an S4 crenulations cleavage. The F4 folds are open to tight.

D5 - F5 folds are tight, symmetric and associated with a N-S striking evenly spacedS5 cleavage. S5 overprints S3 inthe eastern part, S2 in the central part and S0/S1 in the westernpart of the Martimo belt.

Rocks of the Peräpohja belt are divided into two main lithostratigraphic groups—the Kivalo group and Paakkola group (Perttunen et al., 1996; Perttunen and Hanski 2003). These are further subdivided into 17 formations (e.g. Perttunen and Hanski 2003; Kyläkoski et al, 2012). The lithostratigraphy of the PB is shown in the figure 5. The Kivalo group is considered to be deposited generally in shallow water settings, whereas the Paakkola group sediments show signs of a deep-water basin environment, implying progressive evolution of the rifting (e.g. Ranta et al., 2015). Lahtinen et al. (2015) considered the Paakkola group as a lithodemic unit.

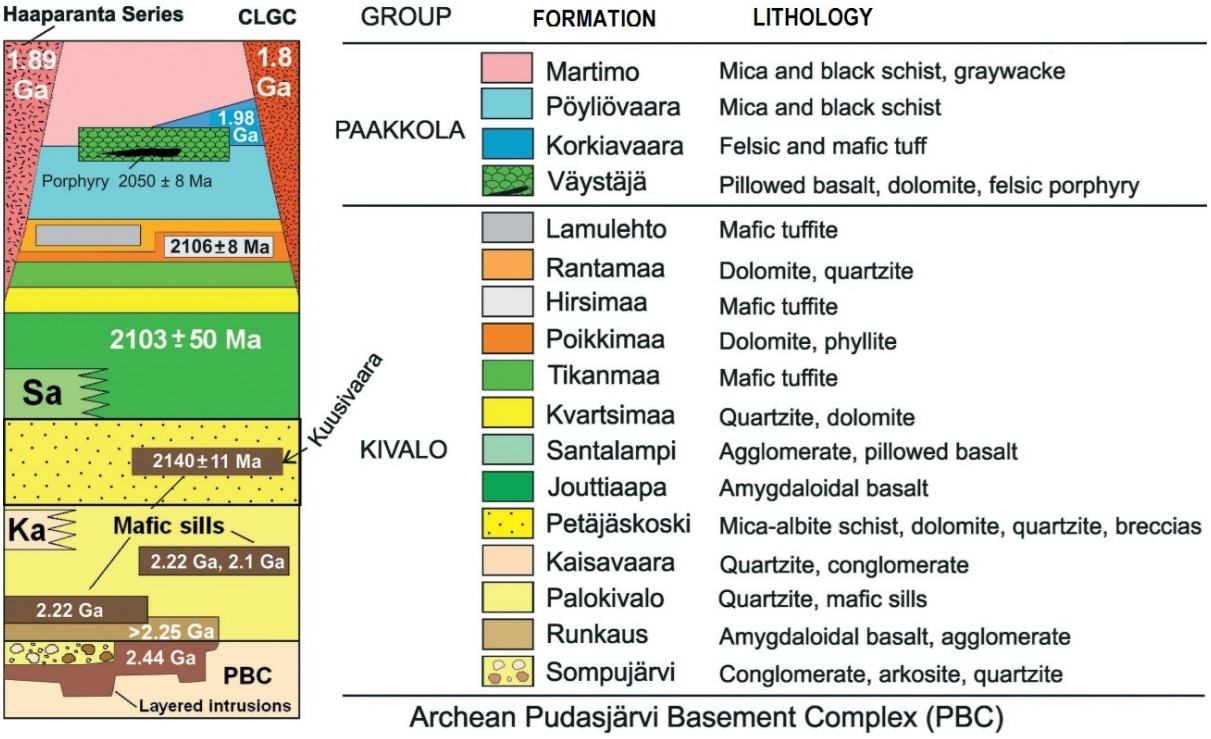


Figure 5. Lithostratigraphy of the Peräpohja belt. Modified after Kyläkoski et al. (2012), Ranta et al. (2015)

## 2.1 Kivalo Group

### *The Sompujärvi formation*

The conglomerates, arkosites and quartzites of the Sompujärvi formation are considered to be the lowest unit in the Kivalo group. It lays directly on top of the Archean Pudasjärvi Basement Complex and locally on remnants of the ~2440 Ma mafic-ultramafic layered intrusions. The unit is around 50 meters thick (Laajoki, 2005). The upper contact is marked by the lava flows of the Runkaus formation.

### *The Runkaus formation*

The Runkaus formation amygdaloidal mafic basalts are estimated to be 100-200m thick (Perttunen and Hanski, 2003). According to Laajoki (2005), the basalts are mainly subalkaline, tholeiitic basalts. In addition to mafic basalts, some layers show agglomerate structures with fragments of mafic volcanic rocks in a tuffitic matrix. The mineral composition of these metamorphic rocks includes actinolite, albite, epidote and chlorite (Perttunen and Hanski, 2003.)

### *The Palokivalo formation and Kaisavaara formation*

The Palokivalo formation is approximately 1 km thick and wide spread quartzitic unit (e.g. Perttunen and Hanski, 2003; Kyläkoski et al., 2012). Crossbedding, ripple marks and signs of mud-cracks preserved in the rocks are evidence of deposition in a shallow water environment. Clastic texture (0.2 – 1 mm in size) in the Palokivalo formation is always distinct. In addition to quartz and feldspars, sericite is often present (Perttunen

and Hanski, 2003). The cutting ca. 2220 Ma ultramafic-mafic sills give the minimum age for the Palokivalo formation (Perttunen and Vaasjoki 2001; Hanski et al. 2005). Detrital zircon population from the quartzites show solely Archean ages (e.g. Perttunen and Vaasjoki, 2001; Hanski et al., 2001; Ranta et al., 2015).

The Kaisavaara Formation comprises of light coloured, schistose, mid- to coarse grained sericite-quartzite, where some original clastic texture can be seen. The stratigraphic location of the Kaisavaara Formation is presently ambiguous but correlation with the Palokivalo formation has been proposed (Perttunen and Hanski, 2003).

*The Petäjäskoski formation*

Petäjäskoski formation comprises mainly of hematite bearing phlogopitic-sericitic and albitic schists with quarzite and dolomite interbeds. The entire formation is intensely deformed, but locally, well-preserved sedimentary structures are visible. Petäjäskoski formation could be considered as claystone-siltstone-sandstone-dolostone association deposited in evaporitic environment (Kyläkoski et al., 2012). The albitic schists are albitised equivalents of the mica-rich clay, and sandstones. The minimum age of the formation is ~2140 Ma, age obtained from the mafic sill intruding the Petäjäskoski formation (Kyläkoski et al., 2013). Older, 2220 Ma differentiated sills, penetrating lower parts of Palokivalo formation, are not known to reach the stratigraphy of Petäjäskoski (Kyläkoski et al. 2012).

*The Santalampi and Jouttiaapa formations*

The Santalampi formation and the Jouttiaapa formation are both comprised of mafic volcanic rocks. However, they are completely different in terms of petrography and in terms of composition. The Santalampi Formation is characterised by very high magnetic susceptibility. The formation can be observed on an aeromagnetic map for about 15 kilometers as a positive anomaly. Thickness of the anomaly is about 500 meters. In outcrops, the Santalampi Formation shows pyroclastic characteristics, such as rounded pyroclastic fragments ranging from 2 to 20 cm in a smaller grained matrix. Smaller 1-2 cm sharp magnetite fragments in tuffitic matrix are common as well. Pillow lavas are found as boulders. (Perttunen and Hanski, 2003).

The Jouttiaapa Formation has only amygdaloidal lavas, but no pillow structures are recorded. It erupted on dry land as tens of lava beds with tuffite or silt layers in between (Perttunen, 1989). According to Kyläkoski (2007) there are two magma types. One high Ti-series, rich in $TiO_2$ and Cu with lower MgO and one more primitive low Ti-series, with low $TiO_2$, Cu and higher MgO. The position of the formation can be determined from the amygdales. Near the lower contact of the lava is a 10 to 30 cm thick part where the amygdales are upright and narrow. The inner parts of the lava beds are void of amygdales but the grain size increases. In the upper parts the amygdales are parallel to the original layering. Mineral assemblage to these rocks are typical to metamorphic mafic lavas in the greenschist facies: albite, amphiboles, chlorite and epidote. Amygdales are also typical for the Peräpohja belt: Quartz, calcite, chlorite and epidote (Perttunen and Hanski, 2003). Sm-Nd data indicates an age of 2105 ± 50 Ma for the Jouttiaapa formation (Huhma et al., 1990; Hölttä et al., 2003).

*The Kvartsimaa formation*

The Kvartsimaa formation comprises of orthoquartzites (Perttunen and Hanski, 2003). Pure quartzites are white or light red in colour. Texture is granoblastic and locally clastic. Layering is hard to determine in the pure quartzites but some can be seen where the quarzites have some mica and carbonate impurities (op. cit.).

*The Tikanmaa formation*

The Tikanmaa formation has layered tuffites and layers range from few millimetres up to tens of centimetres (Perttunen and Hanski, 2003). Besides the layering, some cross-layers have been observed, indicating tidal activity (op.cit.). Magnetic susceptibility of the formation is relatively high; hence it shows on the aeromagnetic map as a positive anomaly.

*The Poikkimaa formation*

Poikkimaa formation is situated between the Tikanmaa and Hirsimaa formations. It is comprised of dolomitic rocks with thin quartz layers accompanied locally fyllitic interlayers. The formation can be seen in aeromagnetic map as area of magnetic low between the magnetic Hirsimaa and Tikanmaa formation. Due to poor exposure of the rocks the formations position is largely based on geophysical data (Perttunen and Hanski, 2003).

*The Hirsimaa formation*

Based on magnetic data, the Hirsimaa formation is estimated to be about 100 - 400 meters thick. It consists of magnetic green mafic tuffitic rocks (Perttunen and Hanski, 2003). U-Pb analysis on the formation's zircons by Karhu et al. (2007) yielded an age of 2106±8 Ma.

*The Rantamaa Formation*

Second youngest unit of the Kivalo Group is dolomitic rocks of the Rantamaa Formation. The rocks are yellowish or grey fine-grained dolomites with some quartzite interlayers. 1-2 mm thick quartzite layers are very well visible in outcrops as they protrude out of the rock (Perttunen and Hanski, 2003). Another distinct feature is the stromatolitic textures, indicating a shallow water environment (op.cit.). The $\delta^{13}C_{tot}$ values in samples taken from Rantamaa show a wide range in composition, from 11.4 % to 2.5%. The carbon isotopes are recording the evidences of so-called Lomagundi-Jatuli event which records the first signs of increasing oxygen and organic matter in earth (Karhu, 1993). A pattern in this variety divides the Rantamaa formation into highly enriched lower Rantamaa and low enrichment of $^{13}C$ in the upper Rantamaa formation (Karhu, 1993).

*The Lamulehto Formation*

Youngest part of the Kivalo group is not outcropped anywhere but can be seen as a magnetic positive anomaly (Perttunen and Hanski, 2003). Based on drill cores, it comprised of green, mafic tuffitic rock. Scarce

geochemical data from the formation suggest that the tuffitic rocks are tholeiitic basalts with incompatible trace element contents (op.cit.).

## 2.2 Paakkola Group

### *Väystäjä formation*

Usually the volcanic rocks of the Peräpohja belt are amygdaloidal lavas, where no pillows structures are observed. However, the Väystäjä formation lavas show consistent pillow lava textures (Perttunen and Hanski, 2003). Although the deformation is strong, some primary features are still visible and amygdaloidal features are rare (op.cit.). In whole, the Väystäjä formation comprises of pillow lavas, small black schist and dolomite parts. The stratigraphic position is currently ambiguous since the contacts with the other lithological units are not exposed and are probably tectonic (e.g. Ranta et al., 2015). Perttunen and Vaasjoki (2001) reported a U-Pb age of 2050 ± 8 Ma for a felsic porphyry cross-cutting the Väystäjä formation.

### *Korkiavaara formation*

According to Hanski et al. (2005), the arkosite-amphibolite Korkiavaara formation have lost all their primary features in the amphibolite facies metamorphism. Mineral assemblage of these rocks includes plagioclase and hornblende. The rocks are currently interpreted to represent tuffs with A-type signature (Hanski et al., 2005; Lahtinen et al., 2015). Zircons dated from the felsic tuffs gave a uniform age of 1973 ± 11 Ma (Hanski et al., 2005). Lahtinen et al. (2015) named this formation as the Rovaniemi Supersuite.

### *Pöyliövaara formation*

The Pöyliövaara formation is considered to represent the youngest sedimentary formation in the Peräpohja belt for a long time (e.g. Perttunen and Hanski, 2003). Pöyliövaara formation primarily consists of mica schists, mica gneisses, graphitic and sulphide bearing schists and amphibolite (Hanski et al., 2005). The contact to the lower units has not been located and due to folding the thickness of the formation is uncertain, but it is estimated to be at least several hundred meters (Perttunen et al., 1996).

### *Martimo formation*

The Martimo Formation, is the most widespread formation in the Paakkola group. According to Lahtinen et al. (2015), the Martimo formation is a poly-deformed fold and thrust belt that despite the lack of clear lithostratigraphic markers can be differentiated into three lithological types. First a graphite and Fe-sulphide-bearing Liekopalo paraschist, second a sequence of turbidites with interlayered pelites with mafic and felsic volcanic rocks and quartzites and the third group corresponds to Ristivuoma greywackes with a more felsic source of origin. Lahtinen et al. (2015) described the rocks mainly as relatively incompetent rocks. In addition, they describe the metamorphic grade increasing from east to west, rather than from south to north, which is

the general trend in the Peräpohja Schist belt. Studies by Ranta et al., (2015) and Lahtinen et al. (2015) allowed to set new depositional constraints between 1.91-1.88 Ga for the sedimentary rocks of the Martimo formation.

### 2.1.3 Mellajoki Suite

According to Perttunen and Hanski (2003) the Mellajoki Suite comprises of mica schists, quarzites and mylonitic quartz-feldspar gneisses. They included the Mellajoki Suite as a lithodemic unit and assigned it to the Central Lapland Granitoid Complex, based on the more deformed nature of the unit compared to the Palokivalo formation. In contrast, Ranta et al. (2015) considered the Mellajoki Suite as a part of the Peräpohja Belt and proposed correlation between the Mellajoki Suite and Palokivalo formations based on the similar detrital zircon populations.

## 2.3 Intrusive rocks

There are both mafic and felsic rock intruding the supracrustal rocks of the Peräpohja belt. According to Perttunen and Hanski (2003), majority of the intrusive mafic sills in Peräpohja belt represents 2220 Ma differentiated gabbro-wehrlite association (e.g. Perttunen and Vaasjoki, 2001; Hanski et al., 2010). In addition, the mafic sill cutting the Petäjäskoski formation, are dated to be 2140 ± 11 Ma (Kyläkoski et al., 2012) and thus, representing a younger phase of mafic intrusives. Supracrustal units are intruded by granitoid intrusions at least in four stages, ca. 1.99 Ga preorogenic Kierovaara granite (Ranta et al., 2015), synorogenic 1.89-1.88 Ga Haaparanta series granitoids (Perttunen and Vaasjoki, 2001), ca. 1.80 Ga appinitic intrusions (Tainio, 2014) and late-orogenic 1.77-1.79 Ga granites (e.g. Ranta et al., 2015).

# 3. Geology of the Rajapalot area

Outcrops in the Rajapalot area are rare, with the bulk of the region covered by swamps, till of variable thickness and small lakes. The outcrops mainly consist of quartzite, albitic metasediments and amphibolites (e.g. Ranta et al., 2018; Cook and Hudson, 2018). Boulders are abundant in the till covered areas and provide some information of the rock types. The rest of the information gathered from the area is from drilling, bottom-of-till (BOT) sampling and geophysical surveys. Descriptions below are mainly based on the Mawson Resources Ltd. press releases and unpublished reports.

The host sequence of the mineralised rocks in the Rajapalot area are divided into two sequences, separated by an interpreted unconformity by Cook and Hudson (2018). First sequence is comprised of a siliclastic, dolomitic carbonate and albite-altered metasedimentary sequence that is interpreted to be formed in a

platformal to continental margin setting. The second sequence is a metasedimentary sequence consisting of pelitic turbidites, arkosic sands, carbonates, various quarzitic sandstones and sulphidic carbonaceous rocks (Cook and Hudson, 2018). According to Ranta et al. (2018), the cordierite-orthoamphibole rocks and interlayered calcsilicate albite rocks are encountered in the drill cores.

### 3.1. Mineralisation types in the Rajapalot area

The mineralisation styles in the Rajapalot area vary between the different prospects, but two main styles can be described by sulphidic K-Fe alteration style of the "Rumajärvi type" and sulphidic Fe-Mg alteration style of the "Palokas type".

#### *Palokas type*

The Palokas type mineral assemblage include chlorite, Fe-Mg amphiboles, tourmaline, cordierite, pyrrhotite, garnets, magnetite and pyrite with bismuth tellurides, scheelite, ilmenite, gold and either cobaltite, cobalt pentlandite or linnaeite. (Ranta et al., 2018; Farajewicz, 2018). Host rock is a metamorphosed Ca-poor, Mg-Fe-rich cordierite-orthoamphibole rock unit with interlayered calcsilicate albite rocks and intrusive amphibolites. (Ranta et al., 2018). Gold occurs as free grains together with tellurides, scheelite and ilmenite and pyrite and pyrrhotite. The same Fe-Mg rich rocks can also be found in Raja and close to Rovaniemi where the rocks are exposed and some of the largest giant's kettles are located.

#### *Rumajärvi type*

Mineralogy of the Rumajärvi type mineralisation which occurs for example in the Raja prospect (Fig. 3) include micas, chlorite, quartz, albite, Mg-Fe amphiboles, tourmaline, pyrrhotite, scheelite, pyrite, chalcopyrite, bismuth tellurides, gold and cobaltite (Cook and Hudson, 2018). Mineralisation is defined by high potassic alteration. Host rocks are quartz-biotite/muscovite schist, albitic metasediments and other mica bearing lithologies. Gold occurs very much like in Palokas, together with pyrrhotite, ilmenite, scheelite and tellurides. Some gold has also been found in just very potassic altered and talc altered rock with little to no association to sulphides.

## 4. Gold and hydrothermal processes

### 4.1. Geochemistry of gold

Together with silver and copper, gold (Au) belongs to group 11 of the periodic classification by the IUPAC (International Union of Pure and Applied Chemistry). The elements are divided into these groups by the electron configuration of their outer most shells. The electron configuration for gold outermost shells are

$4f^{14}5d^{10}6s^1$. Gold has only one stable isotope in nature, $^{197}Au$. The main oxidation states for gold in nature are Au(0), Au(I), and Au (III) in highly oxidising environment (Williams-Jones et al., 2009).

### 4.1.1 Compounds of gold

According to Vlassopoulos and Wood (1990), most important complexes for gold are formed with $HS^-$, $S_2O_3^{2-}$, $CN^-$ and $SCN^-$ ligands. $CN^-$ is the most stable and forms the strongest bond ($Au(Cn)_2^-$). In oxidising conditions, the prevalent complex is $AU(S_2O_3)_2^{3-}$ and in reducing conditions, $Au(HS)_2^-$ is dominant. In hydrothermal fluids produced by geological processes, the most important gold complexes are $AuCl_2$-, which tends to dominate under acidic and oxidising conditions, Au(HS)° at intermediate pH and $Au(HS)_2$- at higher will tend to dominate under acidic (and oxidising) conditions, Au(HS)°at acidic to intermediate pH and Au(HS)2- at more alkaline conditions (Stefánsson and Seward, 2004). Au(OH)° may control gold transportation in very dilute solutions and only at relatively high temperatures. However, it is less stable than HS- and $Cl^-$ species and thus, is considered less important (Williams-Jones et al., 2009)

## 4.2. Hydrothermal fluids

Fluids play a key role in the transportation of elements to form a hydrothermal ore body. Hydrothermal fluids are comprised of liquid, gas or mixture of these. Phase diagram of pure water is presented in the Figure 6 as an example. Water can exist as a liquid, gas or solid phase, depending on the temperature-pressure conditions. In high temperature conditions, above the critical temperature (372 °C) of water, the fluid is said to be in supercritical state where phase boundaries vanish. Powell (1978) divided hydrothermal fluids into silicate fluids (magma), and aqueous fluids that can originate from a range of sources. Such sources could be, metamorphic dehydration reactions, compaction of sediments, meteoric waters, seawater, and mixture of sources mentioned above (Robb, 2005). For aqueous fluids Powell (1978) tells are two different ways of approaching them:

1. Emphasis on the molecular character, like $H_2O$ and $CO_2$. This is usually the case with metamorphic waters

2. Emphasis on ionic character. The interest is towards ion activity derived from the salts in the fluid. This is the case for low temperature and pressure fluids.

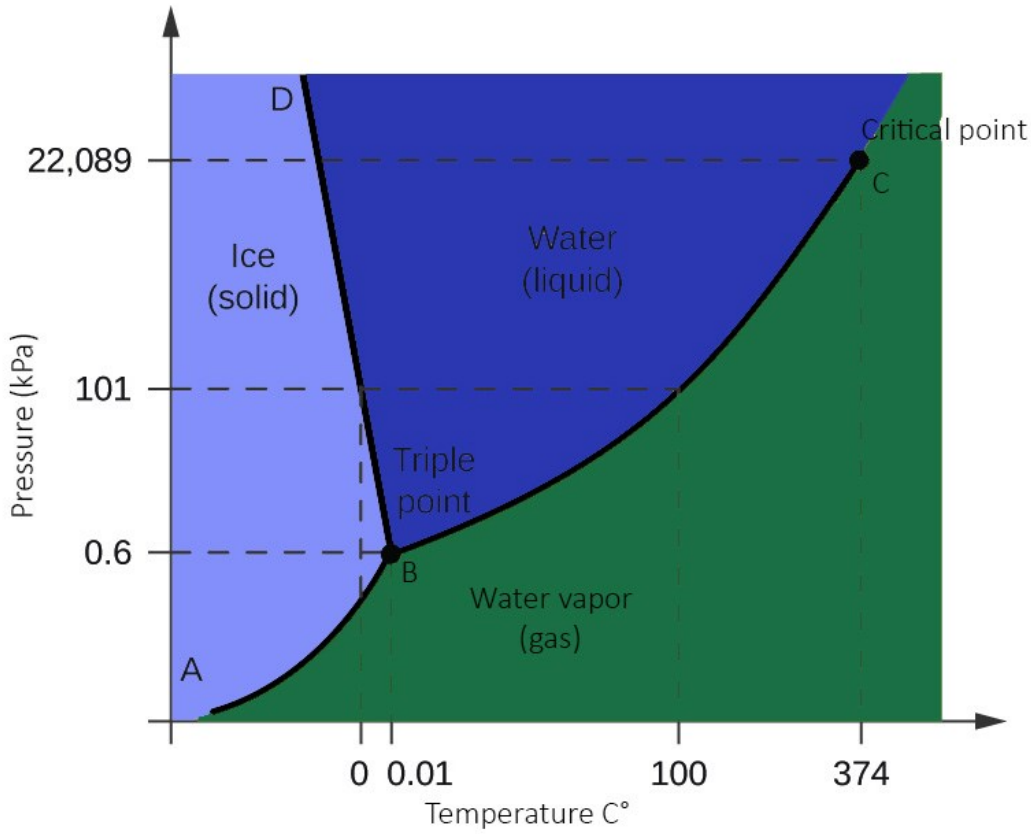


Figure 6. Phase diagram of pure water. Point C represents the critical point in where the density difference between water and gas disappears.

### 4.2.1 Hydrothermal alteration

Hydrothermal alteration is a chemical replacement of minerals in the original rock by new minerals from the hydrothermal fluid, which also removes the aqueous reaction products (Reed, 1997). Alteration takes place in a range of physical (temperature and pressure) and chemical conditions (pH). According to Zhu et al. (2011), hydrothermal alteration includes hydration, hydrolysis, redox reaction and sulphidation. Simplified examples of mentioned alteration reactions include the following:

$3KAlSi_3O_{8\ \text{K-feldspar}} + 2H^+ = 3KAlSi_3O_5(OH)_{2\ \text{muscovite}} + SiO_{2\ \text{quartz}} + 2K^+$

$2KAl_3Si_3O_{10}(OH)_2$ (muscovite) $+2H^+ + 3H_2O = 3Al_2Si_2O_5(OH)_4$ (kaolinite) $+ 2K^+$

$3CaMg(CO_3)_2$ (dolomite) $+ 4SiO_2 + 6H^+ 4H_2O = Mg_3Si_4O_{10}(OH)_2$ (talc) $+ 6H_2CO_3 \ +3Ca^{2+}$

$FeCO_3$ (siderite) $+ 2H_2S + 0{,}5O_2 = FeS_2$ (pyrite) $+CO_2 + 2H_2O$.

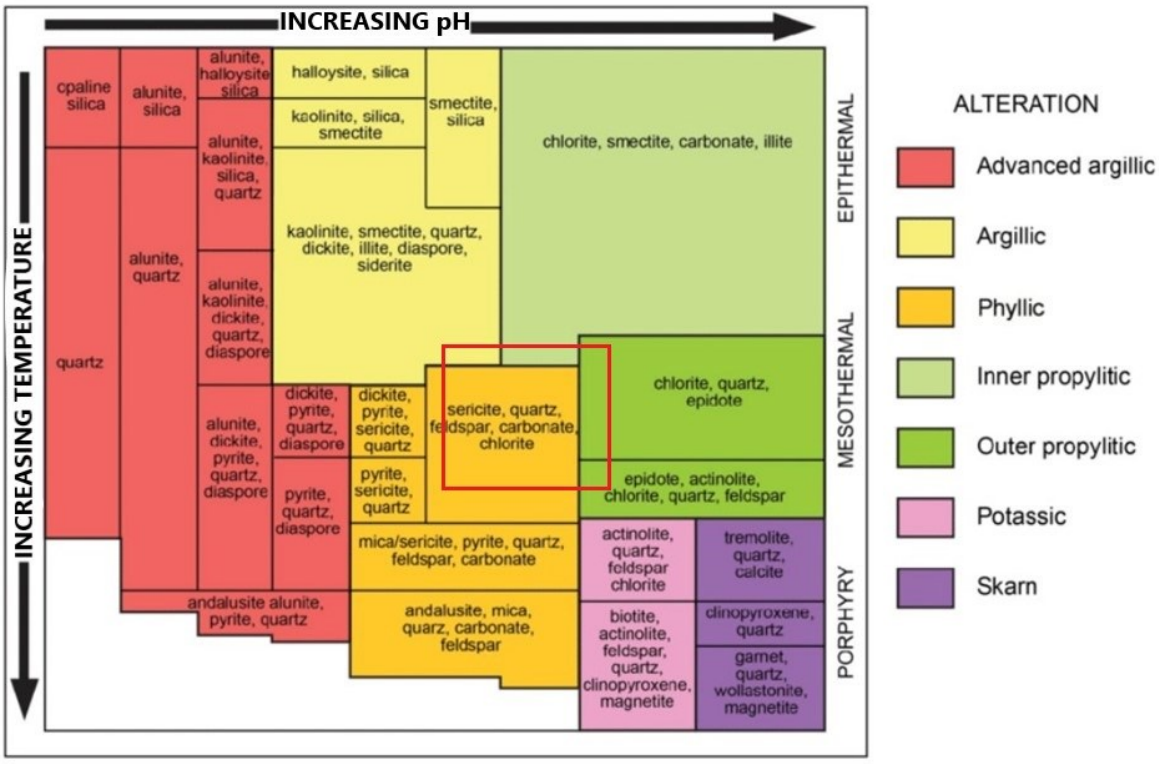


Figure 7. Typical alteration minerals found in various pH and temperature condition. (After Corbett and Leach, 1998).

Besides the composition of the fluids, temperature and pH of the fluid defines the alteration. Figure 7 shows some typical mineral assemblages for changing T and pH conditions. According to Meyer and Hemley (1967), the best way to divide the different alteration types of a hydrothermal system is by the nature of the chemical interchange between the wall rocks and the solution. The most important chemical changes are very likely related to $H^+$ / $OH^-$ balance. Below is the descriptions of the most important hydrothermal alteration types (Robb, 2005)

Advanced argillic alteration is characterised by dickite, kaolinite, pyrophyllite, frequently with sericite, quartz and alunite (Fig. 7). Meyer and Hemley (1967) connects this type of alteration to base metal veins, telescoped pipes or porphyry copper deposits in volcanic field or mountain belts. In addition, the type is found in shallow precious-metal veins in areas with volcanic activity like hot springs. (Meyer and Hemley, 1967). Sulphides in advanced argillic alteration zone tend to have high ratios of sulphur to metal. Argillic alteration happens in lower temperatures and is higher in the pH scale than advanced argillic. Argillic alteration excludes pyrophyllite and andalusite (Guilbert and Park, 2007)

Sericitic, or phyllic alteration shows some similarities with advanced argillic alteration in K-Al-mica composition. In terms of occurrence, sericitic alteration is the most abundant, widespread and significant of all the alteration assemblages (Meyer and Hemley, 1967). It is present in almost all near-surface ore-forming environments where aluminium is available. In addition, it is present in the gold quartz and massive sulphide systems in Precambrian terrains. Phyllic alteration is usually formed by hydrolysis of feldspars to sericite (Robb, 2005).

Propylitic alteration, according to Robb (2005), is most widespread type in terms of mineral assemblages. Meyer and Hemley (1967) states that propylitisation should only describe the weak hydrogen metasomatic alteration. It is a typical alteration in the margins of porphyry Cu deposits and epithermal precious metal ores (Robb, 2005). The stronger propylitic alteration can be indistinguishable from mineral assemblages formed in regional metamorphism in greenschist facies (Robb, 2005). In ore deposits, where the alteration is zoned, propylitic alteration occurs on the outer edges and grades to unaltered rock (Meyer and Hemley, 1967).

Potassic alteration means the formation of new K-feldspar and/or biotite by adding potassium in to the system via $K^+$ metasomatism and hydrolysis. (Robb, 2005). In addition, some sericite, chlorite and quartz are formed. Potassic alteration occurs in high temperatures 500-600ºC and produces adularia in epithermal systems and microcline in granodiorite ore forming systems (Meyer and Hemley, 1967).

# 5. Precipitation of gold

The formation of a hydrothermal ore body occurs, when metallic minerals are formed by the precipitation of solids from hydrothermal solutions called hydrothermal fluids (e.g. Robb, 2005). This reaction takes place when the properties of the environment or hydrothermal fluids change (e.g. temperature-pressure, pH, redox etc.; Robb, 2005). Temperature-pressure conditions change naturally when the fluid gets closer to surface, lowering temperature causes instability in the Au -complexes, particularly gold chloride complexes are sensitive to temperature change (Robb, 2005). In greater depths a more efficient way to cause precipitation is changing the properties of the fluid. For instance, increasing the pH of an acidic gold-chloride complex solution could cause precipitation. Such reactions could occur when the acidic solution react with a carbonate host rock (Robb, 2005). Changes in the gold bearing fluid can occur also via fluid-mixing. When a hot, gold-charged fluid mixes with a more dilute cooler fluid, like meteoric waters, the metal bearing fluid will cool, and the metal-ligands destabilise. Hedenquist and Aoki (1991) suggested that reactions between magmatic fluids and near surface meteoric waters in volcanic regions could be important prerequisite to the formation of epithermal Au-Ag mineralisation.

According to Groves et al. (2018), common site for ore-fluid infiltration, and therefore gold deposition, are contacts between granitic intrusions and volcano sedimentary sequences. Structurally best chances to form a hydrothermal gold deposits are in places with enhanced fluid migration and favourable sites for the gold to precipitate.

According to Goldfarb et al. (1988) gold mineralisation are usually a single widespread event, late in the tectonic evolution. Groves et al. (2018) concurs that data from all around the world indicate that orogenic gold deposits form late in the tectonic and structural evolution, mainly in the D3-D4 sequences.

Experiments done by Loucks and Mavrogenes (1999), in micrometer-sized fluid entrapment, show that solubility of $AuHS(H_2S)_3^0$ is very sensitive to changes in T-P conditions. Cooling from 400º to 340ºC results in precipitation of 90% of the dissolved gold from hydrothermal fluid to metallic Au. Furthermore, the study showed that depressurisation, that happens when fluids ascend from various pathways, decreases the solubility of gold.

# 6. Sampling and analytical methods

The samples are collected from the drill cores owned by Mawson Oy during the winter drill season of 2017-2018. The sampling sites were chosen based on the drill core logging information and represent both mineralised and unmineralised samples. The samples were cut at the Geological Survey of Finland core shed in Rovaniemi, photographed at the Mawson facilities in Rovaniemi. A total of 40 thin sections (see Fig. 8) were made from the core, 27 at the Lapland University of Applied Sciences in Kemi and 13 in Thin Section Lab in Toulou, France. 26 thin section were selected for further study of silicates, sulphides and oxides with electron microprobe analyser (EPMA) at the University of Oulu. Samples are named by drill hole ID and the number indicates the depth from which the sample is taken from.

The study was commenced and funded entirely by Mawson Oy. The majority of the applied research, such as logging of the core and petrographic studies with the polarisation microscope, was done in Rovaniemi at Mawson´s office. Much of the writing, finalising the petrographic studies, theoretical background studies and all the EPMA work was completed at the University of Oulu.

The standards used for the EPMA study can be found in the appendixes (appendix 3). The acceleration voltage used was 15kV and beam current of 15nA. Spot size for the silicate analysis was 10µm

and <1 µm for sulphides. The counting times were set at 10 s and 5 s for the peak and background, respectively.

Elements analysed for silicate studies were: $Na_2O$, $Al_2O_3$, $K_2O$, $SiO_2$, FeO, MgO, CaO, $ZrO_2$, $V2O_3$, Au, PbO, MnO, $Nb_2O_5$, CoO, Cl, NiO, AgO, $P_2O_5$, ZnO, Te and $TiO_2$

Elements analysed for sulphide studies were: Se, U, V, Au, As, S, Co, Pb, Mo, Ni, Ag, Fe, Cu, Sb, Zn, Bi, Te, Ti.

# 7. Results

## 7.1 Petrography

The thin sections used in this study and their name based on the logging information and name based on petrography studies are shown on Table 1. The samples from mineralised parts contained gold from 0.1 ppm to 115 ppm. Separate thin section descriptions for each sample can be found from appendix 4.

Table 1. List of the thin sections and their logged name and name based on microscopic study

| Thin section ID | EPMA | Logged name | Petrographic name | Gold content in the sample interval |
|---|---|---|---|---|
| Pal0083/40.85 | **Yes** | Biotite albite calcsilicate | Hydrothermally altered albite calcsilicate | <0.05 |
| PAL0092/222.95 | **Yes** | Calcsilicate albite | Ca -Metasediment | <0.05 |
| PAL0092/226.85 | **Yes** | albitite | albitite | <0.05 |
| PAL0092/306.90 | **Yes** | Muscovite quartzite | Musvovite quartzite | <0.05 |
| PAL0093/244.30 | **Yes** | Albite calcsilicate | Albitised and chloritised metasediment | **0.61 ppm** |
| PAL0093/248.35 | **Yes** | Albite calcsilicate | Albitised and slightly chloritised metasediment | **0.96 ppm** |
| PAL0093/256.00 | **Yes** | K metasediment | K metasediment | **6.39 ppm** |
| PAL0093/258.95 | **Yes** | K metasediment | Hydrothermal qz-sericite rock | **115 ppm** |
| PAL0093/261.05 | **Yes** | K metasediment | sericite schist | **2.65 ppm** |
| PAL0093/263.35 | **Yes** | Mafic metavolcanic | Intermediary rock | <0.05 |
| PAL0093/266.40 | **Yes** | K metasediment | K metasediment | **5.67 ppm** |
| PAL0093/269.90 | **Yes** | K metasediment | Hydrothermally altered albitised metasediment | **0.57 ppm** |
| PAL0093/274.05 | **Yes** | K metasediment | K metasediment | **6.34 ppm** |
| PAL0093/276.70 | **Yes** | Mg-Fe amphibole msed | Cordierite-cummingtonite-anthophyllite rock | **0.14 ppm** |
| PAL0097/260.73 | **Yes** | Albite calcsilicate | Hydrothermal Mg-Fe metasediment | **4.1 ppm** |
| PAL0097/261.35 | **Yes** | Albite calcsilicate | Hydrothermal Mg-Fe metasediment | **0.1 ppm** |
| PAL0097/272.32 | **Yes** | Albite calcsilicate | hydrothermally altered albitised siltstone | **0.1 ppm** |
| PAL0097/324.8 | **Yes** | Muscovite quartzite | hydrothermally altered siltstone | <0.05 |
| PAL0097/333.45 | **Yes** | Muscovite quartzite | hydrothermally altered quartzite | <0.05 |
| PAL0097/338.2 | **Yes** | Muscovite quartzite | sericitised metasandstone and quartz vein | <0.05 |
| PAL0100/283.3 | **Yes** | Talc altered rock | Chlorite-biotite-tourmaline rock | <0.05 |
| PAL0100/239.15 | **Yes** | Mg-Fe amphibole msed | hydrothermally altered differentiated mafic sill | <0.05 |
| PAL0107/253.6 | **Yes** | K metasediment | Sericitised sediment | <0.05 |
| PAL0107/263.20 | **Yes** | K metasediment | K metasediment | <0.05 |
| PAL111/9.20 | No | Albite calcsilicate | albitic sandstone | <0.05 |
| PAL111/23.75 | No | albitite | albitic sandstone | <0.05 |
| PAL111/139.9 | No | Calcsilicate | propyliticly altered rock | <0.05 |
| PAL116/112.84 | No | Mafic metavolcanic | Basalt | <0.05 |

| | | | | |
|---|---|---|---|---|
| PAL116/116.83 | No | Mafic metavolcanic | Mafic lava | <0.05 |
| PAL0118/381.35 | **Yes** | Mg-Fe amphibole msed | Mg-Fe amphibole metasediment | **3.84** |
| PAL0119/109.50 | **Yes** | Talc altered rock | Talc altered rock | **1.41** |

### Samples from the mineralised areas

14 thin sections representing Au-Co mineralised interval were studied with petrographic microscopes using transmitting light for the inspection of silicate minerals and reflective light for opaque minerals. Samples from the mineralised intervals varied from intensely sericite altered to chlorite altered rocks. Where visible and less altered by overprinting sericite, most of the samples showed granoblastic albite-quartz matrix with cordierite-anthophyllite assemblage (Fig. 11b2 and c2). Grain size of the matrix varies from sample to sample (Fig. 8a2 and Fig. 11b2). Most of the micas seem to be muscovite-sericite and appear as lepidoblastic layers (Fig. 9b2 and 9c2) or in cases pinitised (Fig. 10a2). Biotite occurs as accessory mineral and based on the pleochroism of the crystals, seem to approach phologopitic in composition. It is often also partly chloritised. Cordierite occurs as poikiloblastic grains and are often heavily pinitised. In addition, some talc alteration was found from mineralised rocks that were not in the main mineralised area (Fig. 12b1 and 12b2). One sample from the edge of the main mineralised body included some sillimanite (Fig. 12a2).

Main sulphides are pyrrhotite, pyrite, chalcopyrite with pyrrhotite by far the most common sulphide phase. Pyrrhotite frequently contains Co-pentlandite exsolution lamellae and in places inclusions (Fig. 9a2). Main oxides are ilmenite, rutile. Uraninite occurs as an accessory oxide phase. Other accessory phases identified during petrography include K-feldspar, rutile, tourmaline, zircons, apatite, cobaltite, sphalerite, uraninite, galena and gold. Cobaltite occurs as fine-grained dissemination of nearly euhedral grains (Fig. 11a2). During petrographic examination, one gold grain was found (Fig. 10b2), approximately 0.03 mm in size, among chloritised and biotitised amphibole and rutile. Some uranium, even high amounts, is found within the mineralised zone (like sample PAL0093-248.35, Fig. 8 b2) but it seems to be older since the pyrrhotite brecciates it and it does not correlate with the higher gold grades.

### Samples from non-mineralised areas

17 thin sections were taken from some the immediate vicinity of the mineralised areas, some of representing mafic intrusive rocks within and around the mineralised zones, the muscovite quartzite underlying the mineralised zones and some, from more distal to the mineralised interval.

Samples from the immediate vicinity of the mineralised area are similar to the rocks in the mineralised area, representing albitised metasediments (Fig. 13A and Fig. 14F) that have been slightly chloritised and sulphidised (Fig. 13B). Main sulphides are Fe -sulphides, mainly pyrrhotite and some pyrite. Co-pentlandite occurs as

exsolution lamellae in pyrrhotite. Cobaltite occur as sporadic grains in the matrix. Main oxides are ilmenite and rutile. The difference to the mineralised areas is the lesser extent of sericitisation (Fig. 14D) or the lack of it and a higher amount of carbonates (Fig. 13C and 14E). Also, the amphiboles are generally Ca-amphibole assemblages in contrast to the Fe-Mg-Mn amphiboles in the mineralisation. There are also occurrences of scheelite (Fig. 14A) and tourmaline (Fig. 14B) just outside the mineralised part. Intense sericitisation (Fig. 13E and 13F), in samples outside the mineralised areas, only occurs in the muscovite-quartzite, that underlays the mineralisation.

The samples from mafic rocks represent highly altered, differentiated mafic sills or altered lavas (Fig. 15A). The differentiated sills are generally talc altered (Fig. 15B) and highly chloritised often the chloritisation is zoned (Fig. 15D) and starts from inside the host mineral (Fig. 15C). Pleochroism of the biotite is strongly green, suggesting a high iron content or partial chloritisation. Sulphides include pyrrhotite, pyrite, small amounts of chalcopyrite and some cobalt minerals, mainly cobaltite. Main oxides are ilmenite and rutile.

The underlaying muscovite quartzite is intensely but not evenly sericitised. Main minerals are quartz, sericite and K-feldspar. Sulphidation is minimal to non-existent. Main oxides are ilmenite with accessory uraninite. The quartz is clastic and quite coarse grained compared to the mineralised areas.

Few samples, distal from the mineralised rocks were only slightly albitised and amphibolised sediments to one very intensely propyliticly (actinolite, biotite, chlorite, epidote, feldspar, quartz) altered rock.

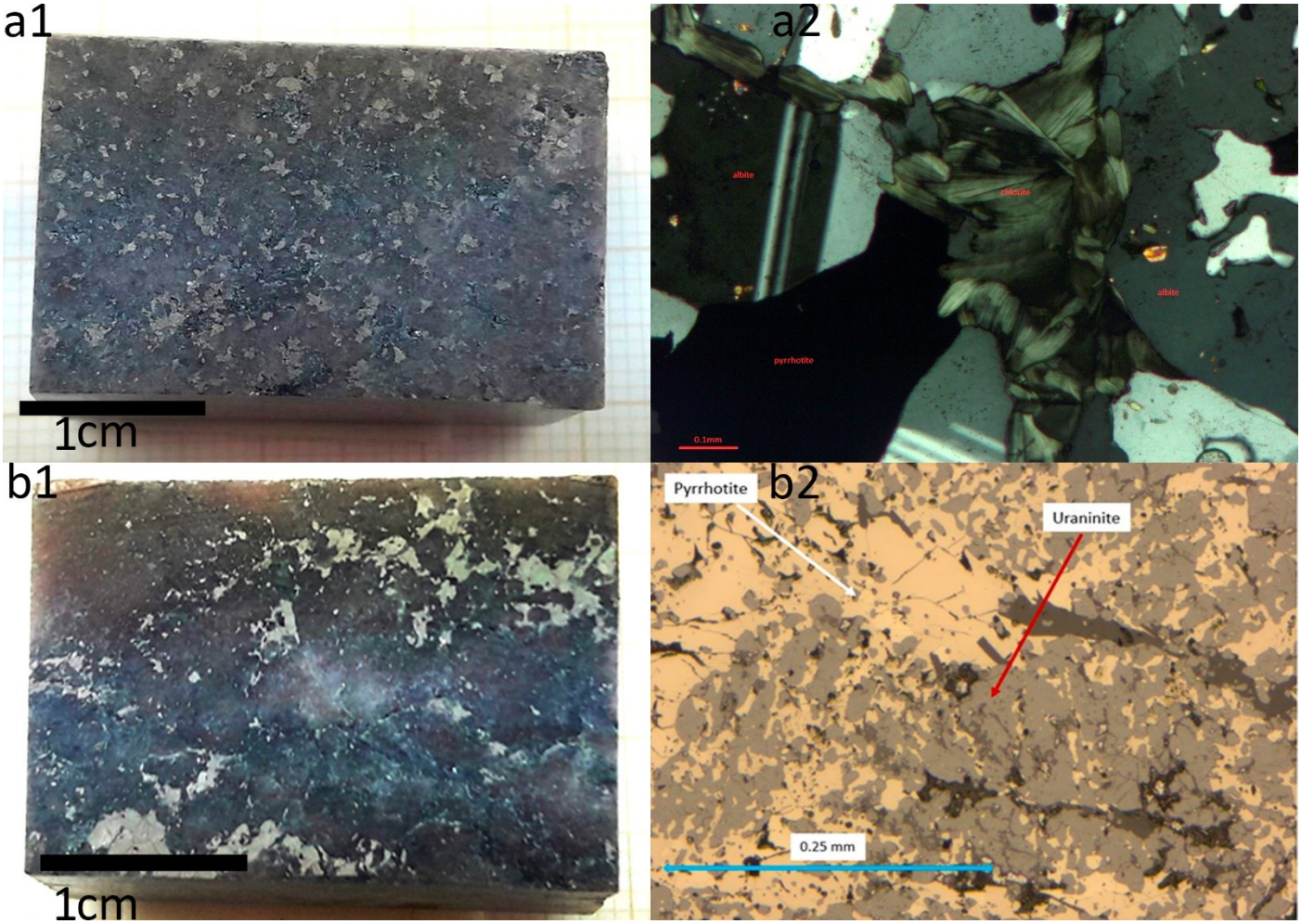


Figure 8. On the left side (a1, b1) hand samples and on the right (a2, b2) microphotographs from the samples in mineralised areas. **a1:** Albitised and chloritised metasediment (sample Pal0093-244.30). **a2:** Coarser grained albite together with pyrrhotite and very green chlorite. Obj. 5x/0.15 XPL (Pal0093-244.30). **b1:** Albitised and chloritised metasediment **(**sample Pal0093-248.35). **b2:** Pyrrhotite brecciating uraninite. Obj. 20x/0.40 XPL (Pal 0093-248.35).

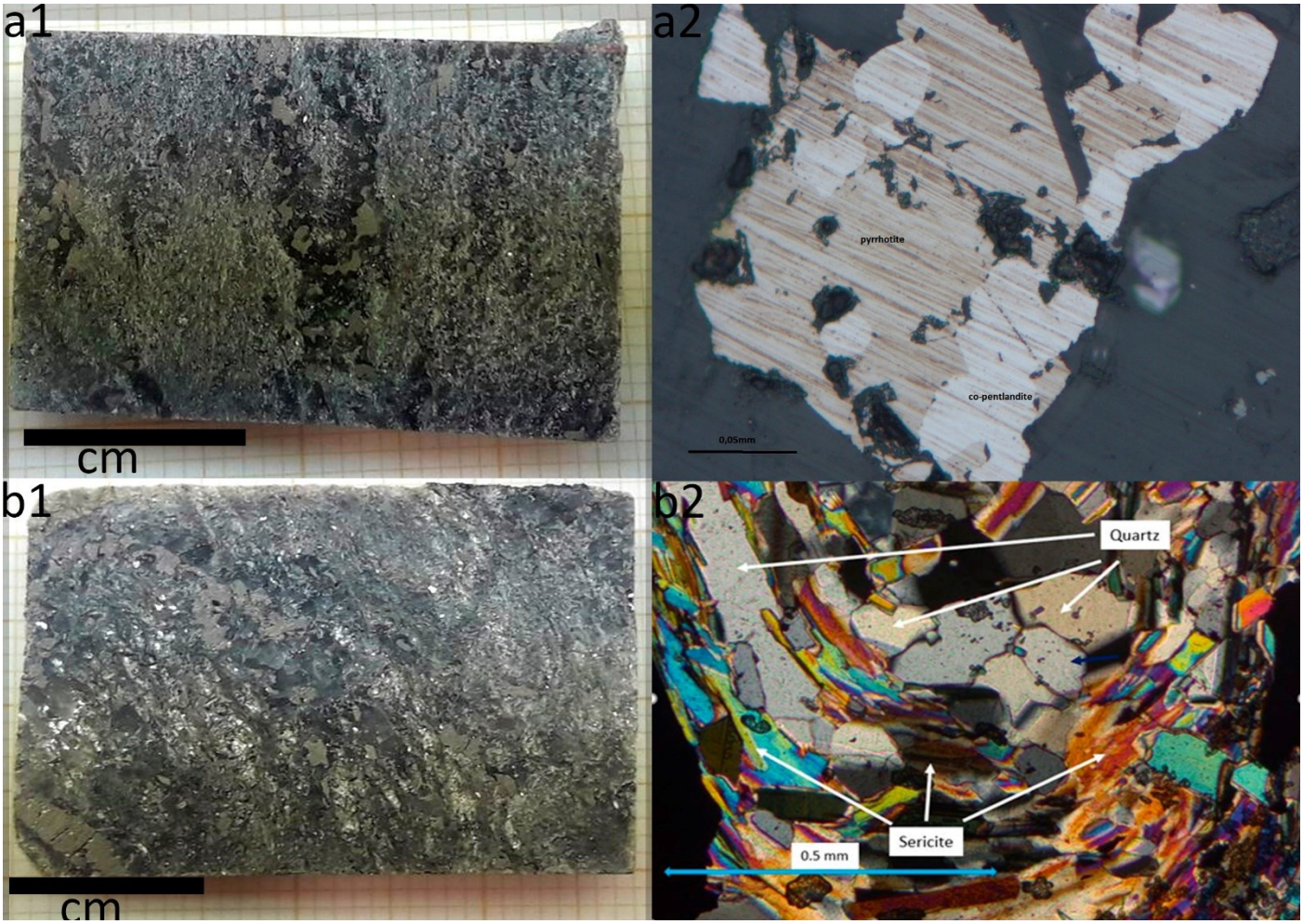


Figure 9. On the left side (a1, b1, c1) handsamples and on the right (a2, b2, c2) microphotographs from the samples in mineralised areas. **a1:** K-metasediment **(**sample Pal0093-256). **a2:** pyrrhotite and co-pentlandite as inclusions Obj. 25x/0.075 reflective light (Pal0093-256). **b1:** Hydrothermal quartz-sericite rock (Sample Pal0093-258.95). **b2:** Sericite and quartz showing a layered appearance and a microfold. Obj. 10x/0.25 XPL (Pal0093-258.95).

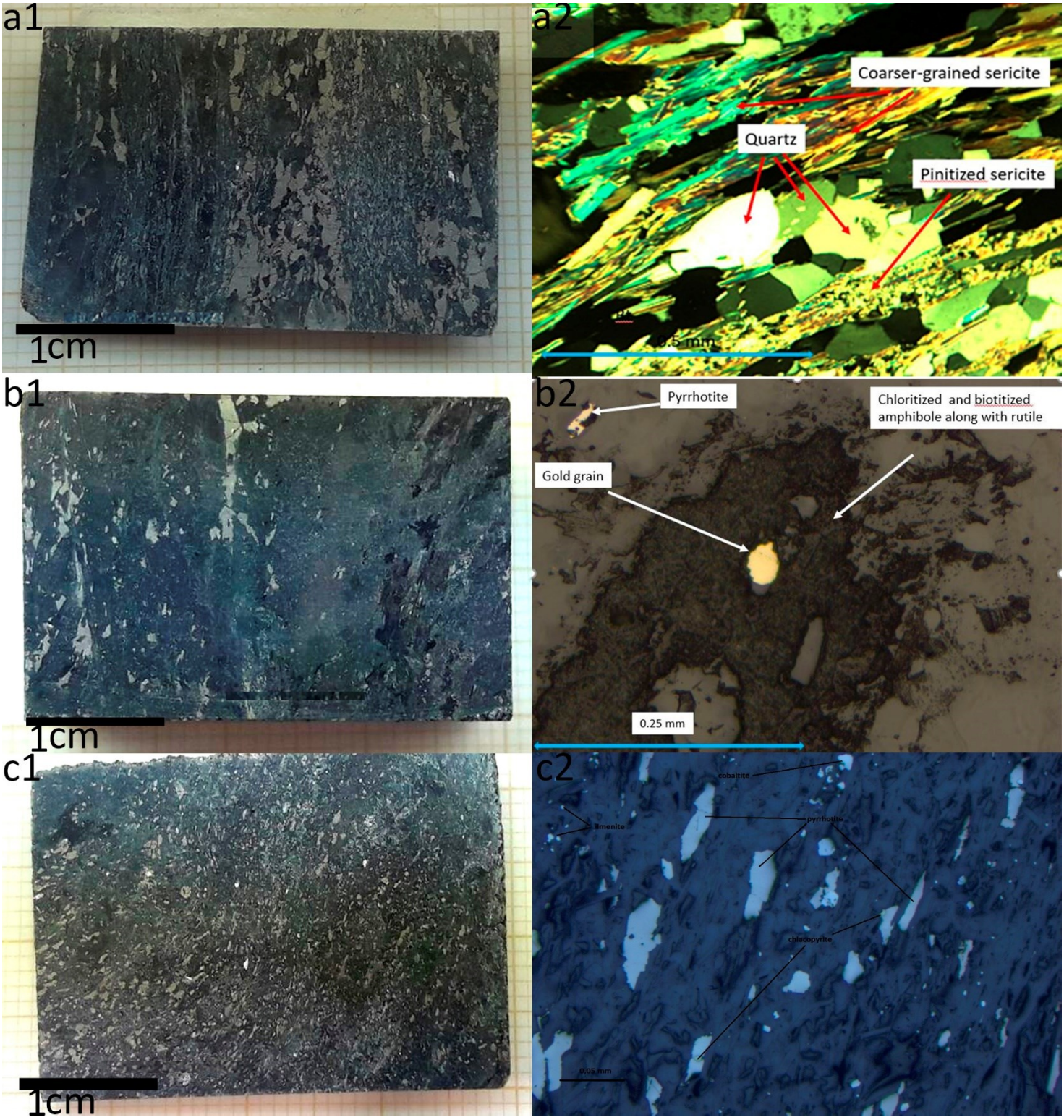


Figure 10. On the left side (a1, b1, c1) hand samples and on the right (a2, b2, c2) microphotographs from the samples in mineralised areas. **a1:** K-metasediment (Sample Pal0093-266.40). **a2:** Pinitisation of sericite together with more coarser grained sericite and quartz grains. Obj 10x/0.25 XPL (Pal0093-266.40) **b1:** Hydrothermally altered albitised metasediment (Sample Pal0093-269.90). **b2:** Occurrence of gold among chloritised and biotitised amphibole along with rutile. Obj 10x/0.25 (Pal0093-269.90). **c1:** K-metasediment (Sample Pal0093-274.05). **c2:** Occurrence of pyrrhotite as oriented elongated grains, cobaltite as semi euhedral grains and ilmenite as small rouded grains. Obj 1.25x/0.035 reflective light (Pal 0093-274.05).

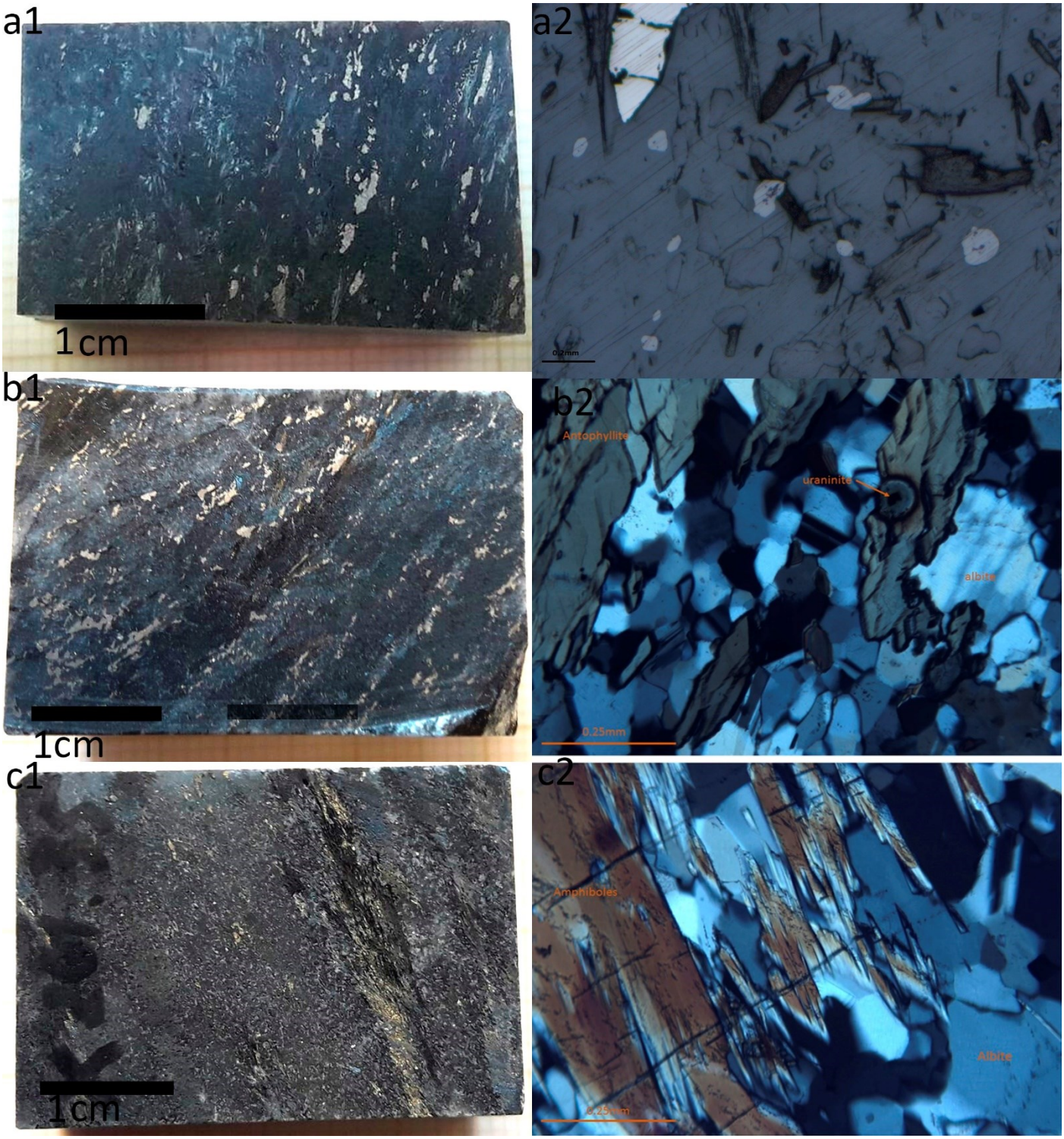


Figure 11. On the left side (a1, b1, c1) hand samples and on the right (a2, b2, c2) microphotographs from the samples in mineralised areas. **a1:** Cordierite-cummingtonite-antophyllite rock (Sample Pal0093-276.70). **a2:** Occurrence of pyrrhotite as elongated grains and cobaltite as almost euhedral grains. Obj 2x/0.075 reflective light (Pal0093-276.70) **b1:** Hydrothermal Mg-Fe metasediment (Sample Pal0097-260.73). **b2:** General overview of the albite matrix and amphiboles. Uraninite grain in the amphibole. Obj 10x/0.25 XPL (Pal0097-269.73). **c1:** Hydrothermal Mg-Fe metasediment (Sample Pal0097-261.35). **c2:** Amphiboles and quite coarse-grained albite. Obj. 10x/0.25 XPL (Pal0097-261.35).

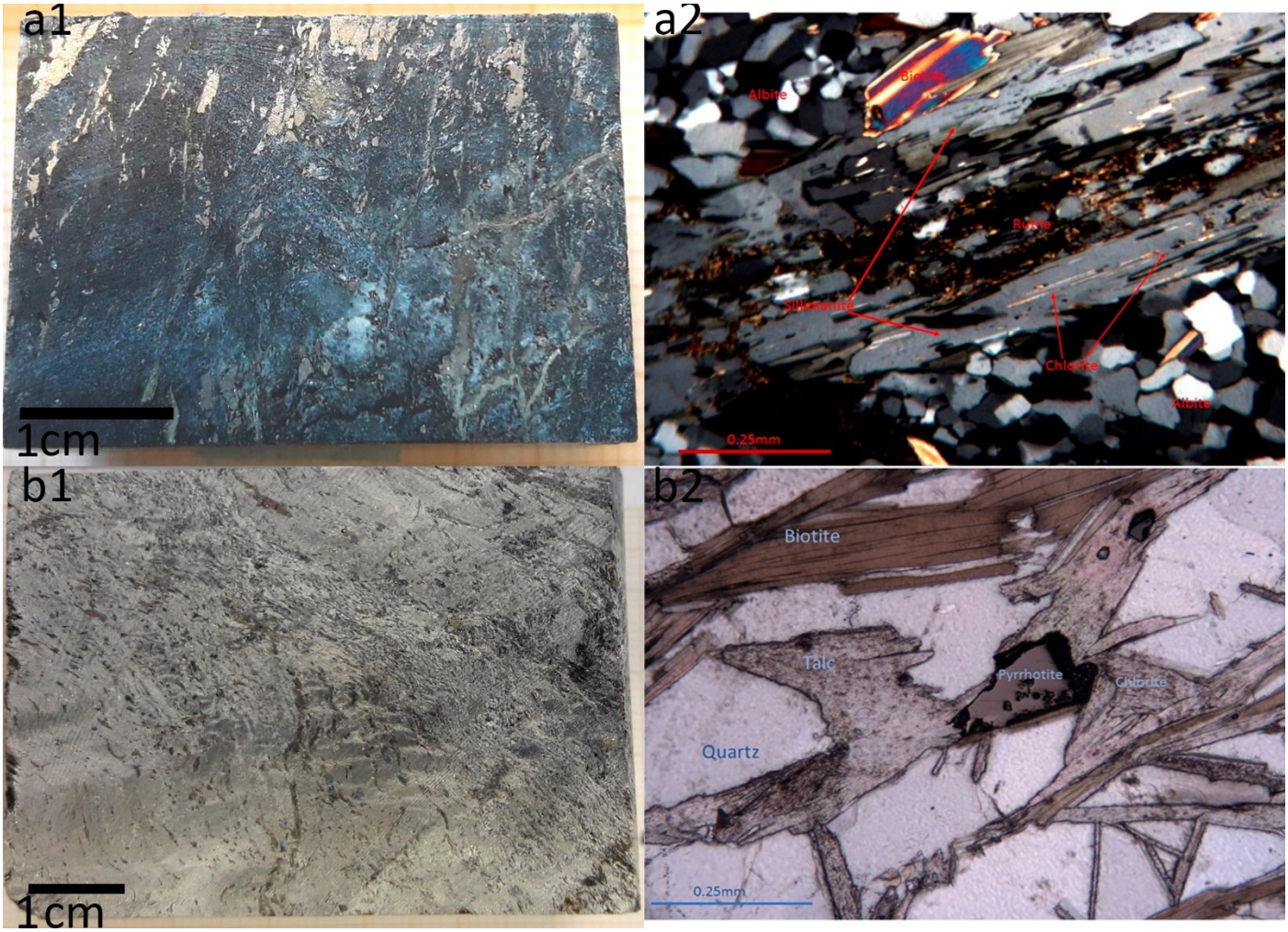


Figure 12. On the left side (a1, b1) hand samples and on the right (a2, b2) microphotographs from the samples in mineralised areas. **a1:** Hydrothermally altered siltstone (Sample Pal0097-272.32). **a2:** Sillimanite being eaten by chlorite surrounded by the albite matrix. Obj 10x/0.25 XPL. **b1:** Talc altered rock (Sample Pal0119-109.5) **b2:** Quartz grains surrounded by biotite, talc and chlorite. Note the sharp edges in quartz. Pyrrhotite grain in the middle. Obj. 10x/0.25 PPL and reflective light.

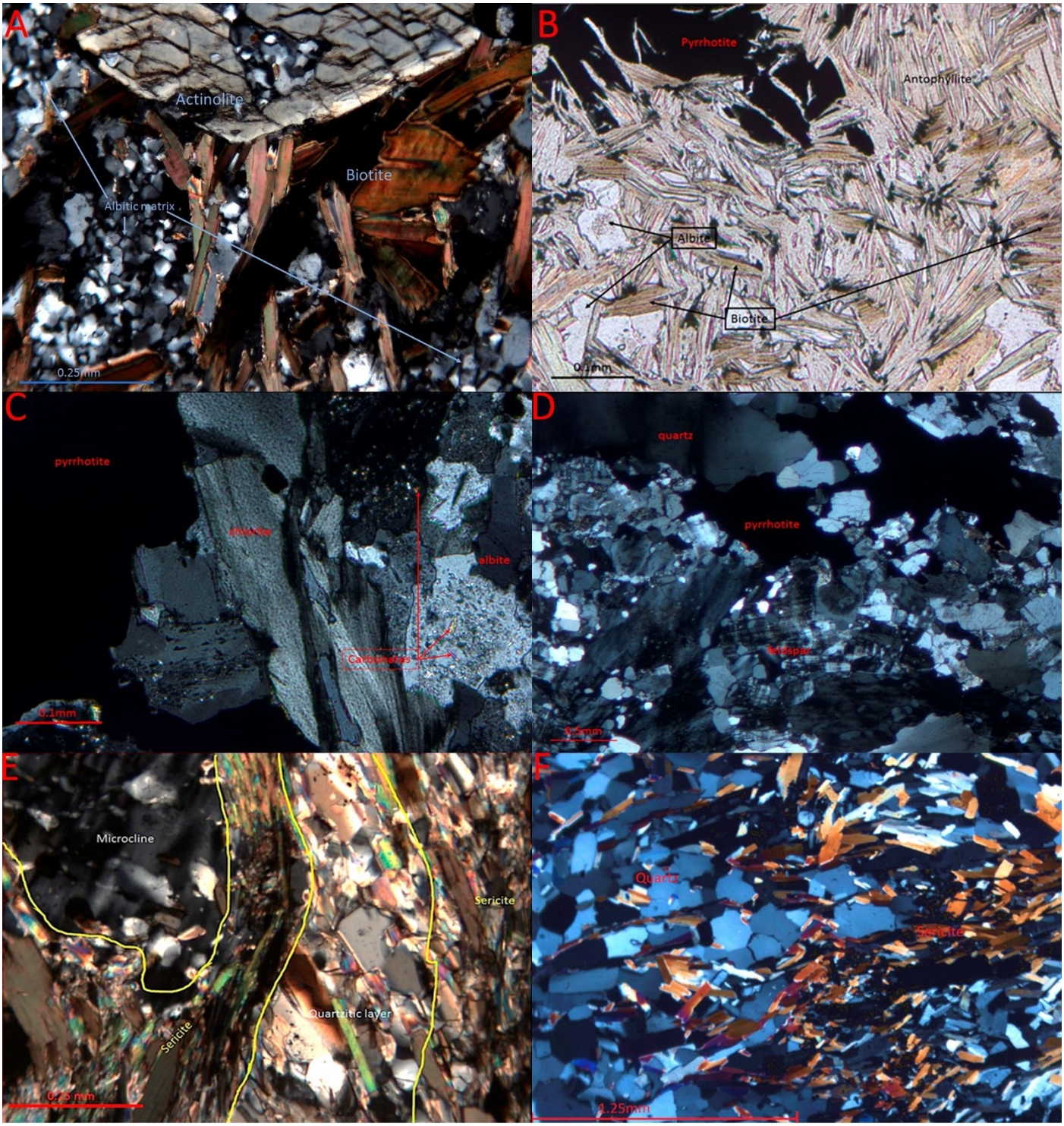


Figure 13. Microphotographs from samples in the non-mineralised areas. A: Overview of the albitic matrix, amphiboles and biotite. Obj. 10x/0.25 XPL (Pal0083-40.85) B: End of a pyrrhotite vein with biotite, amphiboles and albite. Obj. 5x/0.15 PPL (Pal0092-222.95). C: Colourless chlorite around a pyrrhotite vein and some carbonate residue in albite. Obj 10x/0.25 XPL.(Pal0092-226.85) D: Relation of the quartz feldspar matrix, quartz vein and pyrrhotite. Obj. 0.1.25x/0.035 XPL. (Pal0092-306.90) E: Serisitic alteration going around the feldspar. Quartzitic layer outlined and separated from the two sericite layers with different orientation by yellow line. Obj 10x/0.025 XPL.(Pal0097-324.8) F: Sericite coming from the left as a strong overprint fades and goes between the quartz on the right. Obj 4x/0.10 XPL. (Pal0098-333.24)

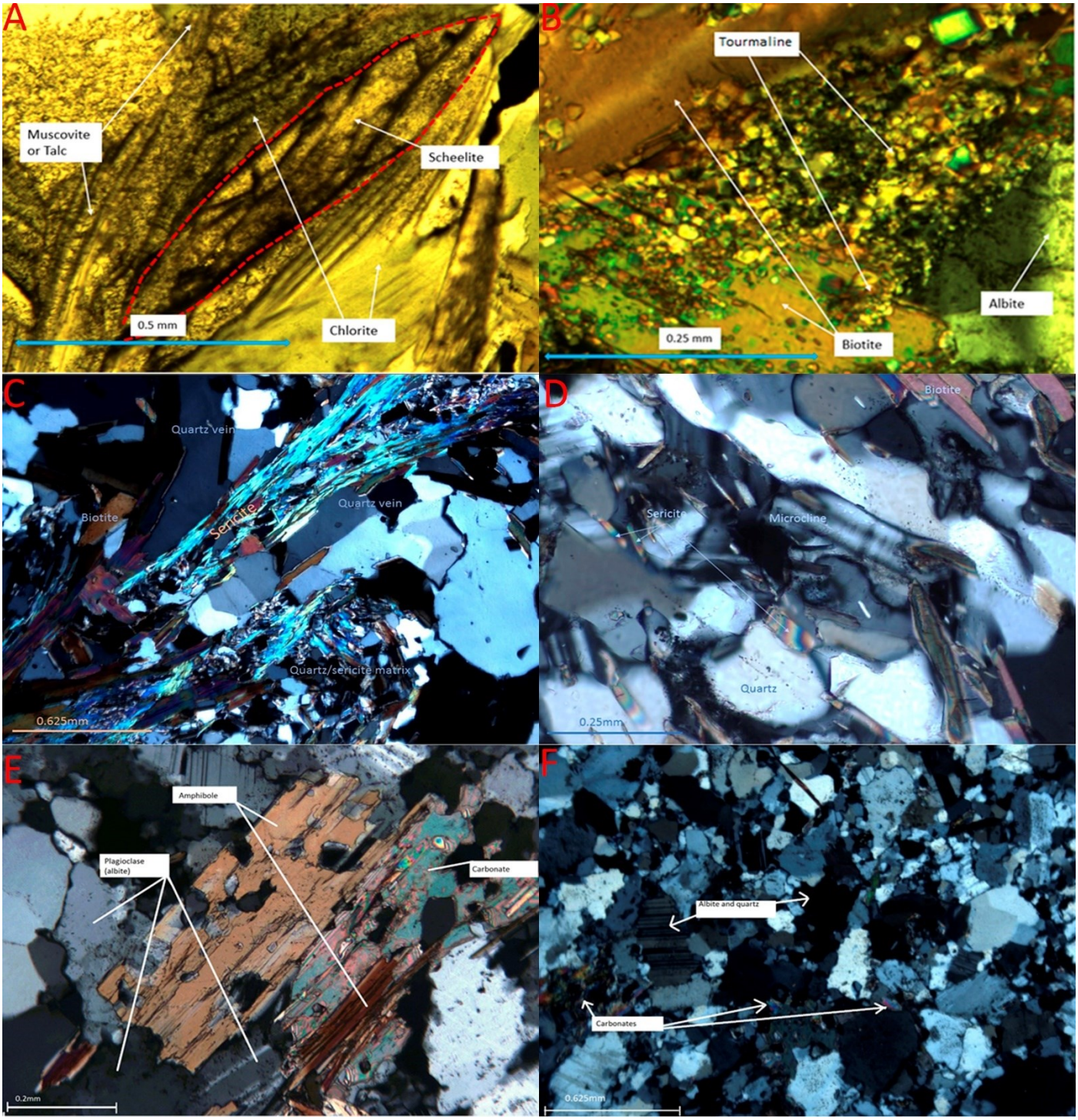


Figure 14. Microphotographs from the non-mineralised areas. A: Scheelite formed a mixed grain with micas. Obj 10x/0.25 PPL (Pal0100-239.15). B: Fine-grained tourmaline mass covering biotite. Obj. 20x/0.40 XPL (Pal0100-283.3). C: Remains of folded quartz vein, schistose sericite and quartz/sericite matrix. Obj 4x/o.10 XPL (Pal0107-253.6). D: General overview and relations of the main minerals and the low amount of sericite 10x/0.25 XPL (Pal0107-263.20). E: Carbonate producing amphibole in albite matrix. Obj. 10x/0.25 XPL (Pal0111-9.20). F: General overview of the relations of albite-quartz matrix and carbonates. 4x/0.10 XPL.

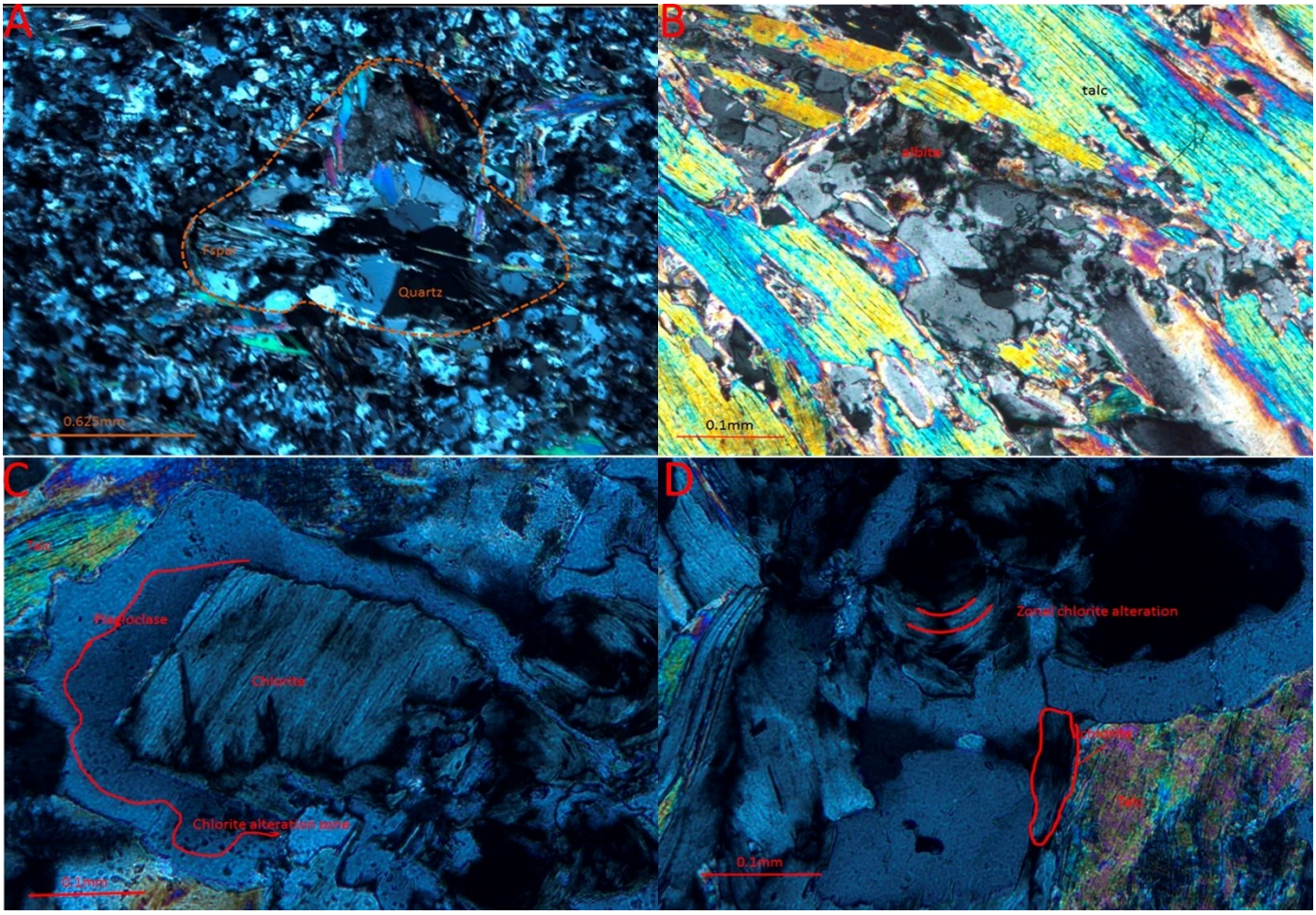


Figure 15. Microphotographs from the non-mineralised areas. A: Cavity or gas pocket in the lava filled with quartz and feldspar. Some of the carbonates have been remobilised. Obj 4x/0.10 XPL (Pal0116-112.84). B: Talc altered amphiboles and albite. Obj 5x/0.15 XPL (Pal0116-116.83). C: Chlorite alteration consuming the plagioclase from the inside. Obj. 10x/0.30 XPL (Pal0116-116.83). D: Zonal chlorite alteration along with evenly altered grains. Obj. 10x/0.30 XPL (Pal0116-116.83).

## 7.2. EPMA

All the results for each measured point can be found from appendix 1 for sulphides and appendix 2 for silicates.

### 7.2.1 Amphiboles and pyroxenes

28 points from six thin sections were identified to belong to the amphibole group and three points to the pyroxene group with composition close to enstatite but with some Fe impurities. The totals for the pyroxenes (all from a mafic intrusion (Pal0100-239.15) ranged from 92 to 94%. The amphiboles are categorised into groups, subgroups and species as recommended by the Commission on New Minerals Nomenclature and Classification (CNMNC) of the International Mineralogical Association (IMA) and published by Hawthorne (2012). From Raja occurrence, two distinct amphibole subgroups were identified: Ca-amphiboles and Mg-Fe-Mn -subgroup. The Ca-amphiboles (Fig. 16) were plotted according to Leake et al. (1997) and the Mg-Fe-Mn amphiboles (Fig. 17) according to Hawthorne et al. (2012).

Calcic amphiboles from 3 different samples plot as actinolite and magnesiohornblende. Notable is that according to Leake (1997) the $Ca_B$ should be ≥1.5 and $Na_B$ should be in the range of 0.5 and 1.5 usually. However, all measured points of calsic amphiboles in this study measure $Na_B$ below 0.1, $Ca_B$ is above the recommendation. Calcic amphiboles were found only just outside of the mineralised area or in the case of PAL0093-263.35 from an intermediary sill inside the mineralised area.

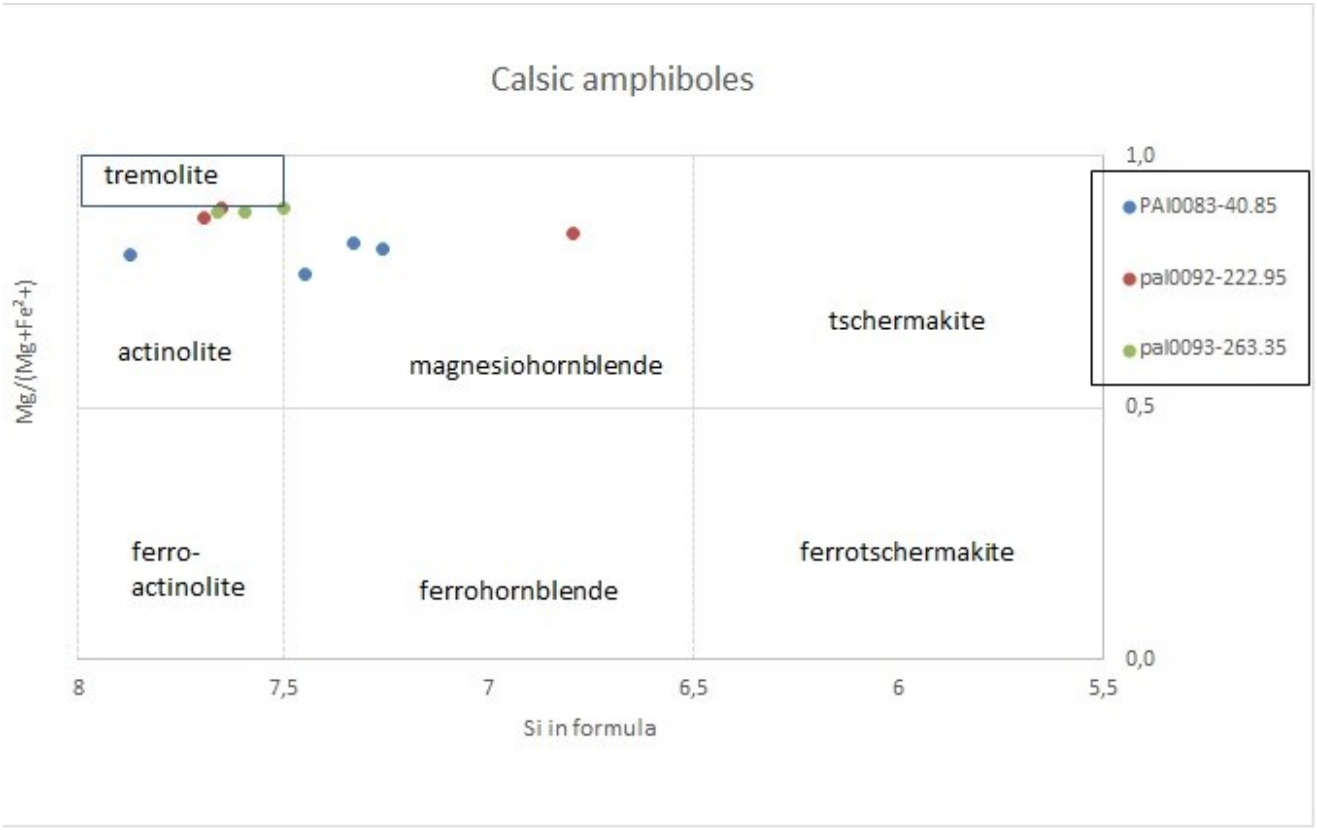


Figure 16. Ca-amphiboles of Raja (After Leake et al. 1997)

Mg-Fe-Mn amphiboles are divided between anthophyllites and gedrites from four different samples. 6 analyses were discarded due to unreliable totals.

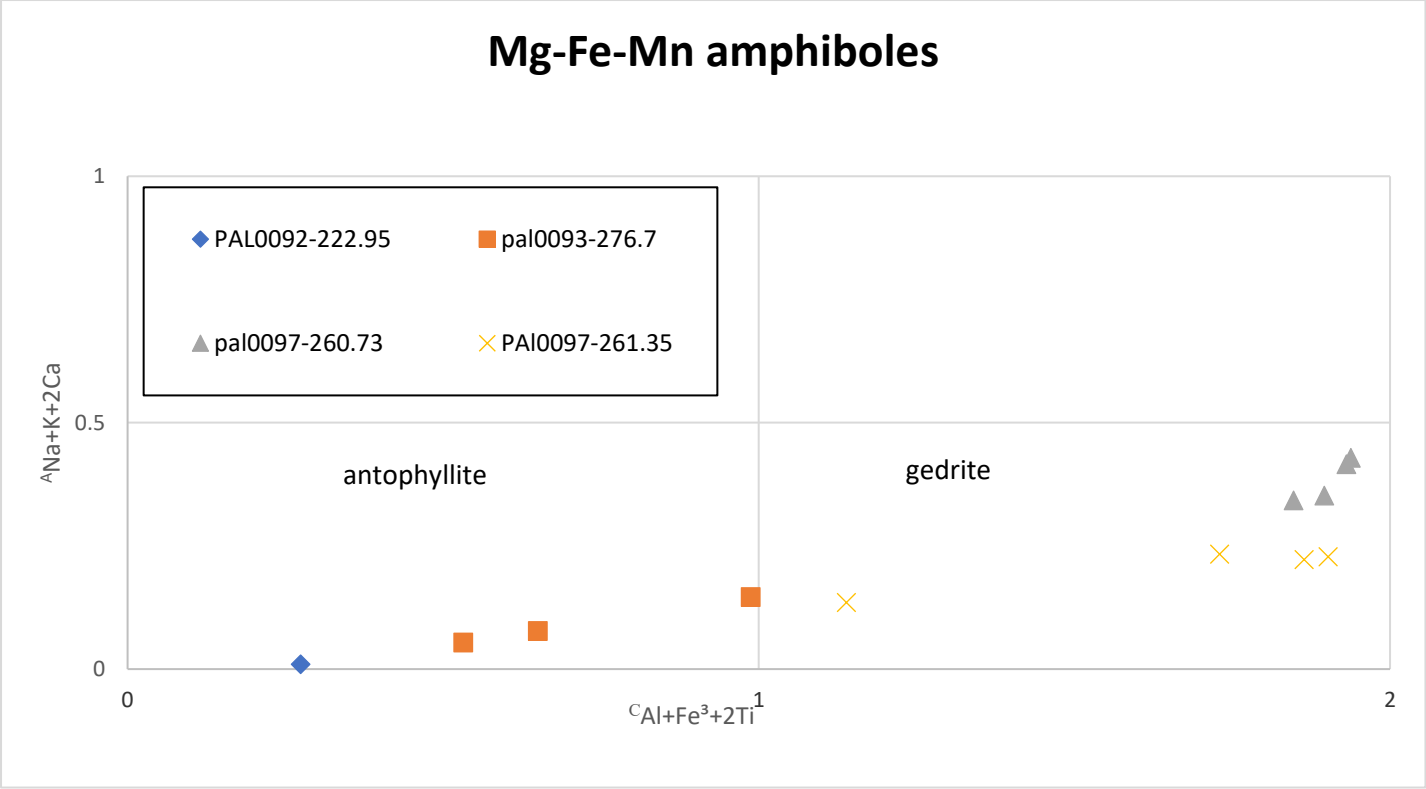


Figure 17. Orthorhombic Mg-Fe-Mn amphiboles in Raja. Classification diagram after Hawthorne et al. (2012).

### 7.2.2. Feldspars

Plagioclases on the anorthite-albite series plot mainly on the albite end (Fig. 18). Feldspars are mainly microcline and found in samples taken from PAL0092, PAL0093 and PAL0097 all near or inside the mineralised zone.

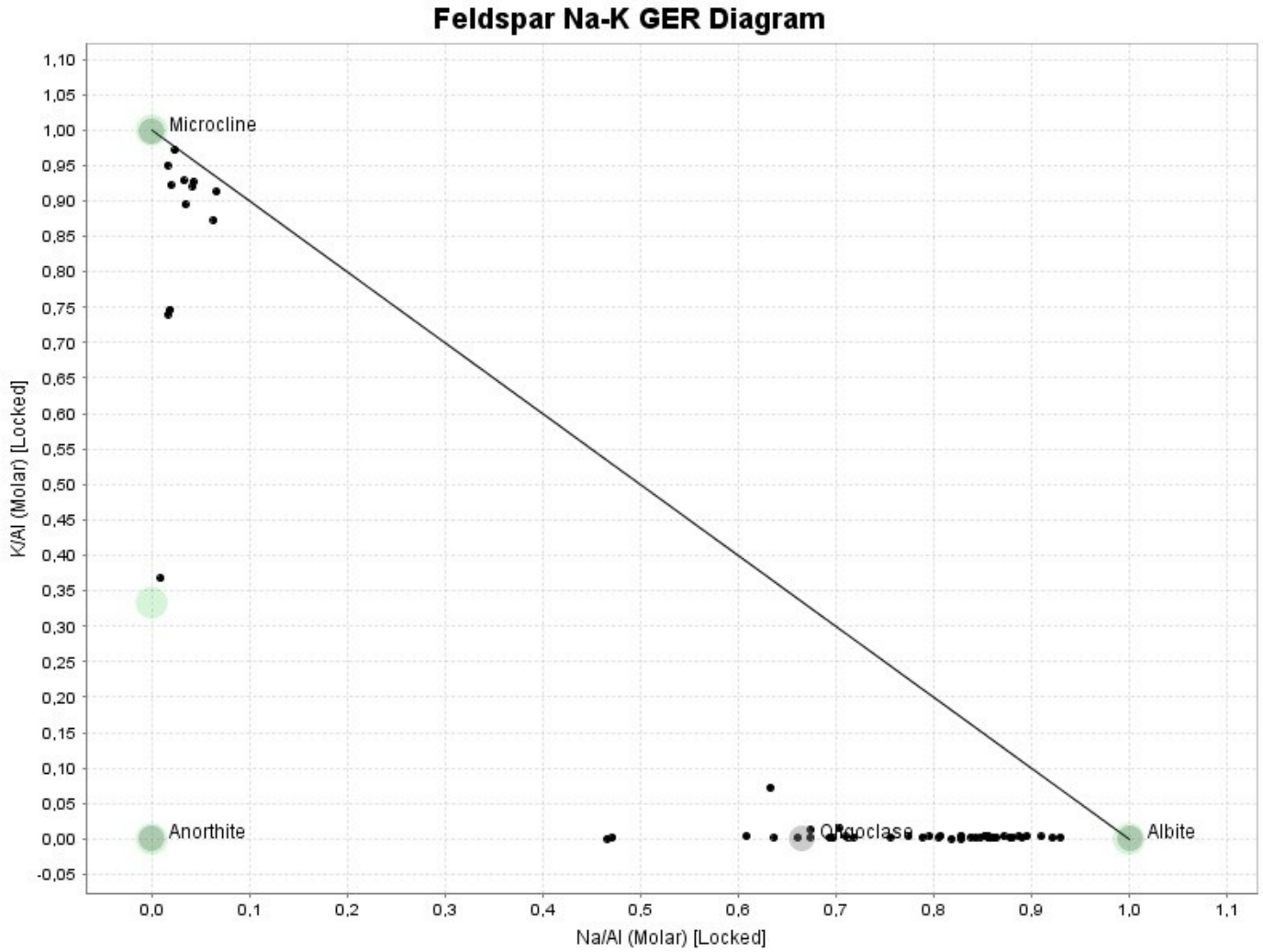


Figure 18. Feldspar compositions in Raja plotted on a Na-K GER diagram.

### 7.2.3. Micas

The analysed micas show two distinct groups in terms of Al content (Fig. 19). The Al-rich muscovite-sericites in the mineralised parts and Al-poor phlogopite and biotite mostly around the mineralisation, but locally in the mineralised parts as well.

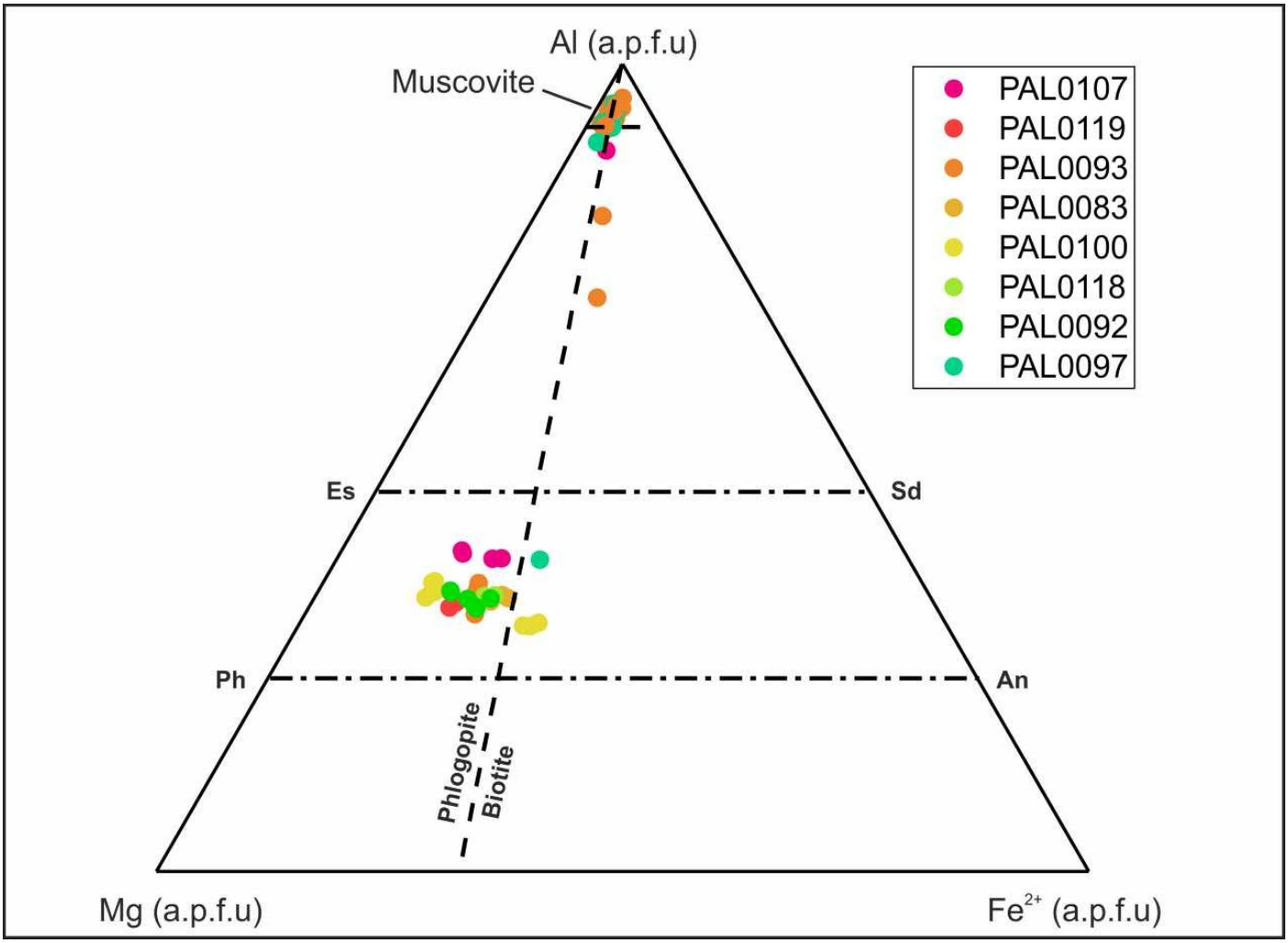


Figure 19. Composition of the analysed micas plotted in Al-Mg-Fe ternary diagram after Bailey (1984). Abbreviations: Es = Eastonite, Ph = Phlogopite, Sd = Siderophyllite, An = Annite.

### 7.2.4 Sulphides, oxides and heavy minerals.

Main sulphides in Raja and studied in this thesis are pyrrhotite, pyrite, cobaltite and cobalt-pentlandite. Oxides analysed represented ilmenite, rutile or uraninite.

Totals for the analyses averaged 98.4%. Some of the pyrite is rich in cobalt, up to 8%. Besides some anomalous contents in pyrite (Fig. 20), cobalt occurs mainly as separate cobaltite grains and Co-pentlandite exsolution lamellae in pyrrhotite.

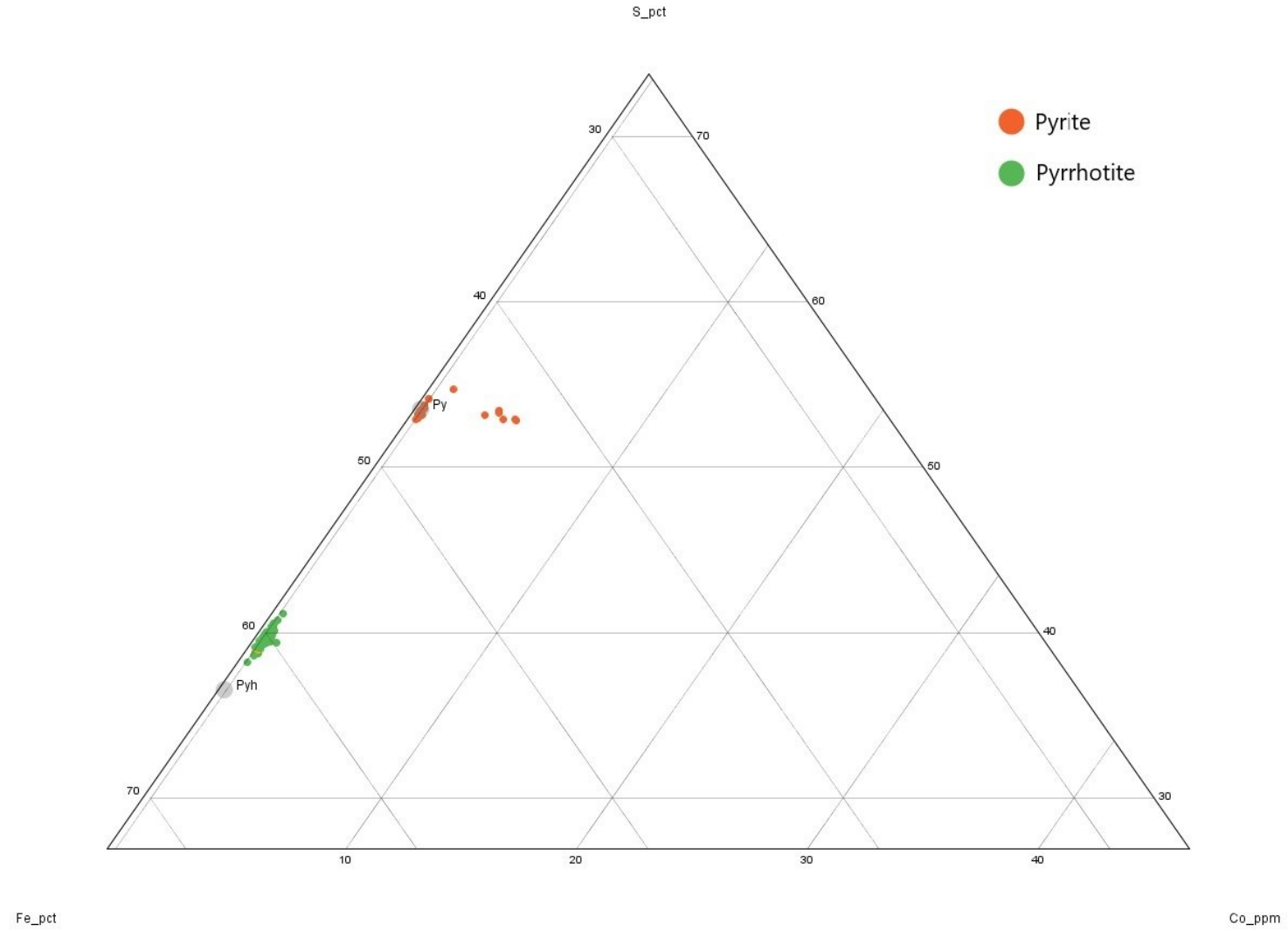


Figure 20. Cobalt content of pyrite and pyrrhotite and the relatively low Fe and high S count of pyrrhotite.

Cobalt content of the Co-pentlandite varies considerably (Fig. 21) (NiAsS) Gersdorffite and ((Ni,Co)AsS) cobaltoan-gersdorffite show as two distinct groups.

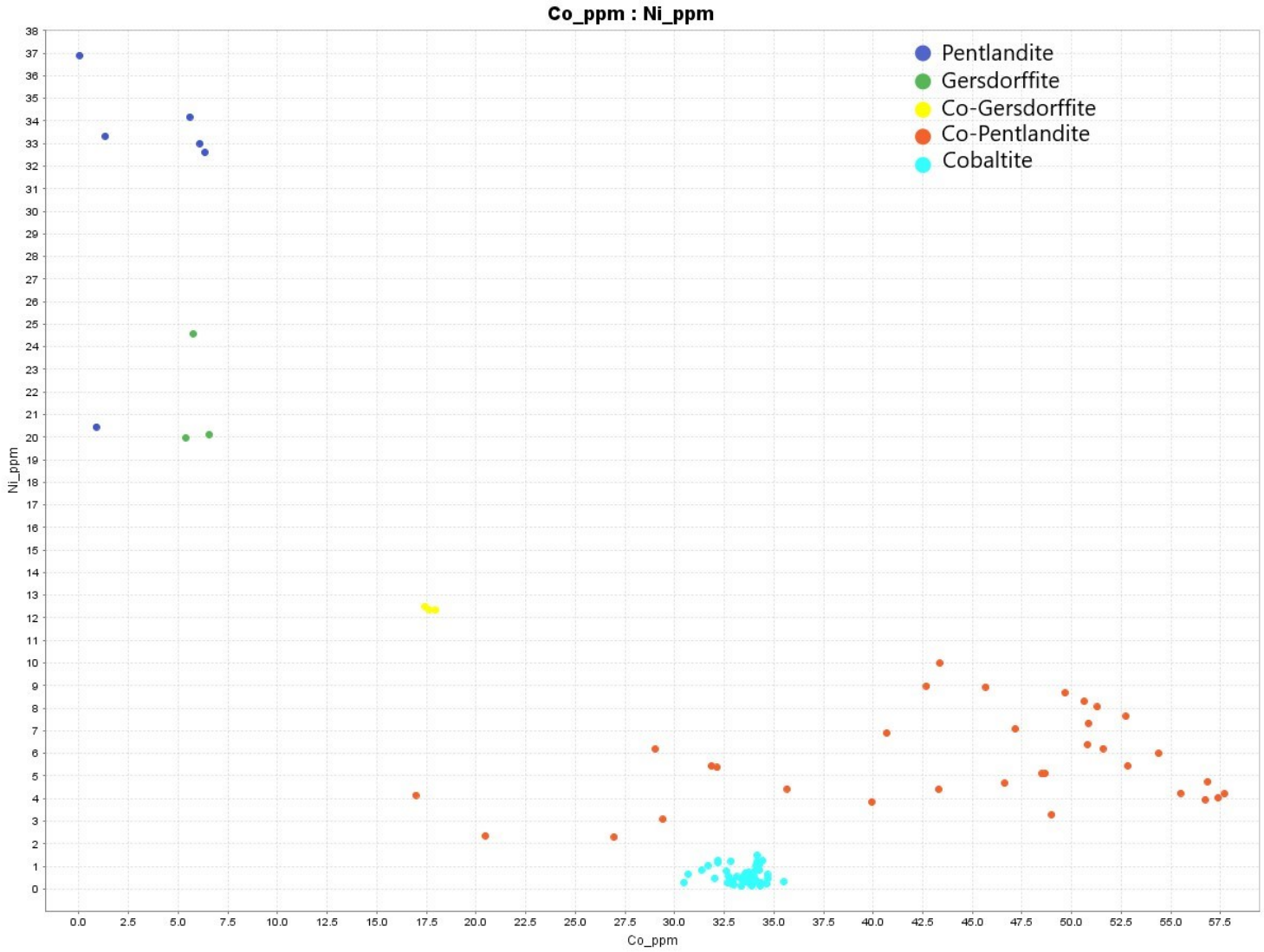


Figure 21. Co-Ni relations of the cobalt bearing minerals. Pyrite excluded.

A small cluster of gold grains (Fig. 22), from 1 to 5 µm in diameter, was found with EPMA from thin section PAL0093-274.05. The grains sit inside and on the sides of silicate minerals and around a grain of cobaltite.

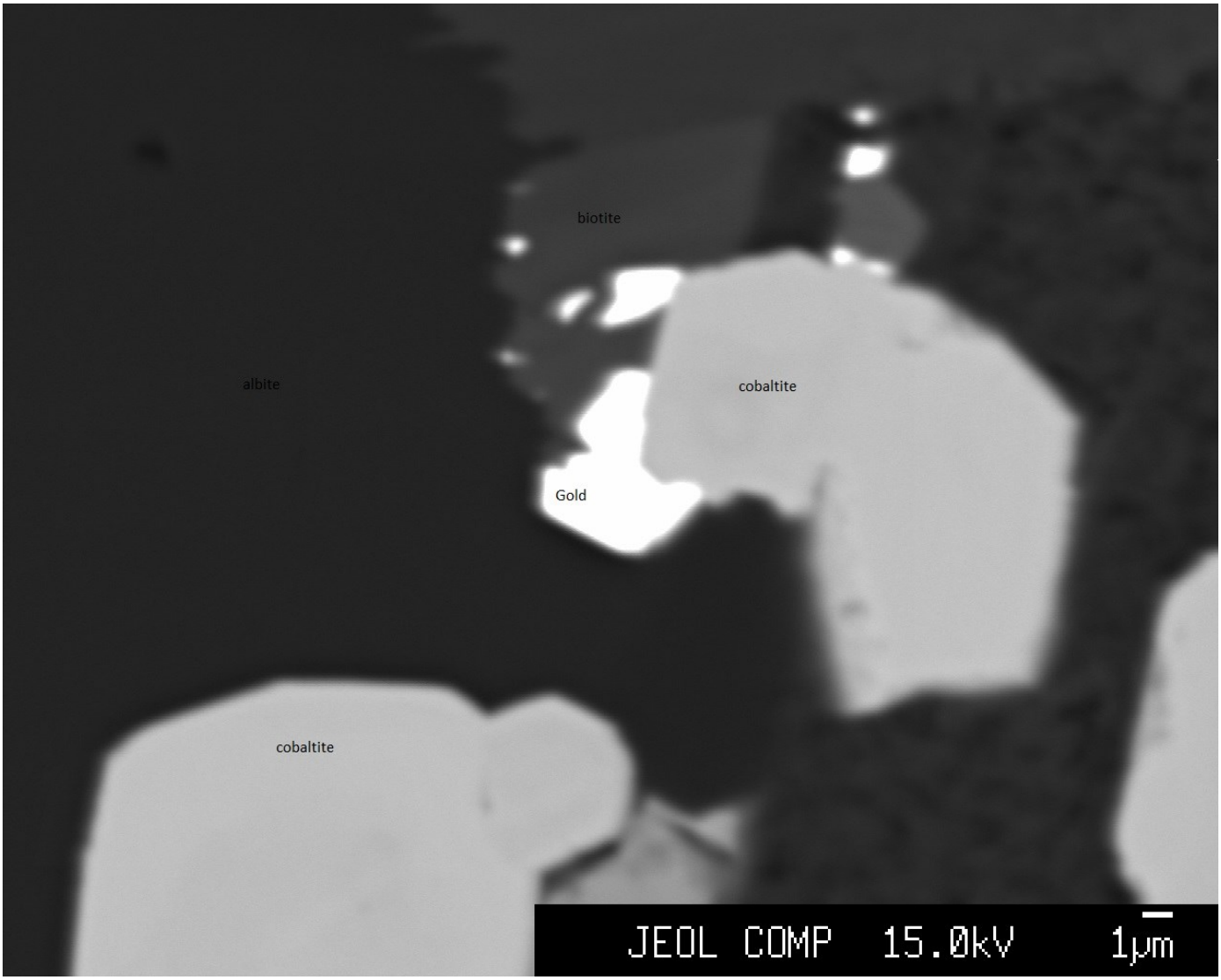


Figure 22. Backscattered electron microprobe image. Occurrence of gold next to cobaltite grains and silicates (Pal0093-274.05).

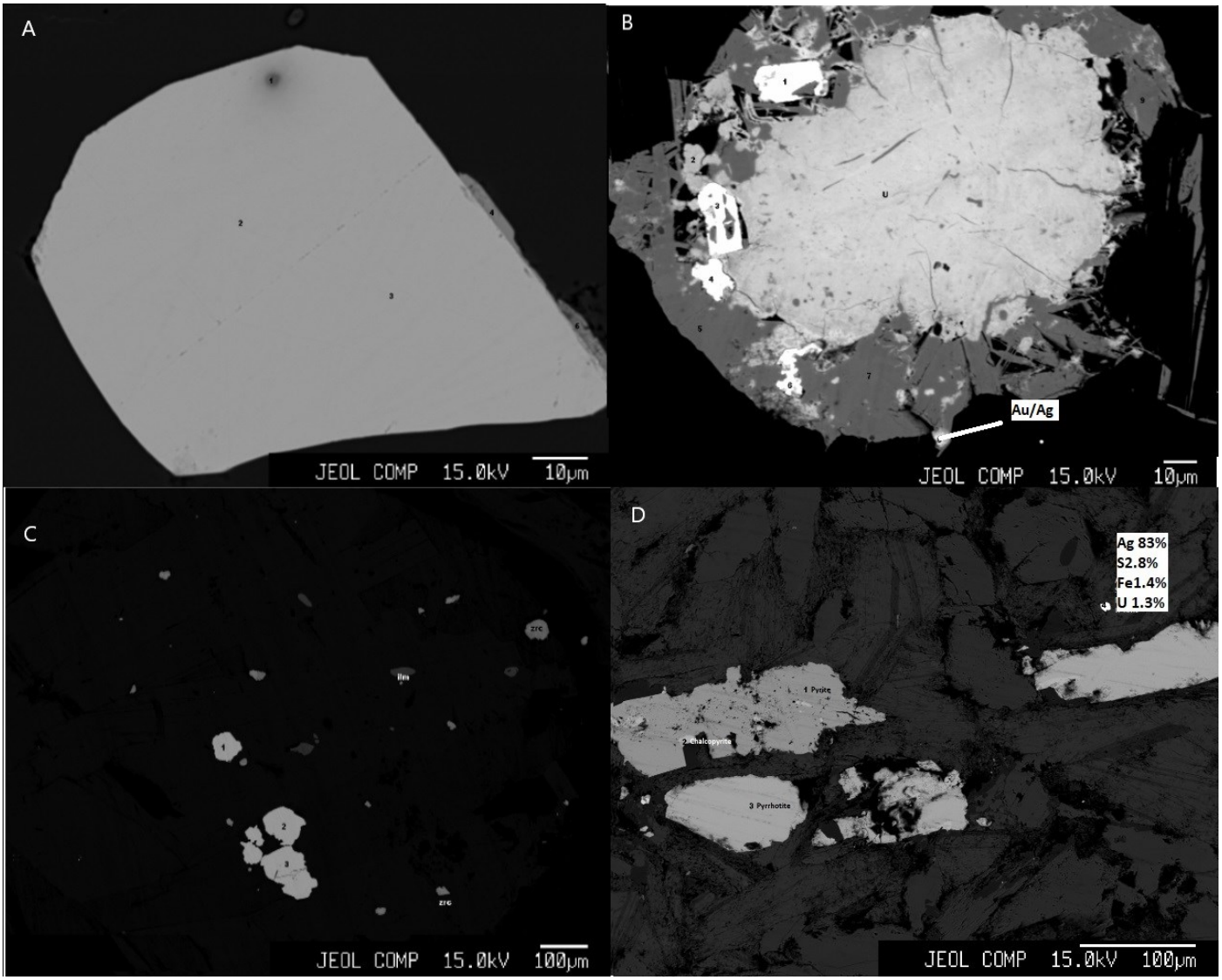


Figure 23. Backscattered electron microprobe images of oxide- and sulphide phases in Raja. A) Semi-idiomorphic gersdorffite grain (Pal0097-261.35) B) Uraninite grain with pyrite, galena and some mixed Ag and Au grain (Pal0097-333.45). C) Co-gersdorffite as semi-idiomorpic grains. (Pal0100-283.3) D) Silver grain with some S, Fe and U impurities (Pal0093-263.35).

One fairly large grain of gersdorffite was found from PAL0097-261.35 (Fig 23A) with contents presented in Table 2. Chemical composition of the cobaltoan gersdorffite (Fig. 23C) are presented in Table 3.

*Table 2. EPMA results for the 3 points in the gersdorffite grain in PAL0097-261.35*

| | As | Ni | S | Co | Fe | Te | Mo | Au | Total |
|---|---|---|---|---|---|---|---|---|---|
| Point1 | 28,96 | 19,97 | 13.02 | 5,38 | 6,07 | 0,10 | 0,14 | 0,00 | 73,69 |
| Point 2 | 46,14 | 24,57 | 16,74 | 5,75 | 8,09 | 0,10 | 0,22 | 0,01 | 101,66 |
| Point 3 | 50,23 | 20,13 | 18,13 | 6,56 | 9,35 | 0,07 | 0,15 | 0,05 | 104,78 |

*Table 3*. EPMA results for the 3 points of the cobaltoan-gersdorffite in PAL0100-283.3

| | As | Ni | S | Co | Fe | Te | Mo | Au | Total |
|---|---|---|---|---|---|---|---|---|---|
| Point 1 | 48,06 | 12,34 | 19,36 | 17,96 | 6,20 | 0,16 | 0,11 | 0,06 | 105,05 |

| | | | | | | | | | |
|---|---|---|---|---|---|---|---|---|---|
| Point 2 | 47,55 | 12,50 | 19,86 | 17,43 | 5,93 | 0,04 | 0,23 | 0,00 | 103,64 |
| Point 3 | 47,54 | 12,37 | 19,69 | 17,56 | 6,02 | 0,09 | 0,22 | 0,00 | 103,71 |

One uraninite grain, with galena and pyrite surrounding it, was found in PAL0097-333.45 (see Fig 23B). The total for the gold/silver grain was 11.68% so the measurement is not reliable. The grain was located at the side of a big uraninite grain surrounded by pyrite and galena and was very small. One silver grain was found, occurring as a single grain in PAL0093-263.35 (Fig 23D). EPMA analysis indicate 83% silver together with small amounts of sulphur, iron and uranium. The total for the analysis is 92.46%.

In addition to sulphides and oxides, few of the samples contained some Bi-Tellurides with high Pb content. They occur as very tiny, 1-2 µm, grains together with bigger sulphide grains (see Fig. 24).

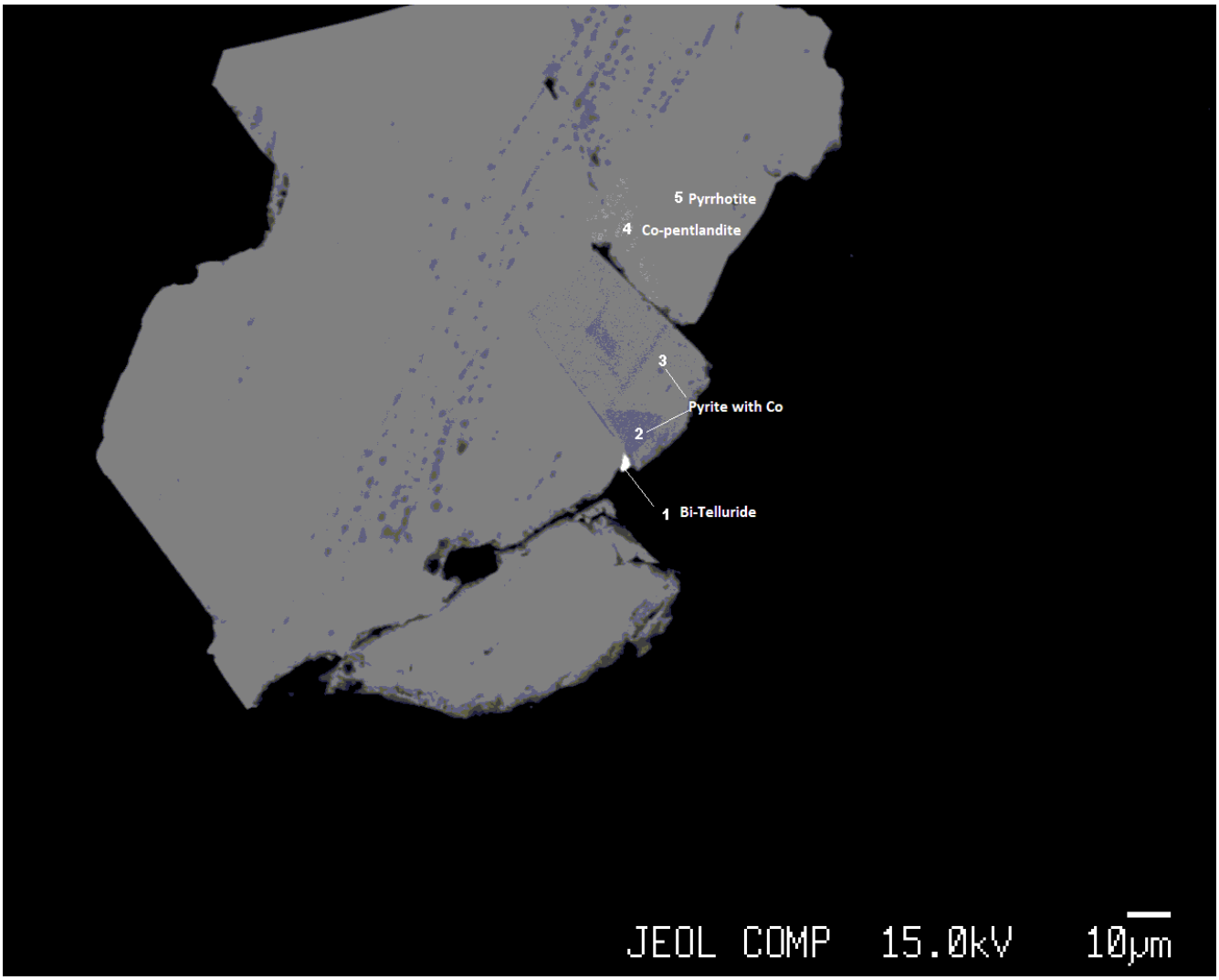


Figure 24. Bi-Telluride grain between pyrrhotite and co-bearing pyrite. Some Co-pentlandite flames in pyrrhotite. PAL0093-244.3.

# 8. Discussion

Systematic variations in and outside of ore deposits are called zonations. The variation can relate to mineral species and assemblages, distribution of major on trace elements or even textures of the ore deposit. Guilbert and Park (2007) explain that zoning can extend from regional scale to a scale of single ore shoot, barren zone, vein or veinlet. Zoning can be observed in almost all hydrothermal ore deposits. For example, in the typical settings of orogenic gold deposit, mineralogy changing from proximal to distal zones in centimetre to meters scale (e.g. Groves et al., 1998). The scale of this alteration depends on the wallrock and crustal depth, usually it is on a meter scale. Proximal alteration assemblages depend on the metamorphic grade, but typically in the greenschist to amphibolite facies, it includes Fe sulphide–carbonate–sericite ± albite. Dominant carbonates include ankerite, dolomite or calcite. Most common sulphides include pyrite, pyrrhotite arsenopyrite. Sericitisation is the typical form of alkali metasomatism and in some cases formation of fuchsite, biotite or K-feldspar, and albitisation. Mafic minerals are usually highly chloritised. Amphibole or diopside occurs at progressively deeper crustal levels at the cost of carbonate minerals. In greenschist facies, wall rock alteration is caused by addition of vast amounts of $CO_2$, S, K, $H_2O$, $SiO_2$ ± Na and LILE. (Groves et al., 2000).

In this study, zonation patterns related to some specific minerals was observed. Most notably is the composition of amphiboles within the mineralised intervals compared to the outside of it. In the mineralisation, amphiboles are almost solely Fe-Mg-Mn amphiboles. In contrast, outside of the mineralisation, Ca-amphiboles dominate. The amphibole distribution seems to suggest that the mineralised part is either leached of calcium or there are differences in the protolith composition. Similar changes from Ca-rich to Mg-Fe-Mn amphiboles has been described from the other mineralised areas within the Rajapalot, like the Palokas occurrence (e.g. Ranta et al., 2018). Micas show a clear increase in Al in the mineralised parts. The white micas associated with the mineralised parts contain a much higher aluminium grade, being mostly sericites. Higher Al content, together with the fact that the mineralised parts are also more Mg rich, has smaller grain size and show distinct layering of the micas, could be further evidence for a more clay rich protolith for the mineralised parts.

Gold occurrences appear to be related to the high aluminium white micas and depletion of Ca or more likely, Mg/Al-clay rich protolith. One gold grain was found inside an amphibole. Gold occurs as separate free gold, but there are some mixed grains with silver and uranium but the data on that is unreliable. Since there are no known minerals of Au-U, the likely cause of this result is a missed analysis and the uranium signal was from the surrounding uraninite. In any case the significance of those grains in term or an ore body is not too high since the supposed grains are extremely small and very scarce.

Overall, petrographic studies are mostly consistent with the observation from drill cores and with earlier studies (Farajewicz, 2018). The rocks in the main mineralisation are comprised mainly of fine-grained sedimentary rocks with early albitisation followed by weak to moderate chloritisation, sulphidation and sericitisation. The sulphides are mainly pyrrhotite and pyrite with traces of chalcopyrite, sphalerite, molybdenite, galena, cobaltite and pentlandite. Main oxides are ilmenite and rutile, generally occurring as sporadic grains as part of matrix. The upper part of mineralised zone (e.g. shown in PAL0093) is intensely sericitised but the amount of sericite varies. There are signs of at least two sulfidation events, based on the distribution of sulphides. Some of the early cobaltite for example occurs as sporadic, idiomorphic or semi-idiomorphic grains (Fig. 10c2) in the silicate matrix and most of the pyrrhotite, pyrite and chalcopyrite occur in veinlets or clumps. The latter representing the later sulfidation event that even recrystallised some quartz and albite since the grains right next to the sulphides are bigger. Co content of the cobalt pentlandite varies considerably, reflecting the fact that it is the Co-end member of solid solution of pentlandite. From cobalt bearing pentlandite to pure cobalt-pentlandite the amount of cobalt content varies considerably and when this kind of monosulphide solid solution crystallises, some variation is to be expected. Other sulphides included pyrrhotite with co-pentlandite lammelaes and cobaltite.

The cobaltoan-gersdorffite found from the very altered mafic sill (PAL0100-283.3) is a curious case. In their paper Béziat et al. (1996) discuss the sources of cobaltoan-gersdorffite in spessartite lamprophyres of Lacaune area in northern France. They conclude that the occurrence of cobaltite gersdorffite in basic rocks can be a result of either orthomagmatic segregation from lamprophyric magmas as well as secondary hydrothermal processes (Béziat et al. 1996). Now while it is improbable, that the cobaltite gersdorffite in Raja is derived straight from the magma and remained there under the conditions of amphibolite facies alteration, it is not impossible and it is curious that the only sample where the more cobalt-bearing gersdorffite was found was from an altered mafic. Based on information gathered for this study, one probable cause is that the mafic sill provided the nickel to interact with a Co-As-S bearing fluid and the cobalt bearing minerals formed as a result of secondary hydrothermal processes. A further study with, for example Mineral Liberation Analyzer (MLA), could be more effective in finding more cobaltoan-gersdorffite and set a more feasible basis for determining the source for it.

# 9. Acknowledgements

I am grateful to Mawson Oy and especially to Dr. Nick Cook for providing me this most interesting topic. The whole Mawson team has been most helpful and a special thanks to Dr. Erkki Vanhanen for assisting me with the thin sections and for the plentiful insights.

I would like to express my gratitude to Dr. Jukka-Pekka Ranta for supervising the work and all the help with presenting the results.

A special thanks also goes to my family for eventually steering me to geology and friends for keeping me on the path.

Finally, I would like to thank my beloved Essi for all the moral support.

# 10. References


Bailey S.W. 1984. Classification and structures of the micas. Crystal chemistry of the true micas. Rev. Mineral., 1984, 13, 1–60

Béziat, D., Monchoux, P., Tollon, F., 1996. Cobaltite-gersdorffite solid solution as a primary magmatic phase in spessartite, Lacaune area, Montagne Noire, France. The Canadian Mineralogist; 34 (3): 503–512

Cook, N., Hudson, M., 2018. Progress Report On The Geology, Mineralization And Exploration Activities On The Rompas-Rajapalot Gold - Cobalt Project, Peräpohja Belt. Lapland, Finland. Mawson Resources Ltd. (http://www.mawsonresources.com/projects/finland/ni43-101-technical-reports)

Corbett, G. J., Leach T. M., 1998. Southwest Pacific Rim Gold-Copper Systems: Structure, Alteration, and Mineralization. Littleton, CO: Society of Economic Geologists, 237.

Eilu, P., 2015. Overview on Gold Deposits in Finland. In: Maier, W. D. et al. (eds.), Mineral Deposits of Finland, Elsevier, 377-410

Farajewicz, M., 2018. Mineral relationships of cobaltite and cobalt pentlandite at Rajapalot, Finland, Master's thesis, University of Exeter, 91 p.

Goldfarb, R. J., Leach, D. L., Pickthorn, W. J., Paterson, C. J., 1988. Origin of lode-gold deposits of the Juneau gold belt, southeastern Alaska. Geology, 16 (5), 440–443

Groves, D.I., Goldfarb, R.J., Gebre-Mariam, M., Hagemann, S.G., Robert, F. 1998. Orogenic gold deposits: A proposed classification in the context of their crustal distribution and relationship to other gold deposit types, Ore Geology Reviews, Volume 13, Issues 1–5, 7-27

Groves, D. I., Goldfarb, R. J., Knox-Robinson, C. M., Ojala, J., Gardoll, S., Yun, G. Y., Holyland, P., 2000. Late-kinematic timing of orogenic gold deposits and significance for computer-based exploration techniques with emphasis on the Yilgarn Block, Western Australia, Ore Geology Reviews, Volume 17, Issues 1–2, 1-38

Groves D. I., Santosh, M., Goldfarb, R. J., Zhang, L., 2018. Structural geometry of orogenic gold deposits: Implications for exploration of world-class and giant deposits, Geoscience Frontiers, Volume 9, Issue 4, 1163-1177

Guilbert, J. M. & Park, C. F. 2007. The geology of ore deposits. Long Grove, IL: Waveland Press.

Hanski, E., Huhma, H., Perttunen, V., 2005. SIMS U-Pb, Sm-Nd isotope and geochemical study of an arkosite-amphibolite suite, Peräpohja Schist Belt: evidence for ca. 1.98 Ga A-type felsic magmatism in northern Finland. Bulletin of the Geological Society of Finland, Vol. 77, 5–2

Hanski, E., Huhma, H. and Vaasjoki, M., 2001a. Geochronology of northern Finland: a summary and discussion. Geological Survey of Finland, Special Paper 33, 255-279.

Hawthorne, F., Oberti, R., Harlow, G. E., Maresch, W. V., Martin, R. F., Schumacher, J. C., Welch, M. D., 2012. Nomenclature of the amphibole supergroup, IMA Report, American Mineralogist, Volume 97, 2031–2048.

Hedenquist, J. W., Aoki, M. (1991). Meteoric interaction with magmatic discharges in Japan and the significance for mineralization. Geology, 19(10)

Huhma, H., Cliff, R., Perttunen, V. and Sakko, M., 1990. Sm/Nd and Pb isotopic study of mafic rocks associated with early Proterozoic continental rifting: the Peräpohja schist belt in northern Finland. Contributions to Mineralogy and Petrology 104, 369-379.

Huttu, M., 2014. Geochemistry and petrography of magnesium-rich intrusive rocks in the Rompas-Rajapalot area, Peräpohja Belt, northern Finland, Master's thesis, Department of Geosciences, University of Oulu., 75.

Hölttä, P., Huhma, H., Lahtinen, R., Nironen, M., Perttunen,V., Vaasjoki, M., Väänänen, J., 2003. Introduction: Modelling of orogeny in northern Fennoscandia. Eklund, O., (ed.) Lapland–2003. Excursion guide to Finnish and Swedish Lapland 1–7.9.2003. Geocenter report nr 20. Turku University –Åbo Akademi University, 6–27.

Iljina, M., Hanski, E., 2005. Layered mafic intrusions of the Tornio–Näränkävaara belt. In: Lehtinen, M. et al. (eds.), Precambrian geology of Finland—Key to the Evolution of the Fennoscandian Shield, Elsevier, Amsterdam, 101-138

Karhu , J. A. 1993. Paleoproterozoic evolution of the carbon isotope ratios of sedimentary carbonates in the Fennoscandian Shield. Geological Survey of Finland, Bulletin 371.

Karhu, J., Kortelainen. N., Huhma, H., Perttunen, V. and Sergeev, S., 2007. New time constraints for the end of the Paleoproteroozoic carbon isotope excursion. 7th International Symposium on Applied Isotope Geochemistry, Steelenbosch, South Africa, 10th–14th September, 2007, Abstracts,76-77.

Kyläkoski, M., 2007. PGE Geochemistry of the Jouttiaapa Formation representing a Palaeoproterozoic Continental Flood Basalt sequence, Peräpohja Belt, Northwestern Finland.

Kyläkoski, M., Hanski E., Huhma H., 2012. The Petäjäskoski Formation, a new lithostratigraphic unit in the Paleoproterozoic Peräpohja Belt, northern Finland. Bulletin of the Geological Society of Finland, Vol. 84, 2012, 85–12

Laajoki, K., 2005. Karelian supracrustal rocks. In: Lehtinen, M. et al. (Eds.), Precambrian Geology of Finland – Key to the Evolution of the Fennoscandian Shield. Elsevier B.V., Amsterdam, 279–342.

Lahtinen, R., Sayab, M., Karell, F., 2015a Near-orthogonal deformation successions in the poly-deformed Paleoproterozoic Martimo belt: Implications for the tectonic evolution of Northern Fennoscandia. Precambrian Res. 270, 22–38

Lahtinen, R., Huhma, H., Lahaye, Y., Jonsson, E., Manninen, T., Lauri, L., Bergman, S.,Hellström, F., Niiranen, T., Nironen, M., 2015b. New geochronological and Sm–Ndconstraints across the Pajala shear zone of northern Fennoscandia: reactivation of a Paleoproterozoic suture. Precambrian Res. 256, 102–119.

Leake, B.E., Woolley, A.R., Arps, C.E.S., Birch, W.D., Gilbert, M.C., Grice, J.D., Hawthorne, F.C., Kato, A., Kisch, H.J., Krivovichev, V.G., Linthout, K., Laird, J., Mandarino, J.A., Maresch, W.V., Nickel, E.H., Rock, N.M.S., Schumacher, J.C., Smith, D.C., Stephenson, N.C.N., Ungaretti, L., Whittaker, E.J.W., and Guo, Y. (1997) Nomenclature of amphiboles: Report of the subcommittee on amphiboles of the International Mineralogical Association, Commission on New Minerals and Mineral Names. Canadian Mineralogist, 35, 219–246

Loucks, R. R., Mavrogenes, J. A., (1999). Gold solubility in supercritical hydrothermal brines measured in synthetic fluid inclusions. *Science (New York, N.Y.), 284*(5423), 2159

Luukas, J., Kousa, J., Nironen, M. & Vuollo, J. 2017. Major stratigraphic units in the bedrock of Finland, and an approach to tectonostratigraphic division. In: Nironen, M. (ed.) Bedrock of Finland at the scale 1:1 000 000 - Major stratigraphic units, metamorphism and tectonic evolution. Geological Survey of Finland, Special Paper 60, 9−40.

Meyer, C. & Hemley J.J., 1967. Wall Rock Alteration. In Geochemistry of Hydrothermal Ore Deposits. 3rd edition. New York: Wiley, 166-235

Molnár, F., Oduro, H., Cook, N.D.J., Pohjolainen, E., Takacs, A., O´Brien, H., Pakkanen, L., Johanson, B. & Wirth, R., 2016. Association of gold with uraninite and pyrobitumen in the metavolcanic rock hosted hydrothermal Au-U mineralization at Rompas, Peräpohja Schist Belt, northern Finland. Mineralium Deposita 51, 681–702.

Molnár, F., O'Brien, H., Stein, H., Cook, N.D.J. (2017). Geochronology of hydrothermal processes leading to the formation of the Au-U mineralization at the Rompas prospect, Peräpohja belt, northern Finland: Application of paired U-Pb dating of uraninite and Re-Os dating of molybdenite to the identification of multiple hydrothermal events in a metamorphic terrane. *Minerals*, 7 (9), art. no. 171.Nekrasov, I. Ya. 1996. Geochemistry, Mineralogy and Genesis of Gold Deposits. A. A. Balkema, Rotterdam, Brookfield. xiv + 329.

Perttunen, V. 1989. Summary: Volcanic rocks in the Peräpohja are, northern Finland. A report of the Lapland Volcanite Project. Report of Investigation 92, Geological Survey of Finland. 42.

Perttunen, V., Hanski, E., Väänänen, J., Eilu, P., Lappalainen, M., 1996. Rovaniemen kartta-alueen kalliopera. Summarv: Pre-Quaternary rocks of the Rovaniemi map-sheet area. Sheet 3612. Geological map of Finland 1:100 000. Geological Survey of Finland, Espoo. 1-63.

Perttunen, V. and Hanski, E., 2003. Törmäsjärven ja Koivun kartta-alueiden kallioperä. Summary: Pre-Quaternary rock of the Törmäsjärvi and Koivu map-sheet areas. Geological Map of Finland 1: 100 000. Explanation to the Maps of Pre-Quaternary Rocks 2631 and 2633. Geological Survey of Finland, 88.

Perttunen, V. and Vaasjoki, M., 2001. U-Pb geochronology of the Peräpohja Schist Belt, northwestern Finland. Geological Survey of Finland, Special Paper 33, 45-84.

Powell, R., 1978. Equilibrium Thermodynamics in Petrology. 294.

Ranta, J.P., Lauri, L.S., Hanski, E., Huhma, H., Lahaye, Y.& Vanhanen, E., 2015. U-Pb and Sm-Nd isotopic constraints on the evolution of the Paleoproterozoic Peräpohja Belt, northern Finland. Precambrian Research 266, 246–259.

Ranta, J.P., Hanski, E., Cook, N. & Lahaye, Y., 2017. Source of boron in the Palokas gold deposit, northern Finland: Evidence from boron isotopes and major element composition of tourmaline. Mineralium Deposita 52,733–746.

Ranta, J.P., Molnár, F., Hanski, E, Cook, N., 2018. Epigenetic gold occurrence in Paleoproterozoic meta-evaporitic sequence in the Rompas-Rajapalot Au system, Peräpohja belt, northern Finland. Bulletin of the Geological Society of Finland, Vol. 90, 69–108

Reed, M, H. 1997. Hydrothermal Alteration and its Relationship to Ore Fluid Composition. In Geochemistry of Hydrothermal Ore Deposits. 3rd edition. New York: Wiley, 303-365

Robb, L., 2005. Introduction to Ore-forming Processes. Blackwell Publishing, Malden, 373.

Stefánsson A, Seward T.M. 2004. Gold(I) complexing in aqueous sulphide solutions to 500°C at 500 bar. Geochimica et Cosmochimica Acta 68: 4121-4143Vlassopoulos, D., Wood, S. A., 1990. Gold speciation in natural waters: I. Solubility and hydrolysis reactions of gold in aqueous solution, Geochimica et Cosmochimica Acta, Volume 54, Issue 1, 3-12.

Tainio, J., 2014. Rovaniemen kunnassa sijaitsevien Vaunttauksen, Lehmikarin ja Äijävaaran appiniitti-intruusioiden petrografinen ja geokemian tutkimus. Master's thesis, Department of Geosciences and Geography, University of Helsinki, 93.

Vanhanen, E., Cook, N.D.J., Hudson, M.R., Dahlenborg, L., Ranta, J.-P., Havela, T., Kinnunen, J., Molnár,F., Prave,A.R., Oliver, N.H.S., 2015. Chapter 5.4 - The Rompas Prospect, Peräpohja Schist Belt, Northern Finland. In: Maier, W. D. et al. (eds.), Mineral Deposits of Finland, Elsevier, 467-484.

Williams-Jones, A., Bowell, Rob., Migdisov, A. 2009. Gold in Solution. Elements. 5. 281-287.

Zhu, Y., An, F., Tan, J., 2011. Geochemistry of hydrothermal gold deposits: A review, Geoscience Frontiers, Volume 2, Issue 3, 367-374

# Appendix 1. EPMA results for sulphides

| No. | S | Fe | Se | U | V | Au | As | Co | Pb | Mo | Ni | Ag | Cu | Sb | Zn | Bi | Te | Ti | Total | Name |
|---|---|---|---|---|---|---|---|---|---|---|---|---|---|---|---|---|---|---|---|---|
| pal0092-222.95.alue2-1 | 52.844 | 42.743 | 0.225 | 0.195 | 0.059 | 0.120 | 0.000 | 4.450 | 0.411 | 0.621 | 0.287 | 0.078 | 0.281 | 0.000 | 0.381 | 0.416 | 0.146 | 0.109 | 103,366 | pyrite |
| pal0092-222.95.alue2-2 | 38.596 | 59.222 | 0.226 | 0.225 | 0.111 | 0.182 | 0.000 | 0.520 | 0.311 | 0.483 | 0.292 | 0.117 | 0.322 | 0.000 | 0.413 | 0.406 | 0.199 | 0.116 | 101,741 | pyrrhotite |
| pal0092-222.95.alue2-3 | 38.977 | 58.554 | 0.228 | 0.251 | 0.093 | 0.126 | 0.000 | 0.569 | 0.360 | 0.563 | 0.278 | 0.102 | 0.323 | 0.000 | 0.335 | 0.396 | 0.194 | 0.105 | 101,454 | pyrrhotite |
| pal0092-222.95.alue3-1 | 33.866 | 30.392 | 0.133 | 0.106 | 0.066 | 0.129 | 0.000 | 0.182 | 0.251 | 0.425 | 0.258 | 0.099 | 33.468 | 0.000 | 0.442 | 0.283 | 0.055 | 0.043 | 100,198 | chalcopyrit |
| pal0092-222.95.alue3-2 | 38.558 | 59.380 | 0.152 | 0.166 | 0.053 | 0.079 | 0.000 | 0.520 | 0.312 | 0.523 | 0.206 | 0.071 | 0.256 | 0.000 | 0.364 | 0.332 | 0.070 | 0.000 | 101,042 | pyrrhotite |
| pal0092-222.95.alue3-3 | 38.114 | 56.761 | 0.000 | 0.119 | 0.004 | 0.022 | 0.000 | 1.808 | 0.000 | 0.250 | 0.259 | 0.029 | 0.000 | 0.019 | 0.016 | 0.000 | 0.000 | 0.002 | 97,403 | pyrrhotite |
| pal0092-222.95.alue3-5 | 38.946 | 58.814 | 0.000 | 0.000 | 0.000 | 0.011 | 0.000 | 0.397 | 0.000 | 0.466 | 0.095 | 0.017 | 0.000 | 0.000 | 0.004 | 0.000 | 0.031 | 0.000 | 98,781 | pyrrhotite |
| pal0092-222.95.alue4-1 | 40.063 | 58.612 | 0.000 | 0.000 | 0.000 | 0.000 | 0.000 | 0.290 | 0.000 | 0.459 | 0.080 | 0.000 | 0.012 | 0.025 | 0.086 | 0.000 | 0.000 | 0.013 | 99,64 | pyrrhotite |
| pal0092-222.95.alue4-2 | 38.749 | 59.490 | 0.035 | 0.060 | 0.004 | 0.000 | 0.016 | 0.316 | 0.000 | 0.437 | 0.074 | 0.017 | 0.010 | 0.030 | 0.000 | 0.000 | 0.000 | 0.101 | 99,339 | pyrrhotite |
| pal0092-226.85-alue1-1 | 38.584 | 59.527 | 0.136 | 0.085 | 0.014 | 0.083 | 0.000 | 0.428 | 0.242 | 0.586 | 0.130 | 0.055 | 0.184 | 0.074 | 0.262 | 0.277 | 0.070 | 0.000 | 100,737 | pyrrhotite |
| pal0092-226.85-alue2-1 | 2.212 | 3.385 | 0.371 | 0.710 | 0.169 | 1.217 | 0.000 | 0.367 | 0.579 | 0.041 | 0.457 | 1.517 | 2.539 | 0.234 | 0.748 | 0.526 | 0.328 | 0.222 | 15,622 | missed |
| pal0092-226.85-alue2-2 | 39.082 | 58.722 | 0.188 | 0.094 | 0.074 | 0.194 | 0.000 | 0.385 | 0.291 | 0.433 | 0.333 | 0.059 | 0.349 | 0.128 | 0.422 | 0.337 | 0.170 | 0.106 | 101,367 | pyrrhotite |
| pal0092-226.85-alue2-3 | 34.959 | 29.828 | 0.268 | 0.153 | 0.094 | 0.217 | 0.000 | 0.227 | 0.309 | 0.543 | 0.336 | 0.084 | 34.237 | 0.162 | 0.554 | 0.356 | 0.233 | 0.106 | 102,666 | chalcopyrit |
| pal0092-226.85-alue2-4 | 39.450 | 58.538 | 0.056 | 0.077 | 0.023 | 0.048 | 0.000 | 0.313 | 0.000 | 0.494 | 0.077 | 0.010 | 0.005 | 0.008 | 0.062 | 0.000 | 0.000 | 0.006 | 99,167 | pyrrhotite |
| pal0092-226.85-alue2-5 | 39.222 | 59.371 | 0.081 | 0.098 | 0.020 | 0.000 | 0.019 | 0.360 | 0.000 | 0.409 | 0.059 | 0.000 | 0.000 | 0.000 | 0.074 | 0.016 | 0.000 | 0.016 | 99,745 | pyrrhotite |
| pal0092-226.85-alue3-1 | 39.607 | 59.074 | 0.035 | 0.090 | 0.008 | 0.000 | 0.046 | 0.271 | 0.000 | 0.511 | 0.083 | 0.008 | 0.000 | 0.000 | 0.008 | 0.046 | 0.005 | 0.000 | 99,792 | pyrrhotite |
| pal0092-226.85-alue3-4 | 38.323 | 57.543 | 0.000 | 0.026 | 0.000 | 0.078 | 0.052 | 0.340 | 0.000 | 0.489 | 0.026 | 0.024 | 0.000 | 0.000 | 0.033 | 0.017 | 0.036 | 0.000 | 96,987 | pyrrhotite |
| PAL0092-306.90-alue1-1 | 11.795 | 0.062 | 0.000 | 0.005 | 0.000 | 0.023 | 0.063 | 0.000 | 0.000 | 0.099 | 0.000 | 0.000 | 0.000 | 0.000 | 0.000 | 0.187 | 0.000 | 0.734 | 12,968 | missed |
| PAL0092-306.90-alue1-2 | 12.230 | 0.076 | 0.000 | 0.138 | 0.000 | 0.000 | 0.000 | 0.000 | 0.000 | 0.166 | 0.000 | 0.013 | 0.000 | 0.044 | 0.000 | 0.172 | 0.000 | 0.727 | 13,566 | missed |
| PAL0092-306.90-alue1-3 | 27.234 | 57.154 | 0.000 | 0.071 | 0.000 | 0.000 | 0.000 | 0.000 | 0.000 | 0.458 | 0.000 | 0.000 | 0.000 | 0.000 | 0.000 | 0.078 | 0.000 | 0.000 | 84,995 | pyrrhotite |
| PAL0092-306.90-alue1-4 | 28.361 | 58.214 | 0.000 | 0.004 | 0.000 | 0.000 | 0.000 | 0.000 | 0.000 | 0.515 | 0.229 | 0.000 | 0.000 | 0.000 | 0.000 | 0.073 | 0.000 | 0.000 | 87,396 | pyrrhotite |
| PAL0092-306.90-alue1-5 | 27.984 | 58.173 | 0.000 | 0.000 | 0.000 | 0.000 | 0.000 | 0.000 | 0.000 | 0.418 | 0.096 | 0.000 | 0.000 | 0.000 | 0.000 | 0.067 | 0.000 | 0.000 | 86,738 | pyrrhotite |
| PAL0092-306.90-alue1-6 | 12.165 | 0.164 | 0.000 | 0.000 | 0.000 | 0.022 | 0.047 | 0.039 | 0.000 | 0.063 | 0.010 | 0.057 | 0.165 | 0.000 | 0.814 | 0.169 | 0.000 | 0.823 | 14,538 | missed |
| PAL0092-306.90-alue1-7 | 25.790 | 28.352 | 0.000 | 0.000 | 0.000 | 0.000 | 0.000 | 0.000 | 0.000 | 0.545 | 0.000 | 0.000 | 32.517 | 0.000 | 0.332 | 0.011 | 0.000 | 0.000 | 87,547 | chalcopyrit |
| PAL0092-306.90-alue1-8 | 23.130 | 4.978 | 0.000 | 0.000 | 0.000 | 0.000 | 0.000 | 0.000 | 0.000 | 0.504 | 0.000 | 0.000 | 0.000 | 0.000 | 58.015 | 0.018 | 0.000 | 0.000 | 86,645 | sphalerite |
| PAL0092-306.90-alue1-9 | 34.056 | 28.481 | 0.048 | 0.038 | 0.024 | 0.005 | 0.065 | 0.050 | 0.000 | 0.379 | 0.000 | 0.026 | 32.670 | 0.012 | 2.704 | 0.024 | 0.011 | 0.000 | 98,593 | chalcopyrit |
| PAL0092-306.90-alue1-10 | 25.712 | 29.728 | 0.014 | 0.000 | 0.000 | 0.000 | 0.000 | 0.000 | 0.000 | 0.557 | 0.000 | 0.000 | 32.607 | 0.000 | 0.000 | 0.014 | 0.000 | 0.000 | 88,632 | chalcopyrit |
| PAL0092-306.90-alue2-1 | 33.314 | 3.488 | 0.000 | 0.000 | 0.010 | 0.000 | 0.000 | 0.034 | 0.000 | 0.331 | 0.000 | 0.027 | 0.037 | 0.032 | 63.252 | 0.000 | 0.011 | 0.000 | 100,536 | sphalerite |
| PAL0092-306.90-alue2-2 | 35.332 | 30.243 | 0.022 | 0.000 | 0.017 | 0.027 | 0.000 | 0.000 | 0.000 | 0.336 | 0.000 | 0.017 | 33.823 | 0.000 | 0.132 | 0.017 | 0.000 | 0.000 | 99,966 | chalcopyrit |
| PAL0092-306.90-alue2-3 | 33.549 | 6.047 | 0.000 | 0.000 | 0.000 | 0.000 | 0.000 | 0.000 | 0.000 | 0.317 | 0.021 | 0.002 | 0.094 | 0.019 | 60.385 | 0.000 | 0.000 | 0.000 | 100,434 | sphalerite |
| PAL0092-306.90-alue2-4 | 38.712 | 58.805 | 0.011 | 0.000 | 0.000 | 0.000 | 0.000 | 0.007 | 0.000 | 0.335 | 0.353 | 0.000 | 0.000 | 0.000 | 0.000 | 0.036 | 0.000 | 0.000 | 98,259 | pyrrhotite |
| PAL0092-306.90-alue2-5 | 33.521 | 6.001 | 0.000 | 0.000 | 0.010 | 0.000 | 0.000 | 0.000 | 0.000 | 0.267 | 0.025 | 0.036 | 0.052 | 0.000 | 59.709 | 0.000 | 0.013 | 0.000 | 99,634 | sphalerite |
| PAL0092-306.90-alue2-6 | 38.037 | 58.479 | 0.000 | 0.000 | 0.052 | 0.019 | 0.018 | 0.130 | 0.000 | 0.466 | 0.379 | 0.000 | 0.021 | 0.036 | 0.000 | 0.000 | 0.000 | 0.000 | 97,637 | pyrrhotite |
| PAL0092-306.90-alue2-7 | 32.687 | 5.740 | 0.000 | 0.000 | 0.014 | 0.000 | 0.000 | 0.028 | 0.000 | 0.423 | 0.084 | 0.000 | 0.135 | 0.068 | 58.849 | 0.001 | 0.061 | 0.028 | 98,118 | sphalerite |
| PAL0092-306.90-alue2-8 | 33.078 | 5.396 | 0.063 | 0.022 | 0.008 | 0.000 | 0.000 | 0.058 | 0.000 | 0.448 | 0.055 | 0.000 | 0.094 | 0.063 | 60.049 | 0.000 | 0.075 | 0.021 | 99,43 | sphalerite |
| PAL0092-306.90-alue2-9 | 38.076 | 58.208 | 0.030 | 0.000 | 0.026 | 0.045 | 0.076 | 0.088 | 0.000 | 0.472 | 0.372 | 0.000 | 0.000 | 0.032 | 0.000 | 0.000 | 0.017 | 0.000 | 97,442 | pyrrhotite |
| PAL0092-306.90-alue3-1 | 38.058 | 58.547 | 0.011 | 0.000 | 0.010 | 0.034 | 0.000 | 0.111 | 0.000 | 0.421 | 0.357 | 0.003 | 0.033 | 0.035 | 0.000 | 0.043 | 0.018 | 0.000 | 97,681 | pyrrhotite |
| PAL0092-306.90-alue3-2 | 12.235 | 0.128 | 0.000 | 0.000 | 0.000 | 0.043 | 0.048 | 0.005 | 0.000 | 0.021 | 0.000 | 0.000 | 0.000 | 0.000 | 0.073 | 0.207 | 0.000 | 0.809 | 13,569 | missed |
| PAL0092-306.90-alue3-3 | 33.200 | 5.205 | 0.000 | 0.000 | 0.010 | 0.000 | 0.119 | 0.025 | 0.000 | 0.467 | 0.000 | 0.002 | 0.007 | 0.000 | 61.081 | 0.000 | 0.000 | 0.000 | 100,116 | sphalerite |
| PAL0092-306.90-alue3-4 | 33.648 | 5.798 | 0.000 | 0.000 | 0.000 | 0.000 | 0.000 | 0.021 | 0.000 | 0.472 | 0.003 | 0.000 | 0.083 | 0.000 | 58.933 | 0.000 | 0.020 | 0.000 | 98,978 | sphalerite |
| PAL0092-306.90-alue3-5 | 34.220 | 29.296 | 0.000 | 0.021 | 0.000 | 0.000 | 0.028 | 0.000 | 0.000 | 0.349 | 0.000 | 0.000 | 33.673 | 0.000 | 0.434 | 0.000 | 0.000 | 0.000 | 98,021 | chalcopyrit |
| PAL0092-306.90-alue3-6 | 33.275 | 5.203 | 0.000 | 0.000 | 0.009 | 0.000 | 0.072 | 0.052 | 0.000 | 0.344 | 0.000 | 0.000 | 0.173 | 0.016 | 60.827 | 0.000 | 0.012 | 0.000 | 99,983 | sphalerite |
| PAL0092-306.90-alue3-7 | 34.450 | 30.102 | 0.060 | 0.064 | 0.011 | 0.061 | 0.019 | 0.055 | 0.000 | 0.384 | 0.029 | 0.000 | 33.598 | 0.000 | 0.252 | 0.000 | 0.006 | 0.000 | 99,091 | chalcopyrit |
| PAL0092-306.90-alue3-8 | 38.465 | 59.320 | 0.076 | 0.089 | 0.000 | 0.000 | 0.082 | 0.070 | 0.000 | 0.398 | 0.472 | 0.000 | 0.000 | 0.023 | 0.004 | 0.000 | 0.000 | 0.000 | 98,999 | pyrrhotite |
| PAL0083-40.85-ALUE1-1 | 39.442 | 59.122 | 0.011 | 0.026 | 0.000 | 0.030 | 0.000 | 0.230 | 0.000 | 0.375 | 0.041 | 0.009 | 0.000 | 0.000 | 0.000 | 0.000 | 0.000 | 0.000 | 99,286 | pyrrhotite |
| PAL0083-40.85-ALUE1-2 | 53.477 | 43.178 | 0.036 | 0.000 | 0.000 | 0.018 | 0.000 | 3.390 | 0.000 | 0.541 | 0.000 | 0.000 | 0.000 | 0.000 | 0.000 | 0.060 | 0.000 | 0.000 | 100,7 | pyrite |
| PAL0083-40.85-ALUE1-3 | 39.104 | 58.321 | 0.030 | 0.043 | 0.000 | 0.086 | 0.000 | 0.248 | 0.000 | 0.420 | 0.029 | 0.000 | 0.000 | 0.000 | 0.000 | 0.000 | 0.007 | 0.000 | 98,288 | pyrrhotite |
| PAL0083-40.85-ALUE1-4 | 53.567 | 44.283 | 0.004 | 0.124 | 0.000 | 0.000 | 0.000 | 2.948 | 0.000 | 0.603 | 0.007 | 0.000 | 0.000 | 0.008 | 0.012 | 0.022 | 0.000 | 0.010 | 101,588 | pyrite |
| PAL0083-40.85-ALUE1-5 | 34.033 | 30.263 | 0.000 | 0.051 | 0.002 | 0.000 | 0.002 | 0.161 | 0.000 | 0.342 | 0.035 | 0.008 | 33.191 | 0.036 | 0.272 | 0.000 | 0.052 | 0.018 | 98,466 | chalcopyrit |
| PAL0083-40.85-ALUE1-6 | 37.681 | 30.874 | 0.498 | 0.185 | 0.054 | 0.000 | 0.015 | 1.588 | 0.000 | 0.345 | 0.214 | 0.136 | 0.182 | 0.285 | 0.287 | 15.316 | 8.558 | 0.066 | 96,284 | Bi-Te |
| PAL0083-40.85-ALUE2-2 | 39.201 | 59.090 | 0.081 | 0.047 | 0.016 | 0.000 | 0.022 | 0.258 | 0.000 | 0.426 | 0.045 | 0.007 | 0.000 | 0.000 | 0.078 | 0.000 | 0.022 | 0.002 | 99,295 | pyrrhotite |
| PAL0083-40.85-ALUE2-3 | 52.727 | 46.692 | 0.000 | 0.000 | 0.000 | 0.000 | 0.000 | 0.129 | 0.000 | 0.558 | 0.076 | 0.005 | 0.012 | 0.000 | 0.021 | 0.109 | 0.003 | 0.004 | 100,336 | pyrite |
| PAL0083-40.85-ALUE2-4 | 39.591 | 59.240 | 0.000 | 0.077 | 0.012 | 0.000 | 0.000 | 0.229 | 0.000 | 0.494 | 0.045 | 0.021 | 0.016 | 0.067 | 0.095 | 0.051 | 0.031 | 0.018 | 99,987 | pyrrhotite |
| PAL0083-40.85-ALUE2-5 | 38.059 | 58.218 | 0.000 | 0.009 | 0.000 | 0.000 | 0.000 | 0.229 | 0.000 | 0.363 | 0.024 | 0.022 | 0.000 | 0.031 | 0.131 | 0.000 | 0.025 | 0.024 | 97,135 | pyrrhotite |
| PAL0083-40.85-ALUE3-1 | 53.425 | 46.866 | 0.000 | 0.053 | 0.000 | 0.000 | 0.020 | 0.197 | 0.000 | 0.591 | 0.089 | 0.008 | 0.000 | 0.014 | 0.067 | 0.003 | 0.000 | 0.000 | 101,333 | pyrite |
| PAL0083-40.85-ALUE3-2 | 39.343 | 60.134 | 0.103 | 0.000 | 0.018 | 0.017 | 0.000 | 0.273 | 0.000 | 0.540 | 0.019 | 0.000 | 0.000 | 0.000 | 0.205 | 0.000 | 0.000 | 0.000 | 100,652 | pyrrhotite |
| PAL0083-40.85-ALUE3-3 | 27.695 | 53.586 | 0.076 | 0.000 | 0.002 | 0.098 | 0.053 | 0.221 | 0.000 | 0.240 | 0.000 | 0.000 | 0.000 | 0.020 | 0.049 | 0.000 | 0.025 | 0.003 | 82,068 | pyrrhotite |
| PAL0083-40.85-ALUE3-4 | 53.448 | 46.663 | 0.022 | 0.000 | 0.013 | 0.080 | 0.000 | 0.005 | 0.000 | 0.547 | 0.000 | 0.000 | 0.000 | 0.000 | 0.113 | 0.007 | 0.000 | 0.000 | 100,898 | pyrite |
| PAL0083-40.85-ALUE3-5 | 39.067 | 58.243 | 0.000 | 0.000 | 0.006 | 0.134 | 0.000 | 0.235 | 0.000 | 0.494 | 0.000 | 0.007 | 0.025 | 0.000 | 0.148 | 0.000 | 0.000 | 0.000 | 98,359 | pyrrhotite |
| PAL0083-40.85-ALUE4-1 | 52.702 | 42.738 | 0.022 | 0.000 | 0.026 | 0.058 | 0.000 | 3.420 | 0.000 | 0.469 | 0.000 | 0.000 | 0.000 | 0.000 | 0.037 | 0.000 | 0.000 | 0.000 | 99,472 | pyrite |
| PAL0083-40.85-ALUE4-2 | 39.048 | 58.612 | 0.000 | 0.124 | 0.000 | 0.048 | 0.002 | 0.272 | 0.000 | 0.454 | 0.069 | 0.028 | 0.000 | 0.024 | 0.058 | 0.000 | 0.000 | 0.012 | 98,751 | pyrrhotite |
| PAL0083-40.85-ALUE4-3 | 38.399 | 58.349 | 0.021 | 0.047 | 0.000 | 0.004 | 0.000 | 0.344 | 0.000 | 0.500 | 0.008 | 0.024 | 0.002 | 0.004 | 0.000 | 0.000 | 0.000 | 0.000 | 97,702 | pyrrhotite |
| PAL0083-40.85-ALUE4-4 | 53.256 | 47.348 | 0.046 | 0.040 | 0.000 | 0.004 | 0.053 | 0.069 | 0.000 | 0.675 | 0.000 | 0.029 | 0.000 | 0.000 | 0.000 | 0.026 | 0.000 | 0.000 | 101,546 | pyrite |
| PAL0083-40.85-ALUE4-5 | 39.990 | 58.538 | 0.000 | 0.026 | 0.000 | 0.049 | 0.000 | 0.369 | 0.000 | 0.442 | 0.033 | 0.018 | 0.074 | 0.014 | 0.000 | 0.004 | 0.000 | 0.017 | 99,574 | pyrrhotite |
| pal0093-244.3-alue1-1 | 20.969 | 1.733 | 0.000 | 0.000 | 0.000 | 0.000 | 44.960 | 34.304 | 0.000 | 0.185 | 0.115 | 0.012 | 0.000 | 0.000 | 0.000 | 0.015 | 0.003 | 0.027 | 102,323 | cobaltite |
| pal0093-244.3-alue1-2 | 22.457 | 3.492 | 0.000 | 0.000 | 0.000 | 0.008 | 43.119 | 33.366 | 0.000 | 0.260 | 0.116 | 0.000 | 0.000 | 0.000 | 0.000 | 0.001 | 0.033 | 0.008 | 102,86 | cobaltite |
| pal0093-244.3-alue1-3 | 39.191 | 58.767 | 0.000 | 0.000 | 0.000 | 0.000 | 0.000 | 0.237 | 0.000 | 0.397 | 0.000 | 0.000 | 0.000 | 0.000 | 0.000 | 0.067 | 0.000 | 0.000 | 98,659 | pyrrhotite |
| pal0093-244.3-alue1-4 | 38.679 | 52.976 | 0.000 | 0.000 | 0.000 | 0.000 | 0.000 | 5.857 | 0.000 | 0.549 | 0.361 | 0.000 | 0.000 | 0.000 | 0.000 | 0.080 | 0.000 | 0.000 | 98,502 | pyrrhotite |
| pal0093-244.3-alue1-5 | 39.132 | 60.279 | 0.000 | 0.000 | 0.000 | 0.000 | 0.000 | 0.168 | 0.000 | 0.464 | 0.000 | 0.000 | 0.000 | 0.000 | 0.000 | 0.112 | 0.000 | 0.000 | 100,155 | pyrrhotite |
| pal0093-244.3-alue1-6 | 39.048 | 58.548 | 0.000 | 0.000 | 0.032 | 0.092 | 0.015 | 0.447 | 0.000 | 0.565 | 0.013 | 0.000 | 0.000 | 0.040 | 0.000 | 0.036 | 0.000 | 0.009 | 98,845 | pyrrhotite |
| pal0093-244.3-alue2-1 | 39.417 | 58.665 | 0.000 | 0.000 | 0.029 | 0.022 | 0.069 | 0.321 | 0.000 | 0.592 | 0.054 | 0.000 | 0.000 | 0.026 | 0.000 | 0.000 | 0.030 | 0.000 | 99,225 | pyrrhotite |
| pal0093-244.3-alue2-2 | 34.863 | 25.011 | 0.073 | 0.021 | 0.025 | 0.000 | 0.000 | 35.660 | 0.000 | 0.603 | 4.431 | 0.000 | 0.000 | 0.064 | 0.000 | 0.048 | 0.018 | 0.022 | 100,839 | Co-pentlan |
| pal0093-244.3-alue2-3 | 36.973 | 39.631 | 0.030 | 0.025 | 0.019 | 0.015 | 0.000 | 20.476 | 0.000 | 0.452 | 2.355 | 0.000 | 0.000 | 0.066 | 0.048 | 0.021 | 0.007 | 0.010 | 100,128 | Co-pentlan |
| pal0093-244.3-alue3-1 | 3.433 | 6.016 | 0.252 | 0.000 | 0.000 | 0.000 | 0.000 | 0.310 | 40.007 | 0.000 | 0.000 | 0.000 | 0.008 | 0.217 | 0.024 | 6.857 | 27.995 | 0.000 | 85,119 | Bi-Te |
| pal0093-244.3-alue3-2 | 52.222 | 42.184 | 0.000 | 0.022 | 0.000 | 0.000 | 1.055 | 4.286 | 0.000 | 0.491 | 0.000 | 0.000 | 0.000 | 0.021 | 0.098 | 0.000 | 0.036 | 0.009 | 100,424 | pyrite |
| pal0093-244.3-alue3-3 | 49.592 | 37.079 | 0.000 | 0.117 | 0.000 | 0.000 | 4.517 | 8.158 | 0.000 | 0.548 | 0.023 | 0.000 | 0.000 | 0.009 | 0.049 | 0.000 | 0.012 | 0.018 | 100,122 | pyrite |
| pal0093-244.3-alue3-4 | 34.260 | 15.872 | 0.000 | 0.108 | 0.037 | 0.000 | 0.000 | 43.287 | 0.000 | 0.297 | 4.407 | 0.036 | 0.000 | 0.054 | 0.140 | 0.000 | 0.101 | 0.037 | 98,636 | Co-pentlan |
| pal0093-244.3-alue3-5 | 38.795 | 58.844 | 0.000 | 0.155 | 0.000 | 0.000 | 0.000 | 0.284 | 0.000 | 0.347 | 0.115 | 0.021 | 0.000 | 0.022 | 0.125 | 0.000 | 0.028 | 0.033 | 98,769 | pyrrhotite |
| pal0093-248.35-alue1-1 | 37.630 | 58.395 | 0.000 | 0.134 | 0.009 | 0.000 | 0.000 | 0.414 | 0.000 | 0.481 | 0.032 | 0.013 | 0.000 | 0.009 | 0.000 | 0.000 | 0.012 | 0.011 | 97,14 | pyrrhotite |
| pal0093-248.35-alue1-2 | 32.661 | 7.289 | 0.001 | 0.004 | 0.000 | 0.023 | 0.045 | 54.380 | 0.000 | 0.230 | 5.992 | 0.000 | 0.000 | 0.010 | 0.000 | 0.000 | 0.019 | 0.005 | 100,659 | Co-pentlan |
| pal0093-248.35-alue1-3 | 52.366 | 42.825 | 0.011 | 0.031 | 0.000 | 0.000 | 0.559 | 3.806 | 0.000 | 0.479 | 0.000 | 0.000 | 0.000 | 0.000 | 0.000 | 0.000 | 0.000 | 0.000 | 100,077 | pyrite |
| pal0093-248.35-alue1-4 | 53.397 | 46.852 | 0.027 | 0.017 | 0.000 | 0.000 | 0.027 | 0.080 | 0.000 | 0.538 | 0.000 | 0.000 | 0.000 | 0.000 | 0.000 | 0.143 | 0.000 | 0.000 | 101,081 | pyrite |
| pal0093-248.35-alue1-7 | 39.061 | 59.037 | 0.025 | 0.000 | 0.000 | 0.000 | 0.000 | 0.359 | 0.000 | 0.363 | 0.035 | 0.000 | 0.000 | 0.008 | 0.000 | 0.000 | 0.001 | 0.002 | 98,891 | pyrrhotite |
| pal0093-248.35-alue1-10 | 38.667 | 57.685 | 0.050 | 0.080 | 0.000 | 0.000 | 0.000 | 0.793 | 0.000 | 0.347 | 0.093 | 0.028 | 0.000 | 0.000 | 0.000 | 0.000 | 0.000 | 0.000 | 97,743 | pyrrhotite |
| pal0093-248.35-alue1-11 | 38.860 | 58.603 | 0.095 | 0.059 | 0.000 | 0.000 | 0.008 | 0.306 | 0.000 | 0.347 | 0.000 | 0.000 | 0.000 | 0.003 | 0.000 | 0.000 | 0.000 | 0.000 | 98,281 | pyrrhotite |
| pal0093-248.35-alue1-12 | 33.652 | 14.712 | 0.021 | 0.000 | 0.001 | 0.091 | 0.012 | 46.619 | 0.000 | 0.371 | 4.671 | 0.011 | 0.000 | 0.000 | 0.000 | 0.000 | 0.019 | 0.000 | 100,18 | Co-pentlan |
| pal0093-248.35-alue1-13 | 32.803 | 9.174 | 0.053 | 0.049 | 0.000 | 0.019 | 0.015 | 52.816 | 0.000 | 0.447 | 5.453 | 0.003 | 0.000 | 0.000 | 0.000 | 0.046 | 0.034 | 0.008 | 100,92 | Co-pentlan |
| pal0093-248.35-alue1-14 | 38.529 | 58.559 | 0.030 | 0.004 | 0.005 | 0.025 | 0.000 | 0.338 | 0.000 | 0.509 | 0.000 | 0.000 | 0.000 | 0.000 | 0.045 | 0.027 | 0.000 | 0.000 | 98,071 | pyrrhotite |
| pal0093-248.35-alue1-15 | 37.802 | 58.618 | 0.055 | 0.000 | 0.011 | 0.099 | 0.000 | 0.245 | 0.000 | 0.464 | 0.000 | 0.014 | 0.000 | 0.000 | 0.000 | 0.000 | 0.000 | 0.000 | 97,308 | pyrrhotite |
| pal0093-248.35-alue2-4 | 38.695 | 58.669 | 0.146 | 0.138 | 0.025 | 0.049 | 0.000 | 0.440 | 0.175 | 0.470 | 0.147 | 0.055 | 0.143 | 0.057 | 0.157 | 0.375 | 0.056 | 0.000 | 99,797 | pyrrhotite |
| pal0093-248.35-alue2-5 | 31.766 | 7.681 | 0.115 | 0.099 | 0.043 | 0.035 | 0.000 | 51.572 | 0.148 | 0.447 | 6.212 | 0.088 | 0.176 | 0.103 | 0.203 | 0.334 | 0.126 | 0.000 | 99,148 | Co-pentlan |
| pal0093-248.35-alue2-7 | 22.361 | 3.797 | 0.062 | 0.004 | 0.004 | 0.051 | 43.464 | 33.265 | 0.000 | 0.196 | 0.542 | 0.000 | 0.000 | 0.074 | 0.000 | 0.057 | 0.085 | 0.000 | 103,962 | cobaltite |
| pal0093-248.35-alue2-8 | 21.999 | 3.239 | 0.000 | 0.082 | 0.000 | 0.000 | 44.187 | 32.751 | 0.000 | 0.120 | 0.381 | 0.000 | 0.000 | 0.037 | 0.011 | 0.022 | 0.062 | 0.000 | 102,891 | cobaltite |
| pal0093-248.35-alue2-9 | 39.307 | 58.835 | 0.000 | 0.000 | 0.000 | 0.000 | 0.000 | 0.607 | 0.000 | 0.441 | 0.000 | 0.000 | 0.000 | 0.000 | 0.000 | 0.139 | 0.000 | 0.000 | 99,329 | pyrrhotite |
| pal0093-248.35-alue2-10 | 39.179 | 59.343 | 0.000 | 0.000 | 0.000 | 0.000 | 0.000 | 0.199 | 0.000 | 0.452 | 0.000 | 0.000 | 0.000 | 0.000 | 0.000 | 0.049 | 0.000 | 0.000 | 99,222 | pyrrhotite |
| pal0093-248.35-alue3-1 | 34.171 | 14.712 | 0.000 | 0.012 | 0.032 | 0.007 | 0.000 | 48.991 | 0.000 | 0.382 | 3.289 | 0.007 | 0.000 | 0.016 | 0.000 | 0.107 | 0.000 | 0.000 | 101,726 | Co-pentlan |
| pal0093-248.35-alue3-2 | 38.756 | 59.715 | 0.000 | 0.000 | 0.015 | 0.000 | 0.000 | 0.271 | 0.000 | 0.397 | 0.000 | 0.000 | 0.000 | 0.017 | 0.008 | 0.106 | 0.017 | 0.000 | 99,302 | pyrrhotite |
| pal0093-248.35-alue3-5 | 33.923 | 27.649 | 0.000 | 0.021 | 0.028 | 0.049 | 0.000 | 0.000 | 0.000 | 0.466 | 0.000 | 0.000 | 25.682 | 0.013 | 0.012 | 0.032 | 0.000 | 0.000 | 87,875 | chalcopyrit |

| | | | | | | | | | | | | | | | | | | | | | |
|---|---|---|---|---|---|---|---|---|---|---|---|---|---|---|---|---|---|---|---|---|---|
| pal0093-256-alue1-1 | 39.368 | 58.937 | 0.005 | 0.000 | 0.000 | 0.025 | 0.078 | 0.307 | 0.000 | 0.302 | 0.078 | 0.045 | 0.000 | 0.000 | 0.000 | 0.098 | 0.029 | 0.000 | 99,272 | pyrrhotite |
| pal0093-256-alue1-2 | 32.722 | 8.879 | 0.000 | 0.000 | 0.000 | 0.000 | 0.006 | 51.286 | 0.000 | 0.276 | 8.054 | 0.042 | 0.025 | 0.000 | 0.052 | 0.000 | 0.095 | 0.000 | 101,437 | Co-pentlan |
| pal0093-256-alue1-3 | 34.234 | 30.732 | 0.000 | 0.033 | 0.000 | 0.011 | 0.018 | 0.111 | 0.000 | 0.337 | 0.091 | 0.053 | 33.965 | 0.003 | 0.067 | 0.022 | 0.045 | 0.015 | 99,737 | chalcopyrit |
| pal0093-256-alue1-4 | 20.696 | 1.569 | 0.267 | 0.134 | 0.039 | 0.041 | 46.662 | 34.081 | 0.000 | 0.108 | 1.046 | 0.093 | 0.225 | 0.140 | 0.130 | 0.000 | 0.152 | 0.056 | 105,439 | cobaltite |
| pal0093-256-alue1-5 | 39.225 | 58.218 | 0.000 | 0.000 | 0.006 | 0.000 | 0.091 | 0.552 | 0.000 | 0.419 | 0.081 | 0.034 | 0.000 | 0.000 | 0.016 | 0.040 | 0.050 | 0.000 | 98,732 | pyrrhotite |
| pal0093-256-alue2-1 | 22.600 | 1.378 | 0.000 | 0.000 | 0.004 | 0.000 | 44.075 | 34.279 | 0.000 | 0.139 | 1.056 | 0.024 | 0.000 | 0.011 | 0.073 | 0.028 | 0.122 | 0.002 | 103,791 | cobaltite |
| pal0093-256-alue2-2 | 4.945 | 0.595 | 0.148 | 0.000 | 0.000 | 0.000 | 0.000 | 9.444 | 43.727 | 0.000 | 0.106 | 0.000 | 0.000 | 0.104 | 0.065 | 0.000 | 21.687 | 0.000 | 80,821 | missed |
| pal0093-256-alue2-3 | 22.173 | 1.132 | 0.000 | 0.000 | 0.000 | 0.012 | 44.034 | 34.714 | 0.000 | 0.216 | 0.474 | 0.016 | 0.000 | 0.000 | 0.000 | 0.000 | 0.119 | 0.000 | 102,89 | cobaltite |
| pal0093-256-alue2-4 | 38.030 | 57.543 | 0.000 | 0.000 | 0.000 | 0.040 | 0.000 | 1.182 | 0.000 | 0.408 | 0.005 | 0.000 | 0.000 | 0.000 | 0.000 | 0.096 | 0.000 | 0.000 | 97,304 | pyrrhotite |
| pal0093-256-alue2-5 | 21.602 | 1.220 | 0.000 | 0.012 | 0.005 | 0.000 | 45.162 | 34.158 | 0.000 | 0.242 | 1.475 | 0.000 | 0.000 | 0.000 | 0.051 | 0.000 | 0.102 | 0.009 | 104,038 | cobaltite |
| pal0093-256-alue2-6 | 22.344 | 2.929 | 0.000 | 0.000 | 0.005 | 0.007 | 42.345 | 33.523 | 0.000 | 0.247 | 0.337 | 0.000 | 0.000 | 0.019 | 0.000 | 0.000 | 0.161 | 0.000 | 101,917 | cobaltite |
| pal0093-256-alue2-7 | 38.234 | 58.826 | 0.000 | 0.000 | 0.000 | 0.000 | 0.000 | 0.194 | 0.000 | 0.458 | 0.000 | 0.000 | 0.000 | 0.000 | 0.000 | 0.058 | 0.000 | 0.000 | 97,77 | pyrrhotite |
| pal0093-256-alue3-2 | 38.125 | 57.894 | 0.000 | 0.000 | 0.000 | 0.000 | 0.000 | 0.115 | 0.000 | 0.457 | 0.000 | 0.000 | 0.000 | 0.000 | 0.000 | 0.000 | 0.000 | 0.644 | 97,235 | pyrrhotite |
| pal0093-256-alue3-3 | 33.064 | 12.885 | 0.000 | 0.000 | 0.000 | 0.000 | 0.000 | 47.157 | 0.000 | 0.372 | 7.084 | 0.000 | 0.000 | 0.000 | 0.000 | 0.000 | 0.000 | 0.097 | 100,659 | Co-pentlan |
| pal0093-256-alue3-4 | 28.162 | 46.114 | 0.088 | 0.041 | 0.067 | 0.114 | 0.000 | 1.889 | 0.000 | 0.279 | 0.711 | 0.000 | 0.000 | 0.012 | 0.000 | 0.000 | 0.013 | 7.282 | 84,772 | missed |
| pal0093-256-alue4-1 | 39.365 | 59.180 | 0.000 | 0.050 | 0.016 | 0.036 | 0.000 | 0.275 | 0.000 | 0.302 | 0.051 | 0.059 | 0.000 | 0.038 | 0.109 | 0.071 | 0.028 | 0.041 | 99,621 | pyrrhotite |
| pal0093-256-alue5-1 | 39.042 | 58.633 | 0.000 | 0.029 | 0.010 | 0.021 | 0.000 | 0.270 | 0.000 | 0.430 | 0.090 | 0.039 | 0.000 | 0.056 | 0.032 | 0.142 | 0.023 | 0.000 | 98,817 | pyrrhotite |
| pal0093-256-alue5-2 | 39.107 | 59.054 | 0.000 | 0.067 | 0.000 | 0.000 | 0.000 | 0.266 | 0.000 | 0.531 | 0.096 | 0.022 | 0.021 | 0.020 | 0.101 | 0.005 | 0.009 | 0.000 | 99,299 | pyrrhotite |
| pal0093-256-alue5-3 | 34.779 | 29.857 | 0.000 | 0.000 | 0.010 | 0.000 | 0.015 | 0.053 | 0.000 | 0.447 | 0.000 | 0.000 | 34.138 | 0.000 | 0.047 | 0.000 | 0.013 | 0.007 | 99,366 | chalcopyrit |
| pal0093-256-alue5-4 | 39.321 | 58.986 | 0.000 | 0.000 | 0.005 | 0.011 | 0.000 | 0.237 | 0.000 | 0.463 | 0.000 | 0.000 | 0.000 | 0.000 | 0.000 | 0.022 | 0.000 | 0.734 | 99,779 | pyrrhotite |
| pal0093-256-alue5-6 | 38.967 | 59.026 | 0.000 | 0.029 | 0.000 | 0.044 | 0.081 | 0.301 | 0.000 | 0.408 | 0.000 | 0.000 | 0.000 | 0.000 | 0.000 | 0.035 | 0.000 | 0.000 | 98,891 | pyrrhotite |
| pal0093-256-alue5-7 | 38.240 | 58.145 | 0.000 | 0.000 | 0.000 | 0.018 | 0.000 | 0.258 | 0.000 | 0.424 | 0.000 | 0.000 | 0.000 | 0.020 | 0.000 | 0.019 | 0.000 | 0.000 | 97,124 | pyrrhotite |
| pal0093-258.95-alue1-1 | 22.154 | 2.416 | 0.104 | 0.029 | 0.027 | 0.000 | 43.358 | 33.933 | 0.000 | 0.246 | 0.221 | 0.029 | 0.000 | 0.048 | 0.000 | 0.000 | 0.000 | 0.020 | 102,585 | cobaltite |
| pal0093-258.95-alue1-2 | 22.135 | 3.400 | 0.000 | 0.008 | 0.022 | 0.017 | 43.645 | 32.020 | 0.000 | 0.390 | 0.482 | 0.028 | 0.000 | 0.000 | 0.000 | 0.014 | 0.008 | 0.000 | 102,169 | cobaltite |
| pal0093-258.95-alue1-3 | 22.073 | 2.479 | 0.007 | 0.000 | 0.014 | 0.030 | 43.116 | 32.888 | 0.000 | 0.208 | 0.231 | 0.023 | 0.000 | 0.002 | 0.000 | 0.000 | 0.000 | 0.033 | 101,104 | cobaltite |
| pal0093-258.95-alue1-4 | 38.069 | 57.763 | 0.000 | 0.000 | 0.000 | 0.055 | 0.000 | 0.175 | 0.000 | 0.334 | 0.000 | 0.005 | 0.000 | 0.000 | 0.000 | 0.124 | 0.000 | 0.000 | 96,525 | pyrrhotite |
| pal0093-258.95-alue1-5 | 34.619 | 10.139 | 0.000 | 0.000 | 0.000 | 0.000 | 0.000 | 43.341 | 0.000 | 0.468 | 9.987 | 0.000 | 0.000 | 0.000 | 0.000 | 0.031 | 0.000 | 0.000 | 98,585 | Co-pentlan |
| pal0093-258.95-alue1-6 | 39.158 | 59.658 | 0.094 | 0.000 | 0.022 | 0.000 | 0.000 | 0.229 | 0.000 | 0.318 | 0.000 | 0.006 | 0.011 | 0.030 | 0.044 | 0.000 | 0.005 | 0.004 | 99,579 | pyrrhotite |
| pal0093-258.95-alue2-1 | 34.781 | 28.501 | 0.134 | 0.000 | 0.038 | 0.044 | 0.000 | 29.019 | 0.000 | 0.368 | 6.189 | 0.000 | 0.036 | 0.050 | 0.112 | 0.000 | 0.018 | 0.002 | 99,292 | Co-pentlan |
| pal0093-258.95-alue2-2 | 38.974 | 58.821 | 0.116 | 0.000 | 0.048 | 0.014 | 0.000 | 0.303 | 0.000 | 0.434 | 0.053 | 0.008 | 0.007 | 0.000 | 0.064 | 0.000 | 0.002 | 0.000 | 98,844 | pyrrhotite |
| pal0093-258.95-alue2-3 | 39.577 | 0.793 | 0.243 | 0.000 | 0.046 | 0.546 | 0.140 | 0.069 | 0.000 | 58.278 | 0.182 | 0.004 | 0.272 | 0.069 | 0.340 | 0.399 | 0.030 | 0.051 | 101,039 | molybdenit |
| pal0093-258.95-alue2-4 | 20.663 | 4.325 | 0.456 | 0.049 | 0.069 | 0.054 | 45.877 | 32.613 | 0.000 | 0.222 | 0.777 | 0.039 | 0.205 | 0.077 | 0.213 | 0.000 | 0.098 | 0.060 | 105,797 | cobaltite |
| pal0093-258.95-alue2-5 | 20.538 | 1.467 | 0.000 | 0.008 | 0.000 | 0.025 | 45.180 | 34.424 | 0.000 | 0.101 | 1.240 | 0.000 | 0.000 | 0.030 | 0.069 | 0.000 | 0.080 | 0.000 | 103,162 | cobaltite |
| pal0093-258.95-alue2-6 | 20.686 | 1.346 | 0.057 | 0.016 | 0.000 | 0.000 | 44.828 | 34.160 | 0.000 | 0.152 | 1.231 | 0.000 | 0.000 | 0.018 | 0.101 | 0.000 | 0.065 | 0.000 | 102,66 | cobaltite |
| pal0093-258.95-alue2-7 | 20.634 | 1.914 | 0.013 | 0.000 | 0.010 | 0.017 | 44.569 | 34.272 | 0.000 | 0.279 | 0.820 | 0.000 | 0.000 | 0.000 | 0.018 | 0.000 | 0.050 | 0.000 | 102,596 | cobaltite |
| pal0093-258.95-alue2-8 | 21.252 | 2.383 | 0.070 | 0.000 | 0.000 | 0.013 | 44.012 | 34.637 | 0.000 | 0.202 | 0.230 | 0.000 | 0.000 | 0.019 | 0.000 | 0.000 | 0.047 | 0.000 | 102,865 | cobaltite |
| pal0093-258.95-alue2-9 | 20.472 | 2.715 | 0.000 | 0.000 | 0.000 | 0.017 | 46.200 | 33.589 | 0.000 | 0.197 | 0.718 | 0.000 | 0.000 | 0.013 | 0.000 | 0.000 | 0.027 | 0.000 | 103,948 | cobaltite |
| pal0093-258.95-alue2-10 | 39.209 | 58.478 | 0.049 | 0.075 | 0.013 | 0.000 | 0.059 | 0.362 | 0.000 | 0.372 | 0.007 | 0.000 | 0.000 | 0.000 | 0.000 | 0.000 | 0.018 | 0.013 | 98,655 | pyrrhotite |
| pal0093-258.95-alue3-1 | 39.219 | 59.780 | 0.034 | 0.033 | 0.000 | 0.000 | 0.026 | 0.287 | 0.000 | 0.367 | 0.022 | 0.040 | 0.000 | 0.020 | 0.000 | 0.016 | 0.000 | 0.007 | 99,851 | pyrrhotite |
| pal0093-258.95-alue3-2 | 33.448 | 15.227 | 0.062 | 0.000 | 0.000 | 0.000 | 0.071 | 42.684 | 0.000 | 0.411 | 8.977 | 0.013 | 0.019 | 0.000 | 0.000 | 0.000 | 0.091 | 0.011 | 101,014 | Co-pentlan |
| pal0093-258.95-alue3-3 | 22.292 | 1.708 | 0.463 | 0.094 | 0.029 | 0.000 | 43.704 | 34.666 | 0.000 | 0.170 | 0.626 | 0.034 | 0.184 | 0.080 | 0.073 | 0.000 | 0.170 | 0.048 | 104,341 | cobaltite |
| pal0093-258.95-alue3-4 | 22.221 | 1.269 | 0.382 | 0.094 | 0.015 | 0.000 | 43.296 | 35.512 | 0.000 | 0.290 | 0.327 | 0.063 | 0.176 | 0.093 | 0.102 | 0.000 | 0.172 | 0.051 | 104,063 | cobaltite |
| pal0093-258.95-alue3-5 | 22.206 | 2.685 | 0.000 | 0.000 | 0.028 | 0.000 | 43.562 | 34.381 | 0.000 | 0.265 | 0.250 | 0.000 | 0.000 | 0.081 | 0.011 | 0.000 | 0.014 | 0.002 | 103,485 | cobaltite |
| pal0093-258.95-alue3-6 | 22.060 | 3.550 | 0.000 | 0.000 | 0.004 | 0.000 | 43.834 | 32.797 | 0.000 | 0.221 | 0.430 | 0.005 | 0.000 | 0.047 | 0.033 | 0.089 | 0.056 | 0.008 | 103,134 | cobaltite |
| pal0093-258.95-alue4-1 | 38.973 | 58.655 | 0.000 | 0.000 | 0.009 | 0.000 | 0.000 | 0.185 | 0.000 | 0.472 | 0.000 | 0.000 | 0.000 | 0.000 | 0.000 | 0.091 | 0.000 | 0.000 | 98,385 | pyrrhotite |
| pal0093-258.95-alue4-2 | 34.396 | 29.610 | 0.000 | 0.000 | 0.008 | 0.000 | 0.000 | 0.000 | 0.000 | 0.410 | 0.000 | 0.000 | 33.037 | 0.000 | 0.000 | 0.086 | 0.000 | 0.000 | 97,547 | chalcopyrit |
| pal0093-258.95-alue4-3 | 34.179 | 29.816 | 0.000 | 0.029 | 0.000 | 0.000 | 0.000 | 0.046 | 0.000 | 0.335 | 0.000 | 0.022 | 33.851 | 0.000 | 0.000 | 0.000 | 0.009 | 0.012 | 98,299 | chalcopyrit |
| pal0093-258.95-alue4-4 | 38.332 | 59.568 | 0.019 | 0.000 | 0.000 | 0.000 | 0.000 | 0.261 | 0.000 | 0.573 | 0.000 | 0.004 | 0.000 | 0.000 | 0.000 | 0.000 | 0.000 | 0.000 | 98,757 | pyrrhotite |
| pal0093-258.95-alue4-5 | 32.417 | 8.443 | 0.021 | 0.000 | 0.005 | 0.000 | 0.000 | 50.613 | 0.000 | 0.303 | 8.295 | 0.024 | 0.000 | 0.000 | 0.000 | 0.000 | 0.048 | 0.000 | 100,169 | Co-pentlan |
| pal0093-258.95-alue4-6 | 34.976 | 28.226 | 0.000 | 0.025 | 0.000 | 0.000 | 0.000 | 31.841 | 0.000 | 0.390 | 5.444 | 0.002 | 0.000 | 0.000 | 0.000 | 0.000 | 0.034 | 0.000 | 100,938 | Co-pentlan |
| pal0093-258.95-alue4-7 | 38.928 | 59.770 | 0.000 | 0.021 | 0.000 | 0.000 | 0.000 | 0.302 | 0.000 | 0.406 | 0.000 | 0.000 | 0.000 | 0.000 | 0.000 | 0.000 | 0.000 | 0.000 | 99,427 | pyrrhotite |
| pal0093-266.40-alue1-1 | 21.565 | 3.691 | 0.000 | 0.045 | 0.000 | 0.106 | 39.434 | 30.464 | 0.000 | 0.195 | 0.291 | 0.000 | 0.000 | 0.046 | 0.025 | 0.000 | 0.062 | 0.000 | 95,924 | cobaltite |
| pal0093-266.40-alue1-2 | 21.077 | 2.336 | 0.153 | 0.000 | 0.000 | 0.154 | 45.626 | 33.985 | 0.000 | 0.241 | 0.549 | 0.000 | 0.000 | 0.034 | 0.007 | 0.000 | 0.067 | 0.011 | 104,24 | cobaltite |
| pal0093-266.40-alue1-3 | 22.339 | 2.787 | 0.095 | 0.000 | 0.021 | 0.110 | 43.016 | 34.231 | 0.000 | 0.258 | 0.290 | 0.001 | 0.000 | 0.047 | 0.000 | 0.000 | 0.082 | 0.000 | 103,277 | cobaltite |
| pal0093-266.40-alue1-4 | 21.686 | 1.889 | 0.075 | 0.000 | 0.000 | 0.097 | 40.650 | 33.782 | 0.000 | 0.251 | 0.213 | 0.003 | 0.000 | 0.073 | 0.000 | 0.000 | 0.180 | 0.000 | 98,899 | cobaltite |
| pal0093-266.40-alue1-5 | 22.895 | 4.094 | 0.087 | 0.000 | 0.000 | 0.055 | 41.186 | 32.669 | 0.000 | 0.245 | 0.262 | 0.011 | 0.000 | 0.043 | 0.040 | 0.000 | 0.055 | 0.000 | 101,642 | cobaltite |
| pal0093-266.40-alue1-6 | 21.056 | 3.038 | 0.000 | 0.000 | 0.000 | 0.124 | 41.860 | 30.688 | 0.000 | 0.107 | 0.648 | 0.000 | 0.000 | 0.000 | 0.069 | 0.000 | 0.018 | 0.000 | 97,608 | cobaltite |
| pal0093-266.40-alue1-7 | 21.645 | 2.095 | 0.081 | 0.016 | 0.000 | 0.106 | 40.793 | 32.993 | 0.000 | 0.126 | 0.197 | 0.000 | 0.000 | 0.000 | 0.000 | 0.052 | 0.057 | 0.000 | 98,161 | cobaltite |
| pal0093-266.40-alue2-1 | 39.113 | 59.040 | 0.000 | 0.000 | 0.000 | 0.102 | 0.000 | 0.192 | 0.000 | 0.494 | 0.000 | 0.000 | 0.000 | 0.000 | 0.000 | 0.079 | 0.000 | 0.000 | 99,02 | pyrrhotite |
| pal0093-266.40-alue2-2 | 33.899 | 29.946 | 0.000 | 0.000 | 0.000 | 0.134 | 0.000 | 0.000 | 0.000 | 0.237 | 0.000 | 0.000 | 32.822 | 0.000 | 0.000 | 0.043 | 0.000 | 0.000 | 97,081 | chalcopyrit |
| pal0093-266.40-alue2-3 | 38.180 | 60.005 | 0.000 | 0.000 | 0.000 | 0.099 | 0.000 | 0.189 | 0.000 | 0.384 | 0.000 | 0.000 | 0.000 | 0.000 | 0.000 | 0.137 | 0.000 | 0.000 | 98,994 | pyrrhotite |
| pal0093-266.40-alue2-4 | 13.205 | 3.341 | 0.000 | 0.000 | 0.000 | 0.000 | 0.000 | 16.962 | 0.000 | 0.142 | 4.147 | 0.015 | 0.000 | 0.352 | 0.044 | 0.035 | 0.000 | 0.000 | 38,243 | Co-pentlan |
| pal0093-266.40-alue2-6 | 36.241 | 53.594 | 0.027 | 0.000 | 0.041 | 0.074 | 0.113 | 0.360 | 0.000 | 0.406 | 0.198 | 0.031 | 0.000 | 0.059 | 0.289 | 0.254 | 0.060 | 0.059 | 91,806 | pyrrhotite |
| pal0093-266.40-alue2-7 | 20.884 | 3.088 | 0.466 | 0.000 | 0.061 | 0.110 | 44.058 | 31.350 | 0.000 | 0.278 | 0.822 | 0.109 | 0.087 | 0.163 | 0.436 | 0.221 | 0.193 | 0.164 | 102,49 | cobaltite |
| pal0093-266.40-alue3-1 | 21.365 | 2.875 | 0.536 | 0.000 | 0.078 | 0.089 | 45.865 | 33.740 | 0.000 | 0.177 | 0.722 | 0.108 | 0.049 | 0.157 | 0.436 | 0.181 | 0.229 | 0.103 | 106,71 | cobaltite |
| pal0093-266.40-alue3-2 | 21.521 | 2.637 | 0.000 | 0.000 | 0.000 | 0.017 | 44.434 | 33.939 | 0.000 | 0.189 | 0.429 | 0.038 | 0.000 | 0.010 | 0.076 | 0.000 | 0.003 | 0.010 | 103,303 | cobaltite |
| pal0093-266.40-alue3-3 | 38.451 | 59.346 | 0.000 | 0.000 | 0.000 | 0.000 | 0.000 | 0.246 | 0.000 | 0.544 | 0.000 | 0.000 | 0.000 | 0.000 | 0.000 | 0.000 | 0.000 | 0.000 | 98,587 | pyrrhotite |
| pal0093-266.40-alue3-4 | 21.634 | 3.085 | 0.000 | 0.000 | 0.000 | 0.041 | 43.781 | 33.333 | 0.000 | 0.372 | 0.437 | 0.000 | 0.000 | 0.031 | 0.185 | 0.000 | 0.000 | 0.000 | 102,899 | cobaltite |
| pal0093-266.40-alue3-5 | 38.232 | 58.477 | 0.000 | 0.000 | 0.000 | 0.000 | 0.000 | 0.389 | 0.000 | 0.472 | 0.000 | 0.000 | 0.000 | 0.000 | 0.000 | 0.028 | 0.000 | 0.000 | 97,598 | pyrrhotite |
| pal0093-266.40-alue3-6 | 39.018 | 58.181 | 0.000 | 0.000 | 0.000 | 0.000 | 0.000 | 0.585 | 0.000 | 0.521 | 0.000 | 0.000 | 0.000 | 0.000 | 0.000 | 0.015 | 0.000 | 0.000 | 98,32 | pyrrhotite |
| pal0093-266.40-alue3-7 | 20.686 | 2.139 | 0.011 | 0.000 | 0.028 | 0.082 | 45.071 | 34.031 | 0.000 | 0.209 | 0.800 | 0.016 | 0.000 | 0.000 | 0.000 | 0.000 | 0.016 | 0.011 | 103,1 | cobaltite |
| pal0093-266.40-alue4-1 | 23.601 | 3.473 | 0.079 | 0.000 | 0.029 | 0.000 | 41.095 | 33.862 | 0.000 | 0.138 | 0.137 | 0.000 | 0.000 | 0.019 | 0.087 | 0.000 | 0.049 | 0.000 | 102,569 | cobaltite |
| pal0093-266.40-alue4-2 | 21.734 | 2.121 | 0.000 | 0.000 | 0.000 | 0.000 | 43.775 | 33.842 | 0.000 | 0.101 | 0.235 | 0.000 | 0.000 | 0.020 | 0.033 | 0.000 | 0.000 | 0.000 | 101,861 | cobaltite |
| pal0093-266.40-alue4-3 | 21.081 | 2.510 | 0.000 | 0.000 | 0.000 | 0.000 | 44.544 | 33.447 | 0.000 | 0.114 | 0.558 | 0.017 | 0.000 | 0.000 | 0.007 | 0.056 | 0.000 | 0.000 | 102,334 | cobaltite |
| pal0093-266.40-alue4-4 | 20.803 | 1.962 | 0.013 | 0.000 | 0.000 | 0.000 | 45.590 | 33.600 | 0.000 | 0.114 | 0.668 | 0.030 | 0.000 | 0.011 | 0.000 | 0.085 | 0.010 | 0.001 | 102,887 | cobaltite |
| pal0093-266.40-alue4-5 | 21.048 | 2.463 | 0.000 | 0.000 | 0.000 | 0.000 | 44.140 | 33.666 | 0.000 | 0.202 | 0.569 | 0.000 | 0.000 | 0.037 | 0.047 | 0.000 | 0.002 | 0.002 | 102,176 | cobaltite |
| pal0093-266.40-alue4-6 | 34.471 | 30.065 | 0.000 | 0.000 | 0.000 | 0.000 | 0.000 | 0.000 | 0.000 | 0.369 | 0.000 | 0.017 | 33.341 | 0.000 | 0.000 | 0.066 | 0.000 | 0.000 | 98,329 | chalcopyrit |
| pal0093-266.40-alue4-7 | 38.516 | 59.376 | 0.000 | 0.000 | 0.000 | 0.044 | 0.000 | 0.160 | 0.000 | 0.422 | 0.000 | 0.000 | 0.000 | 0.000 | 0.000 | 0.000 | 0.000 | 0.000 | 98,518 | pyrrhotite |
| pal0093-266.40-alue4-8 | 33.183 | 12.650 | 0.000 | 0.000 | 0.000 | 0.000 | 0.000 | 45.670 | 0.000 | 0.382 | 8.941 | 0.000 | 0.000 | 0.000 | 0.000 | 0.000 | 0.000 | 0.000 | 100,826 | Co-pentlan |
| pal0093-266.40-alue4-9 | 20.419 | 1.930 | 0.011 | 0.000 | 0.010 | 0.017 | 45.728 | 33.726 | 0.000 | 0.139 | 0.593 | 0.038 | 0.000 | 0.022 | 0.022 | 0.000 | 0.020 | 0.000 | 102,675 | cobaltite |
| pal0093-269.90-alue1-1 | 39.194 | 59.804 | 0.000 | 0.000 | 0.000 | 0.018 | 0.093 | 0.329 | 0.000 | 0.422 | 0.020 | 0.001 | 0.039 | 0.017 | 0.000 | 0.043 | 0.000 | 0.000 | 99,98 | pyrrhotite |
| pal0093-269.90-alue1-5 | 39.502 | 59.748 | 0.023 | 0.000 | 0.000 | 0.003 | 0.075 | 0.238 | 0.000 | 0.427 | 0.005 | 0.046 | 0.050 | 0.000 | 0.092 | 0.000 | 0.035 | 0.078 | 100,322 | pyrrhotite |
| pal0093-269.90-alue1-8 | 39.104 | 59.698 | 0.012 | 0.033 | 0.023 | 0.000 | 0.000 | 0.281 | 0.269 | 0.388 | 0.007 | 0.000 | 0.000 | 0.009 | 0.000 | 0.165 | 0.025 | 0.033 | 100,047 | pyrrhotite |
| pal0093-269.90-alue1-9 | 21.161 | 2.687 | 0.305 | 0.109 | 0.032 | 0.000 | 45.561 | 33.481 | 0.133 | 0.170 | 0.319 | 0.062 | 0.182 | 0.113 | 0.043 | 0.061 | 0.119 | 0.062 | 104,6 | cobaltite |
| pal0093-269.90-alue2-1 | 20.648 | 2.273 | 0.241 | 0.113 | 0.024 | 0.000 | 45.644 | 32.725 | 0.088 | 0.189 | 0.539 | 0.037 | 0.133 | 0.105 | 0.083 | 0.000 | 0.174 | 0.160 | 103,176 | cobaltite |
| pal0093-269.90-alue3-1 | 39.455 | 58.260 | 0.073 | 0.000 | 0.000 | 0.010 | 0.000 | 0.071 | 0.187 | 0.387 | 0.000 | 0.000 | 0.000 | 0.000 | 0.000 | 0.191 | 0.000 | 0.000 | 98,634 | pyrrhotite |
| pal0093-269.90-alue3-2 | 39.231 | 57.431 | 0.089 | 0.000 | 0.000 | 0.000 | 0.000 | 0.055 | 0.141 | 0.432 | 0.000 | 0.000 | 0.000 | 0.000 | 0.000 | 0.125 | 0.000 | 0.000 | 97,504 | pyrrhotite |
| pal0093-269.90-alue3-3 | 39.081 | 58.379 | 0.048 | 0.000 | 0.000 | 0.010 | 0.000 | 0.075 | 0.187 | 0.388 | 0.000 | 0.000 | 0.000 | 0.000 | 0.000 | 0.167 | 0.000 | 0.000 | 98,335 | pyrrhotite |
| pal0093-269.90-alue4-2 | 39.142 | 59.634 | 0.064 | 0.075 | 0.052 | 0.122 | 0.000 | 0.457 | 0.239 | 0.483 | 0.188 | 0.040 | 0.207 | 0.040 | 0.124 | 0.257 | 0.075 | 0.000 | 101,199 | pyrrhotite |
| pal0093-269.90-alue4-3 | 32.977 | 7.903 | 0.103 | 0.098 | 0.022 | 0.099 | 0.000 | 52.734 | 0.209 | 0.490 | 7.642 | 0.034 | 0.295 | 0.077 | 0.170 | 0.257 | 0.110 | 0.000 | 103,22 | Co-pentlan |
| pal0093-269.90-alue4-4 | 39.146 | 59.561 | 0.160 | 0.092 | 0.041 | 0.100 | 0.000 | 0.424 | 0.214 | 0.550 | 0.221 | 0.029 | 0.186 | 0.056 | 0.196 | 0.249 | 0.056 | 0.000 | 101,281 | pyrrhotite |
| pal0093-269.90-alue4-5 | 34.001 | 31.350 | 0.196 | 0.141 | 0.035 | 0.039 | 0.000 | 0.188 | 0.211 | 0.507 | 0.201 | 0.052 | 33.332 | 0.076 | 0.214 | 0.244 | 0.100 | 0.000 | 100,887 | chalcopyrit |
| pal0093-269.90-alue4-6 | 39.104 | 59.168 | 0.000 | 0.063 | 0.000 | 0.000 | 0.021 | 0.350 | 0.000 | 0.494 | 0.017 | 0.038 | 0.000 | 0.000 | 0.120 | 0.020 | 0.000 | 0.000 | 99,395 | pyrrhotite |
| pal0093-269.90-alue4-7 | 34.304 | 30.562 | 0.052 | 0.017 | 0.012 | 0.000 | 0.000 | 0.083 | 0.000 | 0.455 | 0.070 | 0.063 | 33.994 | 0.000 | 0.125 | 0.000 | 0.022 | 0.012 | 99,771 | chalcopyrit |
| pal0093-269.90-alue4-8 | 34.592 | 30.130 | 0.024 | 0.000 | 0.004 | 0.000 | 0.039 | 0.047 | 0.000 | 0.449 | 0.076 | 0.020 | 33.426 | 0.011 | 0.008 | 0.000 | 0.026 | 0.023 | 98,875 | chalcopyrit |
| pal0093-269.90-alue4-9 | 32.323 | 8.716 | 0.037 | 0.086 | 0.015 | 0.000 | 0.000 | 49.657 | 0.000 | 0.421 | 8.671 | 0.000 | 0.000 | 0.064 | 0.075 | 0.000 | 0.025 | 0.000 | 100,09 | Co-pentlan |
| pal0093-269.90-alue5-1 | 33.344 | 12.640 | 0.000 | 0.000 | 0.023 | 0.033 | 0.070 | 48.490 | 0.000 | 0.403 | 5.091 | 0.022 | 0.000 | 0.008 | 0.004 | 0.046 | 0.079 | 0.313 | 100,566 | Co-pentlan |
| pal0093-269.90-alue5-2 | 39.364 | 58.617 | 0.024 | 0.000 | 0.000 | 0.032 | 0.149 | 0.229 | 0.000 | 0.355 | 0.000 | 0.000 | 0.000 | 0.000 | 0.108 | 0.050 | 0.000 | 0.000 | 98,928 | pyrrhotite |
| pal0093-269.90-alue5-3 | 34.681 | 29.661 | 0.000 | 0.025 | 0.000 | 0.000 | 0.000 | 0.023 | 0.000 | 0.455 | 0.032 | 0.010 | 34.301 | 0.000 | 0.062 | 0.000 | 0.022 | 0.019 | 99,291 | chalcopyrit |
| pal0093-269.90-alue5-4 | 39.128 | 59.389 | 0.010 | 0.046 | 0.000 | 0.000 | 0.045 | 0.225 | 0.000 | 0.393 | 0.000 | 0.000 | 0.000 | 0.000 | 0.072 | 0.024 | 0.000 | 0.002 | 99,334 | pyrrhotite |

| | | | | | | | | | | | | | | | | | | | | |
|---|---|---|---|---|---|---|---|---|---|---|---|---|---|---|---|---|---|---|---|---|
| pal0093-269.90-alue5-5 | 33.116 | 9.166 | 0.035 | 0.090 | 0.000 | 0.078 | 0.026 | 50.796 | 0.000 | 0.335 | 6.394 | 0.031 | 0.044 | 0.001 | 0.071 | 0.000 | 0.064 | 0.009 | 100,256 | Co-pentlan |
| pal0093-269.90-alue5-6 | 39.705 | 57.610 | 0.000 | 0.029 | 0.000 | 0.006 | 0.024 | 0.157 | 0.000 | 0.454 | 0.007 | 0.004 | 0.079 | 0.000 | 0.144 | 0.000 | 0.000 | 0.000 | 98,219 | pyrrhotite |
| pal0093-269.90-alue6-1 | 22.103 | 4.203 | 0.000 | 0.077 | 0.000 | 0.050 | 43.719 | 32.945 | 0.000 | 0.188 | 0.368 | 0.019 | 0.000 | 0.000 | 0.152 | 0.000 | 0.000 | 0.000 | 103,824 | cobaltite |
| pal0093-269.90-alue6-2 | 38.360 | 57.813 | 0.000 | 0.008 | 0.000 | 0.051 | 0.000 | 0.076 | 0.000 | 0.404 | 0.000 | 0.000 | 0.000 | 0.000 | 0.000 | 0.044 | 0.000 | 0.000 | 96,756 | pyrrhotite |
| pal0093-269.90-alue6-3 | 34.976 | 26.979 | 0.000 | 0.058 | 0.001 | 0.004 | 0.000 | 32.144 | 0.000 | 0.377 | 5.372 | 0.000 | 0.000 | 0.000 | 0.004 | 0.019 | 0.000 | 0.000 | 99,934 | Co-pentlan |
| pal0093-269.90-alue6-5 | 21.044 | 2.598 | 0.000 | 0.044 | 0.000 | 0.063 | 44.598 | 33.113 | 0.000 | 0.145 | 0.531 | 0.013 | 0.000 | 0.000 | 0.184 | 0.002 | 0.000 | 0.009 | 102,344 | cobaltite |
| pal0093-269.90-alue6-6 | 21.226 | 2.501 | 0.108 | 0.049 | 0.000 | 0.000 | 44.693 | 33.546 | 0.000 | 0.227 | 0.348 | 0.002 | 0.000 | 0.033 | 0.000 | 0.018 | 0.015 | 0.165 | 102,931 | cobaltite |
| pal0093-269.90-alue6-7 | 21.057 | 2.153 | 0.000 | 0.053 | 0.000 | 0.000 | 44.889 | 34.127 | 0.000 | 0.202 | 0.377 | 0.000 | 0.000 | 0.000 | 0.000 | 0.018 | 0.004 | 0.000 | 102,88 | cobaltite |
| pal0093-269.90-alue7-1 | 34.611 | 30.057 | 0.000 | 0.058 | 0.000 | 0.027 | 0.000 | 0.000 | 0.000 | 0.385 | 0.000 | 0.000 | 32.722 | 0.000 | 0.000 | 0.040 | 0.000 | 0.000 | 97,9 | chalcopyrit |
| pal0093-269.90-alue7-2 | 38.493 | 58.202 | 0.000 | 0.079 | 0.000 | 0.000 | 0.000 | 0.028 | 0.000 | 0.548 | 0.000 | 0.000 | 0.000 | 0.000 | 0.000 | 0.058 | 0.000 | 0.000 | 97,408 | pyrrhotite |
| pal0093-269.90-alue7-3 | 26.728 | 39.992 | 0.000 | 0.000 | 0.000 | 0.000 | 0.000 | 0.000 | 0.000 | 0.254 | 0.000 | 0.000 | 0.000 | 0.000 | 0.000 | 0.024 | 0.000 | 0.000 | 66,998 | pyrrhotite |
| pal0093-269.90-alue7-4 | 38.738 | 59.100 | 0.000 | 0.071 | 0.017 | 0.044 | 0.000 | 0.179 | 0.000 | 0.454 | 0.000 | 0.005 | 0.000 | 0.016 | 0.000 | 0.000 | 0.000 | 0.000 | 98,624 | pyrrhotite |
| pal0093-269.90-alue7-5 | 38.585 | 58.586 | 0.033 | 0.125 | 0.023 | 0.073 | 0.005 | 0.754 | 0.000 | 0.443 | 0.014 | 0.018 | 0.033 | 0.018 | 0.036 | 0.000 | 0.008 | 0.002 | 98,756 | pyrrhotite |
| pal0093-269.90-alue7-6 | 39.057 | 58.012 | 0.000 | 0.037 | 0.027 | 0.000 | 0.023 | 0.321 | 0.000 | 0.404 | 0.019 | 0.004 | 0.016 | 0.032 | 0.000 | 0.017 | 0.000 | 0.007 | 97,976 | pyrrhotite |
| pal0093-269.90-alue7-7 | 38.941 | 59.384 | 0.000 | 0.012 | 0.033 | 0.000 | 0.000 | 0.235 | 0.000 | 0.338 | 0.000 | 0.000 | 0.000 | 0.014 | 0.000 | 0.000 | 0.002 | 0.000 | 98,959 | pyrrhotite |
| pal0093-269.90-alue7-8 | 38.792 | 59.385 | 0.000 | 0.017 | 0.012 | 0.025 | 0.000 | 0.349 | 0.000 | 0.454 | 0.000 | 0.000 | 0.024 | 0.004 | 0.000 | 0.054 | 0.000 | 0.009 | 99,125 | pyrrhotite |
| pal0093-261.05-alue2-1 | 39.294 | 59.822 | 0.130 | 0.000 | 0.102 | 0.152 | 0.000 | 0.487 | 0.256 | 0.578 | 0.295 | 0.091 | 0.399 | 0.128 | 0.218 | 0.410 | 0.175 | 0.102 | 102,639 | pyrrhotite |
| pal0093-261.05-alue2-2 | 39.085 | 58.721 | 0.000 | 0.088 | 0.001 | 0.000 | 0.000 | 0.314 | 0.000 | 0.577 | 0.032 | 0.024 | 0.026 | 0.000 | 0.004 | 0.046 | 0.000 | 0.000 | 98,918 | pyrrhotite |
| Pal0093-261.05-alue3-1 | 38.583 | 59.196 | 0.000 | 0.000 | 0.010 | 0.000 | 0.000 | 0.299 | 0.000 | 0.398 | 0.102 | 0.000 | 0.000 | 0.036 | 0.028 | 0.043 | 0.000 | 0.003 | 98,698 | pyrrhotite |
| Pal0093-261.05-alue4-1 | 37.636 | 58.678 | 0.000 | 0.042 | 0.000 | 0.000 | 0.059 | 0.277 | 0.000 | 0.555 | 0.070 | 0.000 | 0.002 | 0.008 | 0.000 | 0.115 | 0.000 | 0.000 | 97,442 | pyrrhotite |
| Pal0093-263.35-alue1-2 | 38.699 | 58.948 | 0.005 | 0.055 | 0.000 | 0.000 | 0.000 | 0.099 | 0.000 | 0.510 | 0.302 | 0.007 | 0.000 | 0.004 | 0.057 | 0.043 | 0.000 | 0.008 | 98,737 | pyrrhotite |
| Pal0093-263.35-alue2-1 | 52.945 | 46.172 | 0.000 | 0.009 | 0.013 | 0.138 | 0.000 | 0.019 | 0.452 | 0.478 | 0.125 | 0.111 | 0.000 | 0.024 | 0.000 | 0.358 | 0.073 | 0.043 | 100,96 | pyrite |
| Pal0093-263.35-alue2-2 | 33.028 | 29.405 | 0.038 | 0.025 | 0.009 | 0.053 | 0.000 | 0.030 | 0.000 | 0.415 | 36.904 | 0.030 | 0.072 | 0.000 | 0.000 | 0.056 | 0.150 | 0.000 | 100,215 | pentlandite |
| Pal0093-263.35-alue2-3 | 31.143 | 29.121 | 0.000 | 0.042 | 0.000 | 0.229 | 0.000 | 1.332 | 0.377 | 0.373 | 33.326 | 0.163 | 0.089 | 0.079 | 0.044 | 0.271 | 0.269 | 0.110 | 96,968 | pentlandite |
| Pal0093-263.35-alue2-4 | 35.115 | 42.028 | 0.000 | 0.000 | 0.006 | 0.141 | 0.000 | 0.871 | 0.426 | 0.430 | 20.455 | 0.154 | 0.046 | 0.038 | 0.053 | 0.254 | 0.198 | 0.224 | 100,439 | pentlandite |
| Pal0093-263.35-alue2-5 | 38.590 | 59.298 | 0.000 | 0.055 | 0.000 | 0.044 | 0.000 | 0.080 | 0.000 | 0.510 | 0.226 | 0.030 | 0.010 | 0.022 | 0.040 | 0.000 | 0.007 | 0.026 | 98,938 | pyrrhotite |
| Pal0093-263.35-alue3-1 | 53.426 | 46.213 | 0.000 | 0.000 | 0.000 | 0.014 | 0.000 | 0.000 | 0.000 | 0.698 | 0.237 | 0.000 | 0.000 | 0.000 | 0.086 | 0.000 | 0.000 | 0.000 | 100,674 | pyrite |
| Pal0093-263.35-alue3-2 | 34.846 | 29.867 | 0.036 | 0.000 | 0.000 | 0.061 | 0.003 | 0.054 | 0.000 | 0.482 | 0.000 | 0.016 | 33.026 | 0.020 | 0.091 | 0.000 | 0.042 | 0.013 | 98,557 | chalcopyrit |
| Pal0093-263.35-alue3-3 | 39.133 | 58.990 | 0.000 | 0.000 | 0.000 | 0.000 | 0.026 | 0.012 | 0.000 | 0.498 | 0.193 | 0.037 | 0.014 | 0.026 | 0.178 | 0.000 | 0.000 | 0.000 | 99,107 | pyrrhotite |
| Pal0093-263.35-alue3-4 | 2.582 | 1.489 | 0.244 | 1.343 | 0.101 | 0.112 | 0.241 | 0.273 | 0.000 | 0.126 | 0.427 | 83.498 | 0.574 | 0.184 | 0.671 | 0.000 | 0.382 | 0.221 | 92,468 | silver |
| Pal0093-274.05-alue1-2 | 21.365 | 3.622 | 0.222 | 0.053 | 0.025 | 0.000 | 44.985 | 32.177 | 0.158 | 0.331 | 1.267 | 0.080 | 0.154 | 0.049 | 0.127 | 0.050 | 0.153 | 0.065 | 104,883 | cobaltite |
| Pal0093-274.05-alue1-3 | 39.295 | 59.937 | 0.000 | 0.071 | 0.010 | 0.000 | 0.000 | 0.321 | 0.201 | 0.504 | 0.071 | 0.021 | 0.000 | 0.000 | 0.000 | 0.170 | 0.026 | 0.008 | 100,635 | pyrrhotite |
| Pal0093-274.05-alue1-4 | 21.293 | 2.937 | 0.110 | 0.074 | 0.025 | 0.000 | 44.444 | 32.837 | 0.166 | 0.324 | 1.233 | 0.067 | 0.164 | 0.056 | 0.102 | 0.138 | 0.156 | 0.062 | 104,188 | cobaltite |
| Pal0093-274.05-alue1-5 | 22.336 | 4.525 | 0.203 | 0.029 | 0.024 | 0.000 | 43.631 | 31.677 | 0.155 | 0.380 | 1.044 | 0.080 | 0.218 | 0.062 | 0.110 | 0.038 | 0.158 | 0.075 | 104,745 | cobaltite |
| Pal0093-274.05-alue2-1 | 38.899 | 59.848 | 0.000 | 0.000 | 0.000 | 0.033 | 0.000 | 0.148 | 0.000 | 0.431 | 0.000 | 0.000 | 0.000 | 0.000 | 0.000 | 0.154 | 0.000 | 0.000 | 99,513 | pyrrhotite |
| Pal0093-274.05-alue2-2 | 21.264 | 2.853 | 0.000 | 0.000 | 0.022 | 0.000 | 44.578 | 32.185 | 0.000 | 0.121 | 1.157 | 0.000 | 0.000 | 0.000 | 0.000 | 0.033 | 0.012 | 0.000 | 102,225 | cobaltite |
| Pal0093-274.05-alue2-3 | 33.194 | 16.671 | 0.000 | 0.000 | 0.015 | 0.004 | 0.000 | 34.024 | 0.000 | 0.369 | 15.716 | 0.000 | 0.000 | 0.000 | 0.000 | 0.079 | 0.000 | 0.000 | 100,072 | Co-pentlan |
| Pal0093-274.05-alue3-1 | 39.203 | 58.625 | 0.000 | 0.000 | 0.000 | 0.000 | 0.226 | 0.241 | 0.000 | 0.521 | 0.115 | 0.007 | 0.000 | 0.000 | 0.101 | 0.000 | 0.008 | 0.007 | 99,054 | pyrrhotite |
| Pal0093-274.05-alue3-2 | 38.847 | 58.559 | 0.006 | 0.000 | 0.016 | 0.000 | 0.000 | 0.244 | 0.000 | 0.616 | 0.148 | 0.000 | 1.130 | 0.000 | 0.024 | 0.000 | 0.021 | 0.021 | 99,632 | pyrrhotite |
| Pal0093-274.05-alue3-3 | 38.866 | 58.952 | 0.086 | 0.000 | 0.000 | 0.000 | 0.159 | 0.487 | 0.000 | 0.526 | 0.301 | 0.000 | 0.033 | 0.000 | 0.000 | 0.013 | 0.040 | 0.017 | 99,48 | pyrrhotite |
| Pal0093-274.05-alue3-4 | 39.173 | 58.255 | 0.013 | 0.000 | 0.015 | 0.026 | 0.021 | 0.256 | 0.000 | 0.470 | 0.118 | 0.000 | 0.001 | 0.000 | 0.000 | 0.000 | 0.000 | 0.000 | 98,348 | pyrrhotite |
| pal0093-276.70-alue1-1 | 37.983 | 59.139 | 0.000 | 0.017 | 0.001 | 0.026 | 0.000 | 0.151 | 0.000 | 0.375 | 0.210 | 0.014 | 0.000 | 0.000 | 0.000 | 0.016 | 0.000 | 0.000 | 97,932 | pyrrhotite |
| pal0093-276.70-alue1-3 | 37.537 | 59.109 | 0.053 | 0.059 | 0.023 | 0.029 | 0.065 | 0.140 | 0.000 | 0.431 | 0.113 | 0.000 | 0.000 | 0.000 | 0.113 | 0.016 | 0.007 | 0.000 | 97,695 | pyrrhotite |
| pal0093-276.70-alue2-2 | 33.747 | 54.540 | 0.190 | 0.033 | 0.006 | 0.041 | 0.263 | 0.094 | 0.000 | 0.431 | 0.065 | 0.008 | 0.004 | 0.023 | 0.000 | 0.000 | 0.000 | 2.949 | 92,394 | pyrrhotite |
| pal0093-276.70-alue2-3 | 39.194 | 57.807 | 0.015 | 0.000 | 0.000 | 0.014 | 0.000 | 0.169 | 0.000 | 0.384 | 0.027 | 0.005 | 0.114 | 0.004 | 0.032 | 0.000 | 0.000 | 1.612 | 99,377 | pyrrhotite |
| pal0093-276.70-alue2-5 | 39.093 | 59.600 | 0.048 | 0.075 | 0.000 | 0.000 | 0.054 | 0.110 | 0.000 | 0.430 | 0.071 | 0.037 | 0.173 | 0.010 | 0.024 | 0.000 | 0.055 | 0.000 | 99,78 | pyrrhotite |
| pal0093-276.70-alue2-6 | 34.113 | 30.130 | 0.247 | 0.138 | 0.054 | 0.157 | 0.000 | 0.265 | 0.250 | 0.523 | 0.330 | 0.109 | 33.905 | 0.192 | 0.451 | 0.331 | 0.211 | 0.135 | 101,541 | chalcopyrit |
| pal0097-324.8-alue1-1 | 37.460 | 58.990 | 0.231 | 0.163 | 0.076 | 0.147 | 0.000 | 0.299 | 0.351 | 0.572 | 0.509 | 0.073 | 0.334 | 0.146 | 0.386 | 0.385 | 0.186 | 0.107 | 100,415 | pyrrhotite |
| pal0097-324.8-alue3-1 | 38.846 | 58.509 | 0.150 | 0.000 | 0.106 | 0.154 | 0.000 | 0.319 | 0.244 | 0.543 | 0.515 | 0.104 | 0.399 | 0.187 | 0.339 | 0.374 | 0.189 | 0.124 | 101,102 | pyrrhotite |
| pal0097-338.2-alue1-1 | 53.102 | 43.224 | 0.203 | 0.000 | 0.086 | 0.194 | 0.000 | 0.741 | 0.590 | 0.766 | 2.416 | 0.074 | 0.383 | 0.171 | 0.314 | 0.416 | 0.159 | 0.102 | 102,941 | pyrite |
| pal0097-338.2-alue1-2 | 10.611 | 7.673 | 0.248 | 0.000 | 0.148 | 0.349 | 0.054 | 0.352 | 0.086 | 0.167 | 0.460 | 0.179 | 0.557 | 0.197 | 0.581 | 0.808 | 0.250 | 0.193 | 22,913 | missed |
| pal0097-260.73-alue1-1 | 38.773 | 60.541 | 0.062 | 0.100 | 0.000 | 0.000 | 0.054 | 0.094 | 0.000 | 0.514 | 0.020 | 0.008 | 0.033 | 0.003 | 0.056 | 0.000 | 0.000 | 0.001 | 100,259 | pyrite |
| pal0097-260.73-alue1-2 | 34.395 | 30.270 | 0.070 | 0.017 | 0.000 | 0.000 | 0.000 | 0.052 | 0.000 | 0.389 | 0.000 | 0.000 | 33.820 | 0.043 | 0.157 | 0.000 | 0.000 | 0.016 | 99,229 | chalcopyrit |
| pal0097-260.73-alue1-3 | 34.238 | 29.423 | 0.000 | 0.054 | 0.000 | 0.000 | 0.000 | 0.026 | 0.000 | 0.412 | 0.011 | 0.033 | 33.349 | 0.006 | 0.145 | 0.000 | 0.028 | 0.036 | 97,761 | chalcopyrit |
| pal0097-260.73-alue2-1 | 38.611 | 60.040 | 0.000 | 0.021 | 0.000 | 0.000 | 0.000 | 0.122 | 0.000 | 0.447 | 0.040 | 0.000 | 0.011 | 0.024 | 0.000 | 0.000 | 0.000 | 0.000 | 99,316 | pyrrhotite |
| pal0097-260.73-alue2-2 | 38.270 | 59.945 | 0.021 | 0.042 | 0.000 | 0.015 | 0.011 | 0.147 | 0.000 | 0.547 | 0.013 | 0.000 | 0.000 | 0.000 | 0.000 | 0.000 | 0.000 | 0.019 | 99,03 | pyrrhotite |
| pal0097-260.73-alue3-1 | 38.556 | 60.050 | 0.000 | 0.013 | 0.001 | 0.000 | 0.110 | 0.189 | 0.000 | 0.357 | 0.009 | 0.000 | 0.000 | 0.000 | 0.020 | 0.000 | 0.017 | 0.005 | 99,327 | pyrrhotite |
| pal0097-260.73-alue3-2 | 37.731 | 1.930 | 0.250 | 0.064 | 0.017 | 0.504 | 0.227 | 0.067 | 0.000 | 55.343 | 0.125 | 0.000 | 0.274 | 0.006 | 0.259 | 0.267 | 0.023 | 0.023 | 97,11 | molybdenit |
| pal0097-260.73-alue3-3 | 38.918 | 59.476 | 0.039 | 0.000 | 0.000 | 0.000 | 0.091 | 0.144 | 0.000 | 0.474 | 0.011 | 0.019 | 0.045 | 0.020 | 0.000 | 0.059 | 0.000 | 0.000 | 99,296 | pyrrhotite |
| pal0097-260.73-alue3-4 | 38.000 | 60.225 | 0.017 | 0.000 | 0.000 | 0.000 | 0.089 | 0.182 | 0.000 | 0.436 | 0.024 | 0.007 | 0.018 | 0.000 | 0.040 | 0.000 | 0.000 | 0.002 | 99,04 | pyrrhotite |
| pal0100-239.15-alue1-1 | 32.974 | 5.241 | 0.029 | 0.062 | 0.004 | 0.000 | 0.076 | 57.697 | 0.000 | 0.355 | 4.203 | 0.010 | 0.053 | 0.033 | 0.000 | 0.009 | 0.023 | 0.010 | 100,779 | Co-pentlan |
| pal0100-239.15-alue1-2 | 39.185 | 59.389 | 0.008 | 0.000 | 0.001 | 0.033 | 0.094 | 0.261 | 0.000 | 0.396 | 0.034 | 0.000 | 0.055 | 0.000 | 0.000 | 0.000 | 0.037 | 0.000 | 99,493 | pyrrhotite |
| pal0100-239.15-alue1-3 | 33.143 | 7.608 | 0.000 | 0.000 | 0.027 | 0.068 | 0.000 | 55.475 | 0.000 | 0.377 | 4.236 | 0.018 | 0.111 | 0.000 | 0.008 | 0.000 | 0.076 | 0.030 | 101,177 | Co-pentlan |
| pal0100-239.15-alue1-4 | 33.527 | 6.021 | 0.067 | 0.000 | 0.028 | 0.000 | 0.014 | 56.720 | 0.000 | 0.400 | 3.956 | 0.023 | 0.078 | 0.029 | 0.000 | 0.027 | 0.100 | 0.027 | 101,017 | Co-pentlan |
| pal0100-239.15-alue2-1 | 39.715 | 59.535 | 0.029 | 0.071 | 0.000 | 0.015 | 0.024 | 0.357 | 0.000 | 0.379 | 0.075 | 0.000 | 0.015 | 0.000 | 0.004 | 0.021 | 0.013 | 0.009 | 100,262 | pyrrhotite |
| pal0100-239.15-alue2-2 | 36.104 | 29.014 | 0.000 | 0.000 | 0.007 | 0.000 | 0.006 | 29.418 | 0.000 | 0.339 | 3.078 | 0.028 | 0.077 | 0.000 | 0.000 | 0.107 | 0.041 | 0.023 | 98,242 | Co-pentlan |
| pal0100-239.15-alue2-3 | 34.216 | 19.152 | 0.041 | 0.000 | 0.000 | 0.000 | 0.000 | 39.928 | 0.000 | 0.392 | 3.847 | 0.026 | 0.000 | 0.000 | 0.000 | 0.000 | 0.004 | 0.000 | 97,606 | Co-pentlan |
| pal0100-239.15-alue2-4 | 35.934 | 34.346 | 0.059 | 0.025 | 0.025 | 0.000 | 0.008 | 26.961 | 0.000 | 0.407 | 2.301 | 0.025 | 0.000 | 0.000 | 0.000 | 0.022 | 0.011 | 0.000 | 100,124 | Co-pentlan |
| pal0100-239.15-alue3-1 | 34.512 | 29.259 | 0.024 | 0.013 | 0.000 | 0.000 | 0.095 | 0.029 | 0.000 | 0.521 | 0.000 | 0.012 | 32.561 | 0.000 | 0.000 | 0.000 | 0.015 | 0.000 | 97,041 | chalcopyrit |
| pal0100-239.15-alue3-2 | 34.024 | 29.990 | 0.075 | 0.079 | 0.003 | 0.000 | 0.064 | 0.042 | 0.000 | 0.394 | 0.045 | 0.024 | 33.461 | 0.012 | 0.059 | 0.000 | 0.019 | 0.000 | 98,291 | chalcopyrit |
| pal0100-239.15-alue3-3 | 39.216 | 59.471 | 0.034 | 0.000 | 0.000 | 0.000 | 0.067 | 0.388 | 0.000 | 0.452 | 0.000 | 0.012 | 0.000 | 0.000 | 0.000 | 0.000 | 0.000 | 0.000 | 99,64 | pyrrhotite |
| pal0100-239.15-alue3-4 | 33.672 | 11.635 | 0.047 | 0.025 | 0.036 | 0.000 | 0.000 | 48.647 | 0.000 | 0.360 | 5.107 | 0.000 | 0.000 | 0.000 | 0.000 | 0.000 | 0.000 | 0.000 | 99,529 | Co-pentlan |
| pal0097-333.45.alue1-1 | 51.822 | 45.675 | 0.014 | 0.000 | 0.016 | 0.000 | 0.002 | 0.000 | 0.000 | 0.537 | 0.000 | 0.000 | 0.000 | 0.000 | 0.000 | 0.040 | 0.000 | 0.100 | 98,206 | pyrite |
| pal0097-333.45.alue1-2 | 51.776 | 44.785 | 0.000 | 0.030 | 0.007 | 0.007 | 0.002 | 0.085 | 0.000 | 0.437 | 0.058 | 0.027 | 0.041 | 0.012 | 0.061 | 0.000 | 0.000 | 0.233 | 97,561 | pyrite |
| pal0097-333.45.alue1-4 | 51.167 | 44.016 | 0.000 | 0.000 | 0.002 | 0.075 | 0.000 | 0.000 | 0.000 | 0.498 | 0.000 | 0.000 | 0.000 | 0.000 | 0.000 | 0.078 | 0.000 | 0.041 | 95,877 | pyrite |
| pal0097-333.45.alue2-1 | 18.357 | 7.397 | 0.908 | 0.000 | 0.000 | 0.000 | 0.000 | 0.034 | 67.372 | 0.000 | 0.103 | 0.024 | 0.000 | 0.000 | 0.000 | 0.000 | 0.000 | 0.005 | 94,2 | galena |
| pal0097-333.45.alue2-3 | 11.698 | 0.844 | 1.762 | 0.153 | 0.000 | 0.000 | 0.000 | 0.144 | 81.246 | 0.000 | 0.217 | 0.045 | 0.178 | 0.100 | 0.260 | 0.000 | 0.000 | 0.090 | 96,737 | galena |
| pal0097-333.45.alue2-4 | 32.076 | 23.825 | 0.459 | 0.000 | 0.000 | 0.000 | 0.000 | 0.000 | 44.425 | 0.000 | 0.040 | 0.000 | 0.000 | 0.000 | 0.000 | 0.000 | 0.000 | 0.000 | 100,825 | galena |
| pal0097-333.45.alue2-5 | 52.654 | 45.670 | 0.000 | 0.000 | 0.000 | 0.000 | 0.000 | 0.000 | 0.000 | 0.000 | 0.000 | 0.000 | 0.000 | 0.000 | 0.000 | 0.000 | 0.000 | 0.000 | 98,324 | pyrite |
| pal0097-333.45.alue2-6 | 12.470 | 1.215 | 0.822 | 0.000 | 0.000 | 0.000 | 0.000 | 0.038 | 79.698 | 0.000 | 0.000 | 0.087 | 0.000 | 0.012 | 0.000 | 0.000 | 0.000 | 0.001 | 94,343 | galena |
| pal0097-333.45.alue2-7 | 52.218 | 45.542 | 0.000 | 0.000 | 0.000 | 0.000 | 0.000 | 0.000 | 0.269 | 0.590 | 0.000 | 0.000 | 0.000 | 0.000 | 0.000 | 0.105 | 0.000 | 0.000 | 98,724 | pyrite |
| pal0097-333.45.alue2-9 | 52.044 | 44.796 | 0.000 | 0.000 | 0.000 | 0.000 | 0.000 | 0.000 | 0.842 | 0.536 | 0.000 | 0.000 | 0.000 | 0.000 | 0.000 | 0.100 | 0.000 | 0.000 | 98,318 | pyrite |
| pal0097-333.45.alue3-1 | 52.896 | 44.858 | 0.000 | 0.000 | 0.000 | 0.000 | 0.000 | 0.000 | 0.142 | 0.574 | 0.000 | 0.000 | 0.000 | 0.000 | 0.000 | 0.082 | 0.000 | 0.000 | 98,552 | pyrite |
| pal0097-333.45.alue3-3 | 51.427 | 45.338 | 0.000 | 0.000 | 0.000 | 0.000 | 0.000 | 0.000 | 0.000 | 0.553 | 0.000 | 0.000 | 0.000 | 0.000 | 0.000 | 0.000 | 0.000 | 0.000 | 97,318 | pyrite |
| pal0097-333.45.alue4-1 | 53.509 | 46.878 | 0.000 | 0.000 | 0.000 | 0.000 | 0.000 | 0.000 | 0.000 | 0.575 | 0.000 | 0.000 | 0.000 | 0.000 | 0.000 | 0.000 | 0.000 | 0.000 | 100,962 | pyrite |
| pal0097-333.45.alue4-2 | 53.660 | 46.757 | 0.000 | 0.000 | 0.000 | 0.000 | 0.000 | 0.000 | 0.000 | 0.553 | 0.000 | 0.000 | 0.000 | 0.000 | 0.000 | 0.000 | 0.000 | 0.000 | 100,97 | pyrite |
| pal0097-333.45.alue4-3 | 52.772 | 46.102 | 0.000 | 0.000 | 0.000 | 0.000 | 0.000 | 0.000 | 0.000 | 0.608 | 0.000 | 0.000 | 0.000 | 0.000 | 0.000 | 0.001 | 0.000 | 0.000 | 99,483 | pyrite |
| pal0097-333.45.alue4-4 | 53.529 | 45.357 | 0.024 | 0.004 | 0.012 | 0.056 | 0.081 | 0.000 | 0.000 | 0.476 | 0.000 | 0.000 | 0.064 | 0.000 | 0.176 | 0.014 | 0.010 | 0.008 | 99,811 | pyrite |
| pal0097-333.45.alue4-5 | 52.015 | 45.749 | 0.002 | 0.087 | 0.000 | 0.039 | 0.064 | 0.057 | 0.000 | 0.438 | 0.000 | 0.000 | 0.000 | 0.011 | 0.094 | 0.000 | 0.000 | 0.000 | 98,556 | pyrite |
| pal0107-253.6-ALUE1-1 | 52.800 | 45.781 | 0.050 | 0.039 | 0.003 | 0.000 | 0.002 | 0.048 | 0.000 | 0.422 | 0.047 | 0.000 | 0.028 | 0.001 | 0.000 | 0.000 | 0.000 | 0.000 | 99,221 | pyrite |
| pal0107-253.6-ALUE1-3 | 52.494 | 45.918 | 0.066 | 0.000 | 0.000 | 0.021 | 0.000 | 0.061 | 0.000 | 0.543 | 0.063 | 0.000 | 0.000 | 0.000 | 0.049 | 0.000 | 0.000 | 0.000 | 99,215 | pyrite |
| pal0118-381.35-alue1-1 | 38.565 | 59.665 | 0.012 | 0.000 | 0.000 | 0.000 | 0.008 | 0.245 | 0.000 | 0.520 | 0.011 | 0.000 | 0.000 | 0.000 | 0.000 | 0.000 | 0.000 | 0.005 | 99,031 | pyrrhotite |
| pal0118-381.35-alue1-2 | 32.720 | 5.760 | 0.027 | 0.000 | 0.000 | 0.000 | 0.028 | 57.366 | 0.000 | 0.407 | 4.037 | 0.041 | 0.036 | 0.066 | 0.012 | 0.000 | 0.052 | 0.021 | 100,573 | Co-pentlan |
| pal0118-381.35-alue1-5 | 38.685 | 59.364 | 0.031 | 0.000 | 0.000 | 0.004 | 0.037 | 0.200 | 0.000 | 0.392 | 0.005 | 0.005 | 0.000 | 0.016 | 0.000 | 0.000 | 0.000 | 0.000 | 98,739 | pyrrhotite |
| pal0118-381.35-alue1-6 | 30.084 | 7.548 | 0.000 | 0.070 | 0.012 | 0.019 | 0.000 | 50.847 | 0.000 | 0.386 | 7.334 | 0.000 | 0.000 | 0.035 | 0.000 | 0.000 | 0.000 | 0.000 | 96,335 | Co-pentlan |
| pal0118-381.35-alue2-1 | 38.611 | 59.520 | 0.000 | 0.017 | 0.006 | 0.018 | 0.000 | 0.156 | 0.000 | 0.492 | 0.000 | 0.000 | 0.000 | 0.011 | 0.000 | 0.000 | 0.000 | 0.000 | 98,831 | pyrrhotite |
| pal0118-381.35-alue2-3 | 38.263 | 59.194 | 0.000 | 0.034 | 0.000 | 0.033 | 0.000 | 0.181 | 0.000 | 0.431 | 0.004 | 0.000 | 0.000 | 0.009 | 0.000 | 0.000 | 0.000 | 0.011 | 98,16 | pyrrhotite |
| pal0118-381.35-alue2-4 | 28.395 | 12.721 | 0.055 | 0.045 | 0.018 | 0.000 | 0.000 | 40.673 | 0.000 | 0.316 | 6.901 | 0.022 | 0.000 | 0.020 | 0.000 | 0.000 | 0.059 | 0.017 | 89,242 | Co-pentlan |
| pal0118-381.35-alue3-1 | 32.576 | 5.995 | 0.064 | 0.074 | 0.017 | 0.000 | 0.000 | 56.850 | 0.000 | 0.345 | 4.748 | 0.000 | 0.000 | 0.037 | 0.028 | 0.023 | 0.053 | 0.014 | 100,824 | Co-pentlan |
| pal0118-381.35-alue3-2 | 38.507 | 59.861 | 0.036 | 0.034 | 0.017 | 0.000 | 0.000 | 0.190 | 0.000 | 0.414 | 0.024 | 0.000 | 0.000 | 0.009 | 0.000 | 0.073 | 0.024 | 0.008 | 99,197 | pyrrhotite |

| | | | | | | | | | | | | | | | | | | | | | |
|---|---|---|---|---|---|---|---|---|---|---|---|---|---|---|---|---|---|---|---|---|---|
| pal0118-381.35-alue3-3 | 34.827 | 30.215 | 0.000 | 0.101 | 0.014 | 0.000 | 0.000 | 0.011 | 0.000 | 0.465 | 0.000 | 0.000 | 32.915 | 0.001 | 0.047 | 0.146 | 0.038 | 0.032 | 98,812 | chalcopyrit |
| pal0118-381.35-alue3-4 | 34.669 | 30.021 | 0.013 | 0.000 | 0.022 | 0.000 | 0.000 | 0.052 | 0.000 | 0.419 | 0.068 | 0.000 | 33.475 | 0.002 | 0.000 | 0.000 | 0.042 | 0.039 | 98,822 | chalcopyrit |
| pal0118-381.35-alue3-5 | 38.961 | 59.034 | 0.049 | 0.050 | 0.000 | 0.000 | 0.081 | 0.239 | 0.000 | 0.353 | 0.000 | 0.034 | 0.000 | 0.000 | 0.008 | 0.000 | 0.000 | 0.000 | 98,809 | pyrrhotite |
| pal0119-109.5-alue1-1 | 32.942 | 27.755 | 0.085 | 0.000 | 0.008 | 0.000 | 0.113 | 6.091 | 0.000 | 0.385 | 33.005 | 0.027 | 0.056 | 0.000 | 0.085 | 0.000 | 0.147 | 0.000 | 100,699 | Co-pentlan |
| pal0119-109.5-alue1-2 | 39.079 | 58.721 | 0.115 | 0.000 | 0.000 | 0.000 | 0.011 | 0.032 | 0.000 | 0.342 | 0.432 | 0.000 | 0.006 | 0.000 | 0.113 | 0.000 | 0.010 | 0.000 | 98,861 | pyrrhotite |
| pal0119-109.5-alue1-3 | 39.539 | 58.276 | 0.021 | 0.000 | 0.000 | 0.000 | 0.003 | 0.077 | 0.000 | 0.425 | 0.352 | 0.000 | 0.000 | 0.000 | 0.170 | 0.009 | 0.039 | 0.000 | 98,911 | pyrrhotite |
| pal0119-109.5-alue2-1 | 39.538 | 57.881 | 0.051 | 0.076 | 0.017 | 0.044 | 0.003 | 0.092 | 0.000 | 0.504 | 0.411 | 0.014 | 0.000 | 0.008 | 0.000 | 0.019 | 0.000 | 0.012 | 98,67 | pyrrhotite |
| pal0119-109.5-alue2-2 | 33.266 | 27.412 | 0.002 | 0.055 | 0.026 | 0.000 | 0.000 | 6.333 | 0.000 | 0.332 | 32.603 | 0.008 | 0.105 | 0.016 | 0.170 | 0.061 | 0.112 | 0.019 | 100,52 | Co-pentlan |
| pal0119-109.5-alue3-1 | 39.079 | 59.352 | 0.029 | 0.046 | 0.010 | 0.015 | 0.000 | 0.038 | 0.000 | 0.325 | 0.222 | 0.000 | 0.005 | 0.018 | 0.000 | 0.078 | 0.000 | 0.021 | 99,238 | pyrrhotite |
| pal0119-109.5-alue3-2 | 38.267 | 58.974 | 0.039 | 0.143 | 0.000 | 0.011 | 0.013 | 0.051 | 0.000 | 0.460 | 0.232 | 0.000 | 0.000 | 0.004 | 0.000 | 0.000 | 0.000 | 0.126 | 98,32 | pyrrhotite |
| pal0097-261.35-alue1-1 | 13.024 | 6.068 | 0.000 | 0.000 | 0.000 | 0.000 | 28.960 | 5.375 | 0.000 | 0.135 | 19.969 | 0.000 | 0.000 | 0.000 | 0.000 | 0.047 | 0.097 | 0.019 | 73,694 | Co-pentlan |
| pal0097-261.35-alue1-2 | 16.743 | 8.092 | 0.000 | 0.000 | 0.030 | 0.008 | 46.139 | 5.749 | 0.000 | 0.223 | 24.572 | 0.003 | 0.000 | 0.000 | 0.000 | 0.000 | 0.102 | 0.000 | 101,661 | Co-pentlan |
| pal0097-261.35-alue1-3 | 18.127 | 9.353 | 0.000 | 0.000 | 0.041 | 0.053 | 50.228 | 6.555 | 0.000 | 0.151 | 20.127 | 0.005 | 0.000 | 0.004 | 0.062 | 0.005 | 0.073 | 0.000 | 104,784 | Co-pentlan |
| pal0097-261.35-alue1-4 | 38.238 | 59.103 | 0.040 | 0.000 | 0.000 | 0.000 | 0.087 | 0.203 | 0.000 | 0.468 | 0.000 | 0.000 | 0.000 | 0.000 | 0.000 | 0.000 | 0.000 | 0.000 | 97,946 | pyrrhotite |
| pal0097-261.35-alue1-5 | 39.438 | 59.760 | 0.000 | 0.000 | 0.000 | 0.000 | 0.135 | 0.340 | 0.000 | 0.124 | 0.173 | 0.000 | 0.000 | 0.000 | 0.000 | 0.000 | 0.000 | 0.000 | 99,971 | pyrrhotite |
| pal0097-261.35-alue2-1 | 38.549 | 59.069 | 0.000 | 0.000 | 0.000 | 0.000 | 0.000 | 0.000 | 0.000 | 0.457 | 0.236 | 0.000 | 0.000 | 0.000 | 0.000 | 0.088 | 0.000 | 0.000 | 98,399 | pyrrhotite |
| pal0097-261.35-alue2-2 | 37.704 | 57.977 | 0.000 | 0.000 | 0.000 | 0.022 | 0.000 | 0.000 | 0.000 | 0.412 | 0.000 | 0.000 | 0.000 | 0.000 | 0.000 | 0.000 | 0.000 | 0.000 | 96,115 | pyrrhotite |
| pal0097-261.35-alue2-3 | 38.031 | 59.236 | 0.000 | 0.000 | 0.000 | 0.000 | 0.000 | 0.000 | 0.000 | 0.502 | 0.150 | 0.000 | 0.000 | 0.000 | 0.000 | 0.096 | 0.000 | 0.000 | 98,015 | pyrrhotite |
| pal0097-261.35-alue2-4 | 38.719 | 59.934 | 0.000 | 0.051 | 0.000 | 0.082 | 0.027 | 0.079 | 0.000 | 0.361 | 0.194 | 0.000 | 0.006 | 0.000 | 0.004 | 0.010 | 0.014 | 0.018 | 99,499 | pyrrhotite |
| pal0097-272.32-alue1-1 | 53.263 | 46.625 | 0.000 | 0.000 | 0.000 | 0.000 | 0.000 | 0.038 | 0.000 | 0.592 | 0.000 | 0.000 | 0.028 | 0.000 | 0.000 | 0.098 | 0.000 | 0.000 | 100,644 | pyrite |
| pal0097-272.32-alue1-2 | 53.463 | 46.290 | 0.000 | 0.000 | 0.000 | 0.000 | 0.000 | 0.020 | 0.000 | 0.642 | 0.000 | 0.000 | 0.000 | 0.000 | 0.000 | 0.011 | 0.000 | 0.000 | 100,426 | pyrite |
| pal0097-272.32-alue1-3 | 52.960 | 46.046 | 0.000 | 0.000 | 0.000 | 0.058 | 0.000 | 0.035 | 0.000 | 0.526 | 0.000 | 0.000 | 0.010 | 0.000 | 0.000 | 0.018 | 0.000 | 0.000 | 99,653 | pyrite |
| pal0097-272.32-alue1-4 | 53.170 | 46.293 | 0.000 | 0.000 | 0.000 | 0.022 | 0.000 | 0.061 | 0.000 | 0.581 | 0.012 | 0.000 | 0.028 | 0.000 | 0.000 | 0.069 | 0.000 | 0.000 | 100,236 | pyrite |
| pal0097-272.32-alue2-1 | 53.109 | 46.869 | 0.008 | 0.000 | 0.006 | 0.000 | 0.065 | 0.051 | 0.000 | 0.510 | 0.000 | 0.000 | 0.017 | 0.000 | 0.000 | 0.000 | 0.000 | 0.016 | 100,651 | pyrite |
| pal0097-272.32-alue2-2 | 33.713 | 30.155 | 0.050 | 0.004 | 0.031 | 0.049 | 0.006 | 0.093 | 0.000 | 0.440 | 0.044 | 0.045 | 33.435 | 0.026 | 0.119 | 0.000 | 0.069 | 0.053 | 98,332 | chalcopyrit |
| pal0097-272.32-alue2-3 | 39.236 | 59.266 | 0.071 | 0.038 | 0.016 | 0.019 | 0.057 | 0.349 | 0.000 | 0.390 | 0.050 | 0.028 | 0.036 | 0.000 | 0.004 | 0.000 | 0.000 | 0.034 | 99,594 | pyrrhotite |
| pal0097-272.32-alue2-4 | 34.329 | 29.946 | 0.000 | 0.017 | 0.024 | 0.042 | 0.043 | 0.044 | 0.000 | 0.440 | 0.042 | 0.035 | 33.571 | 0.033 | 0.107 | 0.000 | 0.036 | 0.055 | 98,764 | chalcopyrit |
| pal0097-272.32-alue2-5 | 38.886 | 59.264 | 0.021 | 0.000 | 0.000 | 0.067 | 0.052 | 0.308 | 0.000 | 0.469 | 0.041 | 0.031 | 0.005 | 0.000 | 0.000 | 0.000 | 0.026 | 0.042 | 99,212 | pyrrhotite |
| pal0097-272.32-alue2-6 | 38.912 | 58.475 | 0.000 | 0.000 | 0.025 | 0.007 | 0.091 | 0.283 | 0.000 | 0.395 | 0.039 | 0.014 | 0.000 | 0.055 | 0.004 | 0.000 | 0.000 | 0.000 | 98,3 | pyrrhotite |
| pal0097-272.32-alue2-7 | 36.796 | 52.465 | 0.066 | 0.013 | 0.013 | 0.048 | 0.105 | 0.176 | 0.000 | 0.457 | 0.000 | 0.010 | 0.000 | 0.015 | 0.000 | 0.083 | 0.009 | 0.000 | 90,256 | pyrrhotite |
| pal0097-272.32-alue2-8 | 53.227 | 45.779 | 0.031 | 0.018 | 0.020 | 0.029 | 0.015 | 0.015 | 0.000 | 0.571 | 0.000 | 0.000 | 0.000 | 0.000 | 0.000 | 0.032 | 0.000 | 0.000 | 99,737 | pyrite |
| pal0097-272.32-alue3-1 | 39.509 | 58.547 | 0.036 | 0.013 | 0.033 | 0.000 | 0.046 | 0.231 | 0.000 | 0.559 | 0.054 | 0.024 | 0.072 | 0.017 | 0.016 | 0.017 | 0.018 | 0.000 | 99,192 | pyrrhotite |
| pal0097-272.32-alue3-2 | 39.371 | 59.842 | 0.000 | 0.064 | 0.019 | 0.000 | 0.106 | 0.241 | 0.000 | 0.441 | 0.039 | 0.000 | 0.000 | 0.003 | 0.000 | 0.028 | 0.002 | 0.000 | 100,156 | pyrrhotite |
| pal0097-272.32-alue3-3 | 39.078 | 58.579 | 0.000 | 0.043 | 0.005 | 0.018 | 0.092 | 0.242 | 0.000 | 0.435 | 0.053 | 0.006 | 0.000 | 0.000 | 0.078 | 0.000 | 0.002 | 0.002 | 98,633 | pyrrhotite |
| pal0097-272.32-alue3-4 | 34.125 | 28.714 | 0.059 | 0.000 | 0.002 | 0.101 | 0.000 | 0.060 | 0.000 | 0.417 | 0.026 | 0.000 | 32.950 | 0.010 | 0.072 | 0.000 | 0.033 | 0.027 | 96,596 | chalcopyrit |
| pal0097-272.32-alue3-5 | 39.351 | 58.903 | 0.000 | 0.068 | 0.011 | 0.045 | 0.060 | 0.227 | 0.000 | 0.481 | 0.098 | 0.000 | 0.000 | 0.000 | 0.000 | 0.000 | 0.018 | 0.003 | 99,265 | pyrrhotite |
| pal0097-272.32-alue3-6 | 38.215 | 58.410 | 0.018 | 0.034 | 0.000 | 0.000 | 0.041 | 0.226 | 0.000 | 0.515 | 0.026 | 0.016 | 0.000 | 0.000 | 0.057 | 0.000 | 0.017 | 0.000 | 97,575 | pyrrhotite |
| pal0100-283.3-alue2-1 | 19.365 | 6.206 | 0.351 | 0.037 | 0.027 | 0.056 | 48.066 | 17.963 | 0.000 | 0.111 | 12.337 | 0.016 | 0.195 | 0.021 | 0.096 | 0.000 | 0.160 | 0.045 | 105,052 | Co-pentlan |
| pal0100-283.3-alue2-2 | 19.863 | 5.938 | 0.000 | 0.050 | 0.027 | 0.000 | 47.552 | 17.431 | 0.000 | 0.228 | 12.509 | 0.000 | 0.000 | 0.000 | 0.000 | 0.000 | 0.042 | 0.004 | 103,644 | Co-pentlan |
| pal0100-283.3-alue2-3 | 19.688 | 6.024 | 0.000 | 0.000 | 0.000 | 0.000 | 47.539 | 17.646 | 0.000 | 0.222 | 12.367 | 0.015 | 0.000 | 0.002 | 0.000 | 0.117 | 0.090 | 0.007 | 103,717 | Co-pentlan |
| pal0100-283.3-alue3-1 | 33.738 | 26.345 | 0.000 | 0.000 | 0.000 | 0.007 | 0.000 | 5.575 | 0.000 | 0.366 | 34.175 | 0.000 | 0.000 | 0.000 | 0.000 | 0.116 | 0.030 | 0.000 | 100,352 | pentlandite |

# Appendix 2. EPMA results for silicates

| No. | Na2O | ZrO2 | V2O3 | Au | MgO | PbO | MnO | Nb2O5 | Al2O3 | K2O | CoO | Cl | SiO2 | CaO | NiO | AgO | P2O5 | FeO | ZnO | Te | TiO2 | Total |
|---|---|---|---|---|---|---|---|---|---|---|---|---|---|---|---|---|---|---|---|---|---|---|
| PAL0107-253.6- | 0 | 0 | 0 | 0,028 | 0 | 0,013 | 0,021 | 0,042 | 0 | 0 | 0,017 | 0 | 99,049 | 0 | 0 | 0,034 | 0 | 0,052 | 0 | 0,031 | 0,004 | 99,291 |
| PAL0107-253.6- | 0,053 | 0,042 | 0,023 | 0,035 | 16,127 | 0,12 | 0,079 | 0,032 | 18,154 | 9,579 | 0,081 | 0,013 | 37,202 | 0,054 | 0,015 | 0,083 | 0 | 11,619 | 0,104 | 0,047 | 1,903 | 95,362 |
| PAL0107-253.6- | 0,218 | 0,071 | 0 | 0,062 | 0,374 | 0 | 0,042 | 0,036 | 21,498 | 14,702 | 0,014 | 0,003 | 59,564 | 0 | 0 | 0,006 | 0 | 0,519 | 0 | 0 | 0,244 | 97,352 |
| PAL0107-253.6- | 0,041 | 0 | 0,002 | 0,028 | 0,007 | 0 | 0,022 | 0 | 0 | 0,005 | 0 | 0,006 | 99,745 | 0,004 | 0 | 0 | 0 | 0 | 0 | 0 | 0,027 | 99,886 |
| PAL0107-253.6- | 0,224 | 0 | 0,042 | 0,004 | 1,945 | 0 | 0,055 | 0,01 | 30,941 | 10,955 | 0 | 0 | 47,52 | 0,002 | 0 | 0,005 | 0 | 1,758 | 0 | 0 | 0,776 | 94,237 |
| PAL0107-253.6- | 0,118 | 0 | 0,054 | 0,035 | 17,003 | 0 | 0,078 | 0,013 | 18,659 | 9,471 | 0,08 | 0,013 | 36,565 | 0,061 | 0,07 | 0,011 | 0 | 11,323 | 0,041 | 0,005 | 1,888 | 95,485 |
| PAL0119-109.5- | 9,547 | 0 | 0 | 0,041 | 0,01 | 0 | 0 | 0,02 | 22,115 | 0,07 | 0,001 | 0 | 65,731 | 2,708 | 0,003 | 0,03 | 0 | 0,07 | 0,067 | 0 | 0,022 | 100,435 |
| PAL0119-109.5- | 0,077 | 0 | 0,081 | 0,065 | 19,35 | 0 | 0,071 | 0,013 | 15,309 | 9,823 | 0,035 | 0,003 | 40,043 | 0,053 | 0,076 | 0 | 0 | 9,978 | 0,121 | 0,009 | 1,155 | 96,261 |
| PAL0119-109.5- | 0,006 | 0 | 0 | 0,064 | 28,413 | 0 | 0,009 | 0 | 0,534 | 0,009 | 0 | 0 | 61,301 | 0,008 | 0,014 | 0 | 0 | 4,379 | 0,071 | 0 | 0,03 | 94,838 |
| PAL0119-109.5- | 0,117 | 0,059 | 0,017 | 0 | 28,445 | 0 | 0,058 | 0 | 0,596 | 0,008 | 0,033 | 0,007 | 61,527 | 0,023 | 0 | 0 | 0 | 4,109 | 0 | 0,014 | 0,025 | 95,036 |
| PAL0119-109.5- | 0,141 | 0,028 | 0,084 | 0 | 18,767 | 0 | 0,051 | 0 | 15,419 | 9,448 | 0,084 | 0,014 | 40,344 | 0,063 | 0,07 | 0,046 | 0 | 10,082 | 0,038 | 0,018 | 1,085 | 95,779 |
| PAL0119-109.5- | 0,018 | 0,073 | 0,033 | 0 | 25,928 | 0 | 0,025 | 0 | 0,304 | 0,018 | 0,056 | 0,005 | 58,141 | 0,004 | 0 | 0,008 | 0 | 4,309 | 0 | 0 | 0,033 | 88,954 |
| PAL0119-109.5- | 0,012 | 0 | 0,004 | 0 | 0,011 | 0 | 0,006 | 0,038 | 0 | 0,012 | 0 | 0,004 | 98,89 | 0 | 0,037 | 0 | 0 | 0 | 0 | 0,001 | 0,005 | 99,019 |
| PAL0119-109.5- | 0,035 | 0,015 | 0,023 | 0,028 | 0,028 | 0 | 0,015 | 0 | 0,006 | 0 | 0 | 0,006 | 100,536 | 0,011 | 0,007 | 0,013 | 0 | 0,071 | 0 | 0,009 | 0,006 | 100,808 |
| PAL0119-109.5- | 0,038 | 0,072 | 0,026 | 0 | 25,369 | 0 | 0,088 | 0 | 16,94 | 0,007 | 0,012 | 0,009 | 33,544 | 0,017 | 0,075 | 0,009 | 0 | 11,16 | 0,027 | 0,006 | 0,103 | 87,5 |
| PAL0107-263.2- | 0,082 | 0,07 | 0,071 | 0 | 17,621 | 0,06 | 0,028 | 0,003 | 18,707 | 10,349 | 0 | 0,013 | 39,172 | 0 | 0,026 | 0 | 0 | 8,542 | 0 | 0 | 2,34 | 97,081 |
| PAL0107-263.2- | 0 | 0,045 | 0 | 0,052 | 0 | 0 | 0 | 0,003 | 0 | 0 | 0 | 0,003 | 99,293 | 0 | 0 | 0 | 0 | 0 | 0 | 0 | 0 | 99,395 |
| PAL0107-263.2- | 0,264 | 0,056 | 0,045 | 0 | 0 | 0,012 | 0 | 0 | 18,339 | 16,454 | 0 | 0 | 64,581 | 0 | 0 | 0 | 0 | 0 | 0,017 | 0 | 0 | 99,768 |
| PAL0107-263.2- | 0,749 | 0,099 | 0 | 0,053 | 0 | 0 | 0 | 0 | 18,592 | 15,682 | 0,01 | 0 | 65,29 | 0,011 | 0 | 0,009 | 0 | 0,033 | 0 | 0 | 0,003 | 100,531 |
| PAL0107-263.2- | 1,861 | 0,014 | 0,068 | 0 | 6,649 | 0 | 0,029 | 0 | 33,802 | 0 | 0,027 | 0 | 36,287 | 0,834 | 0 | 0 | 0 | 5,85 | 0 | 0 | 0,845 | 86,266 |
| PAL0107-263.2- | 0,012 | 0,136 | 0 | 0 | 0 | 0 | 0 | 0,031 | 0,008 | 0 | 0 | 0 | 99,306 | 0 | 0 | 0 | 0 | 0,118 | 0 | 0 | 0 | 99,611 |
| PAL0107-263.2- | 0,063 | 0 | 0,045 | 0 | 17,489 | 0 | 0,077 | 0,016 | 18,379 | 10,196 | 0,007 | 0,011 | 38,63 | 0,017 | 0 | 0,002 | 0 | 8,662 | 0 | 0 | 2,434 | 96,026 |
| pal0093-244.3-1 | 0 | 0 | 0 | 0,066 | 0 | 0,026 | 0 | 0 | 0 | 0 | 0,03 | 0,003 | 99,322 | 0 | 0,039 | 0 | 0 | 0,052 | 0,012 | 0 | 0 | 99,549 |
| pal0093-244.3-2 | 10,542 | 0 | 0,017 | 0,073 | 0 | 0,075 | 0,012 | 0,017 | 19,718 | 0,057 | 0,028 | 0,003 | 68,566 | 0,122 | 0,043 | 0 | 0 | 0,033 | 0,002 | 0,01 | 0 | 99,317 |
| pal0093-244.3-3 | 0,006 | 0 | 0,002 | 0,014 | 0 | 0,077 | 0 | 0,024 | 0 | 0 | 0,021 | 0,004 | 99,795 | 0 | 0,025 | 0 | 0 | 0,08 | 0 | 0,006 | 0 | 100,053 |
| pal0093-244.3-4 | 10,698 | 0 | 0,015 | 0,083 | 0 | 0 | 0 | 0 | 19,748 | 0,048 | 0,012 | 0 | 68,672 | 0,263 | 0 | 0,013 | 0 | 0 | 0,01 | 0,008 | 0,01 | 99,58 |
| pal0093-248.35- | 0,006 | 0,03 | 0,028 | 0,056 | 0 | 0 | 0 | 0 | 0 | 0 | 0,026 | 0,006 | 99,883 | 0,014 | 0 | 0,023 | 0 | 0 | 0,014 | 0,018 | 0 | 100,103 |
| pal0093-248.35- | 0,012 | 0,03 | 0 | 0,089 | 0 | 0,051 | 0,024 | 0 | 0 | 0 | 0,021 | 0,007 | 99,452 | 0 | 0 | 0,013 | 0 | 0,038 | 0 | 0,012 | 0,008 | 99,755 |
| pal0093-248.35- | 10,392 | 0 | 0,004 | 0 | 0,018 | 0,1 | 0 | 0,055 | 19,935 | 0,037 | 0 | 0,001 | 67,727 | 0,492 | 0,039 | 0,001 | 0 | 0 | 0,075 | 0,025 | 0 | 98,901 |
| pal0093-248.35- | 0 | 0,075 | 0,015 | 0 | 0,007 | 0,026 | 0 | 0,042 | 0 | 0,01 | 0 | 0 | 99,586 | 0 | 0,018 | 0 | 0 | 0 | 0,025 | 0 | 0 | 99,804 |
| pal0093-248.35- | 0,012 | 0,03 | 0,024 | 0 | 0,018 | 0,089 | 0 | 0,031 | 0,003 | 0,025 | 0,003 | 0,003 | 98,81 | 0 | 0,021 | 0 | 0 | 0 | 0,048 | 0 | 0 | 99,116 |
| pal0093-248.35- | 10,171 | 0,133 | 0,002 | 0 | 0,009 | 0 | 0,004 | 0,021 | 19,955 | 0,056 | 0 | 0 | 67,88 | 0,501 | 0 | 0,03 | 0 | 0 | 0 | 0 | 0,018 | 98,78 |
| pal0093-256-AL | 10,326 | 0,059 | 0,002 | 0 | 0 | 0 | 0 | 0,003 | 19,699 | 0,055 | 0,014 | 0 | 67,833 | 0,192 | 0,003 | 0 | 0 | 0,014 | 0 | 0 | 0,016 | 98,216 |
| pal0093-256-AL | 10,495 | 0 | 0 | 0 | 0 | 0,038 | 0,001 | 0 | 20,18 | 0,073 | 0,008 | 0,013 | 68,266 | 0,35 | 0 | 0,006 | 0 | 0,023 | 0 | 0 | 0,028 | 99,478 |
| pal0093-256-AL | 0 | 0 | 0,032 | 0 | 0,029 | 0 | 0 | 0 | 0 | 0,008 | 0,017 | 0,003 | 99,515 | 0,015 | 0 | 0,002 | 0 | 0,076 | 0 | 0,023 | 0,017 | 99,736 |
| pal0093-256-AL | 0,863 | 0 | 0,047 | 0 | 1,18 | 0,012 | 0 | 0,017 | 35,169 | 9,905 | 0,052 | 0 | 46,592 | 0,002 | 0,047 | 0 | 0 | 0,761 | 0,032 | 0,021 | 0,682 | 95,382 |
| pal0093-256-AL | 0,875 | 0 | 0,061 | 0,009 | 1,267 | 0,037 | 0 | 0 | 35,239 | 9,812 | 0,031 | 0,002 | 46,79 | 0,021 | 0,024 | 0 | 0 | 0,751 | 0,068 | 0,036 | 0,845 | 95,868 |
| pal0093-256-AL | 10,461 | 0 | 0,004 | 0 | 0 | 0,013 | 0 | 0,01 | 19,389 | 0,071 | 0 | 0,011 | 68,442 | 0,147 | 0 | 0 | 0 | 0,038 | 0 | 0,026 | 0 | 98,61 |
| pal0093-256-AL | 0,92 | 0 | 0,05 | 0 | 1,175 | 0 | 0,009 | 0 | 34,909 | 9,397 | 0 | 0,005 | 46,445 | 0,012 | 0,051 | 0,005 | 0 | 0,883 | 0 | 0,009 | 0,528 | 94,397 |
| pal0093-256-AL | 0,804 | 0 | 0,037 | 0 | 1,226 | 0,024 | 0 | 0 | 34,437 | 9,35 | 0 | 0,01 | 46,795 | 0,029 | 0,049 | 0,008 | 0 | 0,714 | 0,046 | 0,021 | 0,675 | 94,223 |
| pal0093-256-AL | 0,884 | 0,043 | 0,064 | 0 | 1,083 | 0,037 | 0,035 | 0 | 35,155 | 9,836 | 0,011 | 0 | 47,134 | 0 | 0,04 | 0 | 0 | 0,644 | 0 | 0 | 0,7 | 95,666 |
| pal0093-256-AL | 10,496 | 0,029 | 0 | 0 | 0 | 0,025 | 0,004 | 0 | 19,632 | 0,049 | 0,015 | 0 | 68,141 | 0,233 | 0 | 0,014 | 0 | 0 | 0 | 0 | 0 | 98,638 |
| pal0083-40.85-a | 0,046 | 0 | 0,047 | 0 | 17,637 | 0,084 | 0,032 | 0 | 15,756 | 9,959 | 0,042 | 0,008 | 38,338 | 0,005 | 0,021 | 0,019 | 0 | 12,098 | 0 | 0 | 1,285 | 95,375 |
| pal0083-40.85-a | 0,086 | 0 | 0,041 | 0 | 17,398 | 0 | 0,03 | 0 | 15,526 | 9,732 | 0,024 | 0,007 | 39,121 | 0,011 | 0 | 0 | 0 | 12,491 | 0 | 0 | 1,3 | 95,765 |
| pal0083-40.85-a | 0,046 | 0 | 0,043 | 0 | 17,745 | 0,048 | 0,049 | 0 | 15,836 | 9,765 | 0,065 | 0,01 | 38,817 | 0 | 0 | 0 | 0 | 12,273 | 0,015 | 0 | 1,311 | 96,021 |
| pal0083-40.85-a | 0,046 | 0 | 0,024 | 0,009 | 17,514 | 0,012 | 0,059 | 0,019 | 15,733 | 9,843 | 0,034 | 0,002 | 38,946 | 0,021 | 0,001 | 0 | 0 | 12,475 | 0 | 0 | 1,26 | 95,998 |
| pal0083-40.85-a | 0,053 | 0 | 0,032 | 0 | 17,39 | 0,012 | 0,029 | 0 | 15,99 | 10,022 | 0,037 | 0,005 | 38,552 | 0,012 | 0 | 0 | 0 | 12,698 | 0 | 0 | 1,325 | 96,156 |
| pal0083-40.85-a | 0,961 | 0 | 0 | 0,018 | 15,574 | 0 | 0,019 | 0 | 4,784 | 0,042 | 0 | 0 | 45,426 | 9,361 | 0 | 0 | 0,096 | 7,225 | 0 | 0 | 0,096 | 83,602 |
| pal0083-40.85-a | 0,726 | 0 | 0,068 | 0,009 | 16,809 | 0,024 | 0,042 | 0 | 4,978 | 0,072 | 0,056 | 0,004 | 50,726 | 11,778 | 0 | 0 | 0 | 10,328 | 0 | 0 | 0,191 | 95,81 |
| pal0083-40.85-a | 0,97 | 0 | 0,034 | 0 | 16,687 | 0 | 0,047 | 0 | 5,669 | 0,091 | 0,066 | 0,006 | 50,655 | 11,895 | 0 | 0,031 | 0 | 10,448 | 0 | 0 | 0,276 | 96,874 |
| pal0083-40.85-a | 0 | 0 | 0,081 | 0 | 17,002 | 0,132 | 0,037 | 0 | 16,074 | 8,515 | 0,05 | 0,017 | 37,143 | 0,042 | 0 | 0 | 0 | 13,885 | 0 | 0 | 1,793 | 94,767 |
| pal0083-40.85-a | 0,04 | 0,028 | 0,088 | 0,052 | 16,252 | 0,012 | 0,035 | 0 | 15,368 | 10,265 | 0,061 | 0 | 38,148 | 0 | 0,014 | 0 | 0 | 12,612 | 0 | 0 | 2,047 | 95,022 |
| pal0083-40.85-a | 10,279 | 0 | 0 | 0,005 | 0 | 0 | 0 | 0 | 19,768 | 0,033 | 0 | 0 | 68,657 | 0,191 | 0 | 0 | 0 | 0,038 | 0 | 0 | 0 | 98,971 |
| pal0083-40.85-a | 10,323 | 0 | 0 | 0,037 | 0 | 0,126 | 0 | 0 | 19,727 | 0,031 | 0 | 0 | 68,321 | 0,192 | 0 | 0 | 0 | 0,066 | 0 | 0 | 0 | 98,823 |
| pal0083-40.85-a | 11,211 | 0,029 | 0 | 0 | 0 | 0 | 0,038 | 0 | 19,835 | 0,046 | 0,007 | 0 | 67,794 | 0,199 | 0 | 0,003 | 0 | 0,023 | 0 | 0,025 | 0,012 | 99,222 |
| pal0083-40.85-a | 0,314 | 0 | 0,031 | 0 | 18,506 | 0,036 | 0,119 | 0,01 | 1,198 | 0,068 | 0,04 | 0,016 | 55,785 | 11,967 | 0,024 | 0,009 | 0,099 | 9,254 | 0,112 | 0,072 | 0,14 | 97,796 |
| pal0083-40.85-a | 0,464 | 0,014 | 0,069 | 0,053 | 16,167 | 0 | 0,097 | 0 | 3,828 | 0,163 | 0,108 | 0,008 | 51,68 | 12,384 | 0,018 | 0,032 | 0,11 | 11,387 | 0,14 | 0,083 | 0,396 | 97,199 |
| pal0083-40.85-a | 8,831 | 0,058 | 0 | 0,023 | 2,44 | 0,075 | 0,041 | 0 | 18,417 | 0,043 | 0,045 | 0,012 | 61,066 | 0,229 | 0,057 | 0 | 0 | 6,466 | 0,057 | 0,002 | 0 | 97,859 |
| pal0093-258.95- | 0,84 | 0,057 | 0,078 | 0,049 | 1,104 | 0,086 | 0,012 | 0,04 | 34,396 | 10,044 | 0 | 0,014 | 46,264 | 0,013 | 0 | 0 | 0 | 0,813 | 0,021 | 0 | 0,514 | 94,342 |
| pal0093-258.95- | 0,724 | 0,028 | 0,078 | 0,022 | 1,704 | 0,086 | 0,01 | 0 | 33,049 | 10,046 | 0,007 | 0,012 | 47,506 | 0 | 0,029 | 0 | 0 | 0,677 | 0,036 | 0 | 0,524 | 94,535 |
| pal0093-258.95- | 0,781 | 0,014 | 0,082 | 0,022 | 1,47 | 0 | 0,022 | 0 | 32,666 | 9,715 | 0,018 | 0,028 | 45,947 | 0,027 | 0 | 0,001 | 0 | 0,738 | 0 | 0 | 0,516 | 92,041 |
| pal0093-258.95- | 0,064 | 0,045 | 0,017 | 0 | 0 | 0 | 0,004 | 0 | 0 | 0 | 0,014 | 0 | 99,553 | 0 | 0 | 0 | 0 | 0 | 0 | 0 | 0 | 99,697 |
| pal0093-258.95- | 0,754 | 0,043 | 0,116 | 0,027 | 1,491 | 0,012 | 0 | 0 | 33,059 | 10,059 | 0,029 | 0 | 47,476 | 0 | 0 | 0,002 | 0 | 0,79 | 0,011 | 0 | 0,54 | 94,409 |
| pal0093-258.95- | 0 | 0 | 0 | 0 | 0 | 0 | 0,029 | 0 | 0 | 0 | 0,018 | 0,004 | 99,211 | 0 | 0 | 0,016 | 0 | 0,038 | 0 | 0 | 0,001 | 99,316 |
| pal0093-258.95- | 0,762 | 0,014 | 0,074 | 0 | 1,72 | 0 | 0,016 | 0 | 32,862 | 9,877 | 0,014 | 0,009 | 47,465 | 0,015 | 0,029 | 0 | 0 | 1,084 | 0,03 | 0 | 0,5 | 94,469 |
| pal0093-258.95- | 0 | 0 | 0 | 0 | 0 | 0 | 0 | 0 | 0 | 0,003 | 0,015 | 0,005 | 98,419 | 0,007 | 0,014 | 0 | 0 | 0,08 | 0 | 0 | 0,015 | 98,557 |
| pal0093-258.95- | 0,731 | 0,142 | 0,108 | 0 | 1,291 | 0 | 0,023 | 0,04 | 33,817 | 10,073 | 0 | 0,012 | 46,896 | 0 | 0,001 | 0,005 | 0 | 0,804 | 0,021 | 0,021 | 0,525 | 94,507 |
| pal0093-258.95- | 0 | 0,076 | 0 | 0,014 | 0 | 0 | 0,015 | 0,08 | 0,007 | 0,014 | 0 | 0,002 | 98,656 | 0 | 0 | 0 | 0 | 0 | 0 | 0 | 0 | 98,864 |
| pal0093-258.95- | 0,957 | 0,028 | 0,092 | 0,08 | 0,928 | 0,049 | 0,036 | 0,02 | 34,761 | 9,899 | 0,003 | 0,003 | 45,486 | 0,01 | 0 | 0 | 0 | 0,893 | 0 | 0 | 0,627 | 93,871 |
| pal0093-258.95- | 0,806 | 0,071 | 0,082 | 0,04 | 1,32 | 0 | 0,034 | 0,007 | 34,149 | 10,331 | 0 | 0 | 46,458 | 0,015 | 0,053 | 0 | 0 | 0,743 | 0 | 0 | 0,488 | 94,597 |
| pal0093-258.95- | 0,076 | 0,015 | 0 | 0,019 | 0 | 0 | 0,034 | 0 | 0 | 0,003 | 0 | 0 | 99,289 | 0 | 0,025 | 0 | 0 | 0,028 | 0 | 0 | 0,004 | 99,493 |
| pal0097-260.73- | 10,306 | 0,03 | 0 | 0,041 | 0 | 0 | 0 | 0 | 19,628 | 0,045 | 0 | 0 | 67,959 | 0,181 | 0,05 | 0 | 0 | 0,08 | 0 | 0 | 0 | 98,32 |
| pal0097-260.73- | 9,923 | 0,015 | 0 | 0,009 | 0,013 | 0,025 | 0,019 | 0 | 19,705 | 0 | 0 | 0 | 68,002 | 0,243 | 0,011 | 0 | 0 | 0,014 | 0 | 0 | 0 | 97,979 |
| pal0097-260.73- | 9,732 | 0 | 0,019 | 0,041 | 0 | 0,138 | 0,004 | 0,017 | 19,559 | 0,009 | 0 | 0 | 68,131 | 0,245 | 0,018 | 0,005 | 0 | 0,014 | 0 | 0 | 0 | 97,932 |
| pal0097-260.73- | 1,997 | 0 | 0,084 | 0,075 | 8,568 | 0,072 | 0,17 | 0,039 | 20,001 | 0,038 | 0,102 | 0,014 | 39,322 | 0,075 | 0,104 | 0,059 | 0,04 | 28,436 | 0,14 | 0,072 | 0,206 | 99,611 |
| pal0097-260.73- | 1,868 | 0 | 0,055 | 0,04 | 9,001 | 0 | 0,087 | 0 | 18,721 | 0 | 0,046 | 0,005 | 40,165 | 0,038 | 0,034 | 0 | 0 | 27,507 | 0 | 0 | 0,168 | 97,734 |
| pal0097-260.73- | 1,824 | 0 | 0,08 | 0,004 | 8,928 | 0,024 | 0,108 | 0 | 19,516 | 0,001 | 0,036 | 0,007 | 39,751 | 0,015 | 0 | 0,024 | 0 | 27,816 | 0 | 0 | 0,168 | 98,3 |
| pal0097-260.73- | 1,944 | 0 | 0,027 | 0 | 8,984 | 0,024 | 0,115 | 0 | 19,401 | 0,006 | 0,036 | 0,007 | 39,608 | 0,038 | 0,003 | 0,021 | 0 | 28,266 | 0 | 0 | 0,175 | 98,653 |
| pal0097-260.73- | 1,802 | 0,028 | 0,09 | 0,04 | 8,717 | 0 | 0,115 | 0 | 19,72 | 0,038 | 0,052 | 0,001 | 39,251 | 0,022 | 0 | 0,084 | 0 | 28,233 | 0,051 | 0 | 0,115 | 98,359 |
| pal0097-260.73- | 1,626 | 0,028 | 0,037 | 0,004 | 8,495 | 0,085 | 0,075 | 0 | 20,23 | 0,018 | 0,043 | 0 | 38,961 | 0,011 | 0 | 0,034 | 0,006 | 29,003 | 0,03 | 0 | 0,14 | 98,826 |
| pal0097-260.73- | 2,115 | 0 | 0,088 | 0 | 8,723 | 0 | 0,094 | 0,01 | 19,666 | 0,019 | 0,08 | 0 | 39,3 | 0,053 | 0 | 0,034 | 0 | 28,356 | 0,009 | 0 | 0,182 | 98,729 |
| pal0097-260.73- | 2,09 | 0 | 0,064 | 0,018 | 9,001 | 0,048 | 0,092 | 0 | 19,322 | 0,011 | 0,07 | 0,007 | 39,436 | 0,054 | 0,034 | 0 | 0 | 28,162 | 0,082 | 0 | 0,168 | 98,657 |
| pal0097-260.73- | 0,008 | 0,028 | 0,096 | 0,039 | 14,567 | 0,048 | 0 | 0 | 22,837 | 0 | 0,04 | 0 | 25,281 | 0 | 0 | 0 | 0 | 26,12 | 0 | 0 | 0,078 | 89,142 |
| pal0097-260.73- | 1,588 | 0 | 0,046 | 0,009 | 9,101 | 0,073 | 0,117 | 0 | 18,631 | 0 | 0,087 | 0,007 | 40,286 | 0,025 | 0 | 0 | 0 | 28,095 | 0,129 | 0 | 0,242 | 98,434 |
| pal0097-260.73- | 2,269 | 0,042 | 0,062 | 0 | 8,606 | 0 | 0,105 | 0,03 | 19,489 | 0 | 0,059 | 0 | 39,32 | 0,053 | 0 | 0,002 | 0 | 28,5 | 0,024 | 0,003 | 0,216 | 98,78 |
| pal0097-260.73- | 0,119 | 0 | 0,047 | 0,013 | 15,516 | 0,06 | 0 | 0,046 | 22,939 | 0,002 | 0 | 0,005 | 25,607 | 0 | 0 | 0,013 | 0 | 23,773 | 0 | 0 | 0,086 | 88,225 |
| pal0093-276.7-A | 0,378 | 0,097 | 0,156 | 0 | 13,075 | 0,048 | 0,027 | 0 | 18,066 | 8,03 | 0,09 | 0,009 | 36,38 | 0,099 | 0,051 | 0,02 | 0 | 17,319 | 0,009 | 0,006 | 1,334 | 95,192 |
| pal0093-276.7-A | 0,419 | 0 | 0,134 | 0 | 13,044 | 0 | 0,004 | 0 | 17,522 | 7,925 | 0,057 | 0,007 | 36,296 | 0,071 | 0 | 0 | 0 | 16,898 | 0,028 | 0 | 1,317 | 93,72 |
| pal0093-276.7-A | 0,383 | 0 | 0,113 | 0,009 | 15,888 | 0,037 | 0,097 | 0,007 | 5,123 | 0 | 0,085 | 0 | 51,276 | 0,103 | 0,001 | 0 | 0 | 25,599 | 0,023 | 0 | 0,091 | 98,835 |
| pal0093-276.7-A | 0,34 | 0 | 0,154 | 0 | 12,911 | 0 | 0 | 0,026 | 17,672 | 8,35 | 0,059 | 0,005 | 36,94 | 0 | 0,014 | 0 | 0 | 16,182 | 0,047 | 0 | 1,386 | 94,085 |
| pal0093-276.7-A | 0,329 | 0,07 | 0,085 | 0 | 12,962 | 0,012 | 0,023 | 0,032 | 17,481 | 7,335 | 0,058 | 0,015 | 36,334 | 0,318 | 0,029 | 0,003 | 0 | 17,071 | 0 | 0 | 1,316 | 93,47 |
| pal0093-276.7-A | 0,983 | 0 | 0,009 | 0,049 | 14,72 | 0,036 | 0,177 | 0 | 8,795 | 0,029 | 0,048 | 0,004 | 47,747 | 0,139 | 0 | 0,002 | 0 | 24,963 | 0 | 0 | 0,097 | 97,797 |
| pal0093-276.7-A | 0,243 | 0 | 0 | 0 | 9,288 | 0,062 | 0,019 | 0,007 | 33,485 | 0,002 | 0 | 0,005 | 48,859 | 0 | 0 | 0 | 0 | 7,157 | 0 | 0 | 0 | 99,126 |
| pal0093-276.7-A | 0,543 | 0 | 0,01 | 0,022 | 15,959 | 0 | 0,1 | 0,017 | 5,378 | 0,008 | 0,055 | 0 | 50,88 | 0,112 | 0 | 0,015 | 0 | 26,342 | 0,047 | 0 | 0,037 | 99,525 |
| pal0093-276.7-A | 0,249 | 0 | 0 | 0,005 | 9,198 | 0 | 0 | 0,014 | 33,001 | 0 | 0 | 0 | 48,632 | 0 | 0 | 0 | 0 | 7,037 | 0 | 0 | 0 | 98,136 |
| pal0100-283.3-A | 10,096 | 0,103 | 0 | 0,014 | 0 | 0 | 0 | 0 | 19,291 | 0,052 | 0 | 0 | 66,238 | 0,284 | 0 | 0 | 0 | 0 | 0 | 0 | 0 | 96,078 |
| pal0100-283.3-A | 10,555 | 0 | 0 | 0 | 0,029 | 0,138 | 0,004 | 0,01 | 19,732 | 0,05 | 0 | 0,003 | 67,555 | 0,346 | 0 | 0 | 0 | 0,033 | 0,002 | 0 | 0 | 98,456 |
| pal0100-283.3-A | 0 | 0 | 0 | 0 | 0,011 | 0 | 0 | 0,024 | 0,031 | 0,008 | 0,008 | 0,004 | 98,154 | 0,008 | 0 | 0 | 0 | 0,024 | 0,068 | 0,029 | 0 | 98,368 |
| pal0100-283.3-A | 0 | 0 | 0,034 | 0 | 0,017 | 0 | 0 | 0,045 | 0,034 | 0,007 | 0,001 | 0 | 98,424 | 0 | 0 | 0 | 0 | 0 | 0 | 0 | 0 | 98,562 |

| | | | | | | | | | | | | | | | | | | | | | | | |
|---|---|---|---|---|---|---|---|---|---|---|---|---|---|---|---|---|---|---|---|---|---|---|---|
| pal0100-283.3-A | 0 | 0 | 0,034 | 0 | 0,017 | 0 | 0 | 0,045 | 0,034 | 0,007 | 0,001 | 0 | 98,424 | 0 | 0 | 0 | 0 | 0 | 0 | 0 | 0 | 98,562 |
| pal0100-283.3-A | 10,223 | 0 | 0 | 0 | 0,016 | 0,075 | 0 | 0 | 19,817 | 0,057 | 0,019 | 0,005 | 67,884 | 0,357 | 0,013 | 0 | 0 | 0,042 | 0,04 | 0 | 0,001 | 98,548 |
| pal0100-283.3-A | 10,715 | 0 | 0 | 0,037 | 0 | 0,113 | 0,026 | 0 | 19,681 | 0,071 | 0 | 0,006 | 68,401 | 0,087 | 0,004 | 0,014 | 0 | 0,005 | 0,01 | 0 | 0 | 99,169 |
| pal0100-283.3-A | 0,095 | 0 | 0,161 | 0,083 | 19,608 | 0,072 | 0,025 | 0 | 16,41 | 10,005 | 0,049 | 0,015 | 39,262 | 0,029 | 0,091 | 0,043 | 0 | 8,072 | 0,152 | 0,009 | 1,243 | 95,421 |
| pal0100-283.3-A | 0,157 | 0 | 0,159 | 0,026 | 19,477 | 0,012 | 0,022 | 0 | 16,165 | 9,731 | 0,008 | 0,005 | 39,859 | 0,001 | 0,028 | 0,026 | 0 | 8,265 | 0 | 0 | 1,211 | 95,151 |
| pal0100-283.3-A | 0,182 | 0,042 | 0,148 | 0,07 | 18,994 | 0,048 | 0,067 | 0,007 | 16,532 | 9,786 | 0,037 | 0,002 | 38,95 | 0,005 | 0,035 | 0,041 | 0 | 7,701 | 0,064 | 0 | 1,234 | 93,945 |
| pal0100-283.3-A | 0,088 | 0 | 0,132 | 0,048 | 19,438 | 0,048 | 0,016 | 0 | 16,463 | 9,775 | 0,005 | 0,001 | 39,443 | 0 | 0,017 | 0 | 0 | 7,983 | 0,002 | 0 | 1,194 | 94,653 |
| pal0100-283.3-A | 0,219 | 0,084 | 0,194 | 0 | 19,258 | 0,145 | 0,087 | 0,013 | 16,56 | 9,477 | 0,027 | 0 | 39,335 | 0 | 0,044 | 0,008 | 0 | 7,641 | 0,038 | 0 | 1,218 | 94,348 |
| pal0100-283.3-A | 0 | 0,07 | 0,207 | 0,044 | 19,732 | 0,036 | 0,123 | 0,016 | 15,619 | 10,006 | 0,018 | 0 | 40,185 | 0 | 0 | 0,005 | 0 | 7,742 | 0,015 | 0 | 1,12 | 94,938 |
| pal0100-283.3-A | 2,026 | 0,044 | 0,502 | 0 | 8,64 | 0,025 | 0,051 | 0 | 30,747 | 0,003 | 0 | 0 | 36,709 | 0,393 | 0 | 0,011 | 0 | 2,611 | 0 | 0 | 0,361 | 82,123 |
| pal0100-283.3-A | 2,442 | 0,029 | 0,397 | 0 | 9,112 | 0,012 | 0 | 0,007 | 30,869 | 0,026 | 0,029 | 0 | 37,232 | 0,407 | 0 | 0,019 | 0 | 3,025 | 0,01 | 0 | 0,662 | 84,278 |
| pal0100-239.15 | 0 | 0,071 | 0,034 | 0,075 | 22,55 | 0,073 | 0,036 | 0,003 | 20,055 | 0,049 | 0,088 | 0 | 27,6 | 0,045 | 0,026 | 0,026 | 0 | 16,858 | 0,079 | 0,011 | 0,105 | 87,784 |
| pal0100-239.15 | 0,2 | 0,014 | 0,071 | 0,004 | 16,669 | 0,036 | 0,032 | 0,065 | 14,102 | 9,507 | 0,132 | 0 | 38,924 | 0,115 | 0,073 | 0,026 | 0 | 15,757 | 0,19 | 0,014 | 0,883 | 96,814 |
| pal0100-239.15 | 9,24 | 0 | 0 | 0,091 | 0 | 0,013 | 0 | 0 | 21,928 | 0,042 | 0,015 | 0 | 66,026 | 2,261 | 0 | 0 | 0 | 0,033 | 0 | 0,008 | 0 | 99,657 |
| pal0100-239.15 | 8,827 | 0 | 0 | 0,1 | 0 | 0,025 | 0 | 0,02 | 21,97 | 0,044 | 0 | 0 | 64,556 | 2,569 | 0 | 0 | 0 | 0 | 0 | 0 | 0 | 98,111 |
| pal0100-239.15 | 0 | 0 | 0 | 0,028 | 0 | 0,038 | 0 | 0 | 0 | 0 | 0,019 | 0,003 | 98,72 | 0 | 0 | 0 | 0 | 0,175 | 0,054 | 0 | 0 | 99,036 |
| pal0100-239.15 | 0 | 0 | 0,018 | 0,013 | 23,204 | 0 | 0,039 | 0,017 | 19,728 | 0,04 | 0,089 | 0,004 | 28,88 | 0,02 | 0,046 | 0 | 0 | 16,034 | 0,04 | 0,049 | 0,065 | 88,285 |
| pal0100-239.15 | 0,208 | 0 | 0 | 0 | 27,316 | 0 | 0 | 0 | 1,061 | 0,015 | 0,033 | 0,003 | 59,088 | 0,008 | 0 | 0 | 0 | 5,107 | 0 | 0,013 | 0,036 | 92,887 |
| pal0100-239.15 | 0 | 0 | 0,022 | 0,084 | 22,913 | 0 | 0,065 | 0 | 20,085 | 0,052 | 0,068 | 0 | 26,843 | 0,045 | 0 | 0 | 0 | 15,843 | 0 | 0,035 | 0,088 | 86,143 |
| pal0100-239.15 | 0 | 0 | 0,066 | 0,022 | 21,924 | 0 | 0,023 | 0 | 19,489 | 0,065 | 0,049 | 0,003 | 27,39 | 0 | 0 | 0 | 0 | 16,924 | 0 | 0 | 0,056 | 86,01 |
| pal0100-239.15 | 0,144 | 0 | 0 | 0 | 27,194 | 0 | 0,004 | 0 | 0,567 | 0,003 | 0,019 | 0 | 59,641 | 0,016 | 0,013 | 0 | 0 | 5,988 | 0 | 0 | 0,013 | 93,602 |
| pal0100-239.15 | 0,056 | 0,042 | 0,015 | 0 | 15,861 | 0,024 | 0,027 | 0 | 13,267 | 8,789 | 0,038 | 0,005 | 38,123 | 0,047 | 0,061 | 0 | 0 | 16,516 | 0,032 | 0,011 | 0,964 | 93,877 |
| pal0100-239.15 | 0,085 | 0 | 0 | 0 | 26,788 | 0,012 | 0 | 0,037 | 0,68 | 0,001 | 0,032 | 0 | 60,041 | 0,034 | 0 | 0,042 | 0 | 6,369 | 0,027 | 0,018 | 0,034 | 94,2 |
| pal0100-239.15 | 0 | 0 | 0,098 | 0,013 | 16,235 | 0 | 0,06 | 0 | 13,941 | 9,125 | 0,085 | 0,006 | 38,841 | 0,145 | 0,084 | 0,051 | 0 | 16,11 | 0,147 | 0,056 | 1,259 | 96,255 |
| pal0100-239.15 | 0 | 0,097 | 0,03 | 0,078 | 15,685 | 0 | 0,088 | 0,029 | 13,994 | 9,389 | 0,142 | 0,014 | 38,109 | 0,082 | 0,092 | 0,054 | 0 | 16,397 | 0,192 | 0,026 | 0,999 | 95,494 |
| pal0097-261.35 | 1,526 | 0,028 | 0,031 | 0,013 | 10,481 | 0,024 | 0,179 | 0 | 17,11 | 0,003 | 0,052 | 0 | 41,597 | 0,038 | 0,048 | 0 | 0 | 27,018 | 0,139 | 0 | 0,155 | 98,442 |
| pal0097-261.35 | 0 | 0,014 | 0,01 | 0 | 16,915 | 0 | 0,003 | 0,003 | 22,666 | 0 | 0,024 | 0,003 | 25,4 | 0 | 0,032 | 0 | 0 | 23,272 | 0 | 0 | 0,074 | 88,415 |
| pal0097-261.35 | 0,029 | 0,056 | 0,024 | 0 | 17,049 | 0 | 0,043 | 0 | 22,625 | 0 | 0,028 | 0,004 | 25,484 | 0 | 0,025 | 0 | 0 | 22,83 | 0 | 0 | 0,055 | 88,251 |
| pal0097-261.35 | 1,585 | 0,043 | 0,009 | 0,004 | 10,504 | 0,085 | 0,1 | 0 | 17,852 | 0 | 0,042 | 0 | 41,497 | 0,049 | 0,054 | 0 | 0 | 26,681 | 0,03 | 0 | 0,168 | 98,703 |
| pal0097-261.35 | 0 | 0,06 | 0 | 0 | 0 | 0 | 0 | 0 | 0 | 0 | 0 | 0 | 99,497 | 0 | 0,027 | 0 | 0 | 0 | 0 | 0 | 0 | 99,584 |
| pal0097-261.35 | 1,653 | 0,028 | 0,053 | 0,031 | 11,121 | 0,097 | 0,135 | 0 | 15,896 | 0,014 | 0,04 | 0 | 42,694 | 0,05 | 0,092 | 0 | 0 | 26,563 | 0 | 0 | 0,183 | 98,65 |
| pal0097-261.35 | 1,085 | 0 | 0,023 | 0 | 13,054 | 0 | 0,099 | 0 | 10,543 | 0,018 | 0,035 | 0,002 | 47,042 | 0,03 | 0 | 0,003 | 0 | 26,165 | 0,072 | 0,015 | 0,092 | 98,278 |
| pal0097-261.35 | 0,064 | 0 | 0 | 0 | 0 | 0 | 0 | 0 | 0,025 | 0,009 | 0 | 0 | 99,304 | 0,004 | 0 | 0 | 0 | 0 | 0 | 0 | 0 | 99,406 |
| pal0097-261.35 | 10,217 | 0 | 0 | 0 | 0 | 0 | 0 | 0 | 19,607 | 0,033 | 0 | 0 | 67,777 | 0,167 | 0 | 0 | 0 | 0,085 | 0 | 0 | 0 | 97,886 |
| pal0097-261.35 | 1,151 | 0,184 | 0 | 0,044 | 11,883 | 0 | 0,125 | 0 | 13,208 | 0 | 0,07 | 0 | 44,773 | 0,061 | 0,047 | 0,029 | 0 | 26,789 | 0,004 | 0 | 0,114 | 98,482 |
| pal0093-263.35 | 0,085 | 0,125 | 0 | 0 | 17,43 | 0 | 0,068 | 0 | 15,561 | 9,364 | 0,012 | 0,003 | 37,94 | 0,187 | 0,039 | 0,045 | 0 | 11,206 | 0 | 0 | 1,546 | 93,61 |
| pal0093-263.35 | 7,064 | 0,102 | 0 | 0 | 0 | 0 | 0 | 0,003 | 24,924 | 0,006 | 0 | 0 | 59,666 | 6,292 | 0 | 0,006 | 0 | 0 | 0 | 0 | 0 | 98,063 |
| pal0093-263.35 | 0 | 0,045 | 0 | 0 | 0,008 | 0 | 0 | 0,007 | 0 | 0 | 0,036 | 0 | 100,122 | 0,03 | 0,011 | 0,011 | 0 | 0,147 | 0 | 0 | 0 | 100,417 |
| pal0093-263.35 | 0,159 | 0,042 | 0,024 | 0 | 18,441 | 0 | 0,162 | 0,049 | 14,868 | 8,107 | 0,113 | 0,009 | 39,148 | 0,685 | 0,108 | 0,028 | 0 | 11,997 | 0,11 | 0,017 | 1,713 | 95,778 |
| pal0093-263.35 | 0,192 | 0 | 0 | 0 | 19,621 | 0 | 0,254 | 0,02 | 3,322 | 0,064 | 0,086 | 0 | 54,653 | 12,266 | 0,123 | 0,007 | 0 | 7,482 | 0,105 | 0,03 | 0,102 | 98,327 |
| pal0093-263.35 | 7,155 | 0,159 | 0 | 0 | 0,004 | 0,012 | 0,047 | 0,024 | 24,949 | 0,052 | 0,055 | 0 | 59,923 | 6,617 | 0,028 | 0,013 | 0 | 0,07 | 0 | 0 | 0 | 99,108 |
| pal0093-263.35 | 0,315 | 0,099 | 0,029 | 0,022 | 19,024 | 0 | 0,231 | 0,02 | 3,826 | 0,052 | 0,034 | 0,003 | 52,725 | 11,91 | 0,142 | 0,03 | 0 | 7,559 | 0,01 | 0,023 | 0,073 | 96,126 |
| pal0093-263.35 | 0,118 | 0,07 | 0,064 | 0 | 17,967 | 0 | 0,111 | 0,065 | 16,084 | 9,277 | 0,11 | 0,016 | 38,439 | 0,113 | 0,129 | 0,022 | 0 | 11,255 | 0,053 | 0,027 | 1,621 | 95,537 |
| pal0093-263.35 | 0,098 | 0 | 0,006 | 0,009 | 17,519 | 0,012 | 0,087 | 0 | 16,619 | 10,256 | 0,035 | 0 | 38,912 | 0,042 | 0,1 | 0 | 0 | 10,958 | 0,026 | 0 | 1,675 | 96,354 |
| pal0093-263.35 | 0,137 | 0 | 0 | 0,026 | 17,801 | 0,072 | 0,066 | 0 | 16,36 | 10,014 | 0,031 | 0 | 38,033 | 0,013 | 0,039 | 0 | 0 | 11,178 | 0 | 0 | 1,618 | 95,388 |
| pal0093-263.35 | 0,065 | 0 | 0 | 0,035 | 17,512 | 0 | 0,067 | 0 | 16,071 | 9,879 | 0,019 | 0 | 39,399 | 0,028 | 0,077 | 0 | 0 | 11,03 | 0 | 0 | 1,647 | 95,829 |
| pal0093-263.35 | 0,166 | 0,057 | 0,021 | 0 | 20,295 | 0 | 0,193 | 0 | 2,82 | 0,031 | 0,023 | 0 | 55,925 | 12,539 | 0,11 | 0 | 0 | 7,1 | 0,074 | 0 | 0,091 | 99,445 |
| pal0093-274.05 | 0 | 0,056 | 0,195 | 0 | 17,811 | 0 | 0,116 | 0 | 21,675 | 0,525 | 0,075 | 0,004 | 26,633 | 0,045 | 0,025 | 0 | 0 | 20,387 | 0 | 0 | 0,321 | 87,867 |
| pal0093-274.05 | 1,021 | 0,014 | 0,14 | 0 | 0,806 | 0 | 0 | 0,007 | 34,653 | 9,435 | 0 | 0,003 | 45,013 | 0 | 0,024 | 0 | 0 | 1,365 | 0 | 0 | 0,444 | 92,924 |
| pal0093-274.05 | 8,257 | 0 | 0 | 0,027 | 0,001 | 0,137 | 0,01 | 0,01 | 22,323 | 0,084 | 0 | 0,006 | 64,858 | 3,044 | 0,031 | 0,024 | 0 | 0,127 | 0 | 0 | 0 | 98,938 |
| pal0093-274.05 | 0 | 0,07 | 0,154 | 0,07 | 17,9 | 0,109 | 0,124 | 0,01 | 21,981 | 0,322 | 0,09 | 0,015 | 26,45 | 0,019 | 0,044 | 0,025 | 0 | 20,652 | 0,068 | 0,025 | 0,456 | 88,581 |
| pal0093-274.05 | 0,955 | 0,043 | 0,137 | 0,013 | 0,731 | 0,061 | 0 | 0 | 35,332 | 9,612 | 0,007 | 0,016 | 46,197 | 0,046 | 0,011 | 0,028 | 0 | 1,238 | 0 | 0 | 0,518 | 94,941 |
| pal0093-274.05 | 0 | 0 | 0,197 | 0,009 | 17,707 | 0 | 0,098 | 0 | 21,69 | 0,034 | 0,007 | 0,009 | 26,156 | 0,051 | 0 | 0 | 0 | 21,451 | 0,006 | 0,012 | 0,152 | 87,577 |
| pal0093-274.05 | 0,9 | 0 | 0,252 | 0 | 0,618 | 0 | 0 | 0 | 35,56 | 9,339 | 0 | 0 | 45,109 | 0 | 0 | 0,043 | 0 | 1,098 | 0 | 0 | 0,433 | 93,352 |
| pal0093-274.05 | 0,127 | 0 | 0,266 | 0 | 12,042 | 0 | 0,08 | 0,003 | 19,704 | 8,69 | 0,061 | 0,013 | 35,017 | 0,007 | 0 | 0,022 | 0 | 17,515 | 0,064 | 0,027 | 1,827 | 95,462 |
| pal0093-274.05 | 0,243 | 0 | 0,227 | 0 | 11,741 | 0,06 | 0,042 | 0,003 | 19,893 | 9,515 | 0,069 | 0,007 | 36,297 | 0 | 0 | 0 | 0 | 16,297 | 0,07 | 0 | 1,672 | 96,134 |
| pal0093-274.05 | 0,007 | 0 | 0,235 | 0 | 16,965 | 0,012 | 0,081 | 0 | 21,581 | 0,557 | 0,008 | 0,012 | 25,54 | 0 | 0 | 0,003 | 0 | 20,883 | 0 | 0 | 2,475 | 88,356 |
| pal0093-274.05 | 0,125 | 0 | 0,284 | 0 | 16,956 | 0 | 0,085 | 0 | 21,892 | 0,191 | 0,063 | 0 | 25,989 | 0,015 | 0 | 0 | 0 | 22,754 | 0,002 | 0 | 0,151 | 88,507 |
| pal0093-274.05 | 0,167 | 0,028 | 0,243 | 0,017 | 11,762 | 0 | 0,047 | 0,019 | 19,873 | 9,598 | 0,024 | 0,018 | 36,4 | 0 | 0 | 0,007 | 0 | 16,635 | 0,038 | 0 | 1,651 | 96,523 |
| pal0093-274.05 | 0,028 | 0 | 0,219 | 0 | 11,396 | 0 | 0,088 | 0,01 | 20,443 | 9,416 | 0,034 | 0,006 | 35,368 | 0,02 | 0,057 | 0 | 0 | 16,538 | 0 | 0 | 1,65 | 95,272 |
| pal0093-274.05 | 8,619 | 0,015 | 0 | 0 | 0 | 0 | 0 | 0,01 | 22,249 | 0,049 | 0 | 0,003 | 64,182 | 3,194 | 0 | 0 | 0 | 0 | 0 | 0 | 0 | 98,32 |
| pal0093-274.05 | 0,046 | 57,046 | 0,015 | 22,353 | 1,131 | 0,043 | 0,021 | 0 | 1,894 | 1,014 | 0,02 | 0,009 | 33,241 | 0,247 | 0 | 0,037 | 0,855 | 2,122 | 0,01 | 0,006 | 0,206 | 120,314 |
| pal0092-306.90 | 0,044 | 0 | 0 | 0 | 5,969 | 0 | 1,575 | 0,019 | 0,029 | 0 | 0,018 | 0,008 | 0 | 47,277 | 0,032 | 0,034 | 0,336 | 1,445 | 0,075 | 0 | 0,01 | 56,869 |
| pal0092-306.90 | 0 | 0 | 0,002 | 0 | 0,065 | 0 | 0,885 | 0 | 0,038 | 0,011 | 0 | 0,008 | 0 | 55,967 | 0,033 | 0,046 | 0,431 | 0,272 | 0,056 | 0 | 0,032 | 57,844 |
| pal0092-306.90 | 10,366 | 0 | 0 | 0 | 0,013 | 0 | 0 | 0 | 19,56 | 0,069 | 0 | 0 | 67,177 | 0,096 | 0 | 0,008 | 0 | 0,366 | 0 | 0 | 0 | 97,655 |
| pal0092-306.90 | 0,183 | 0,057 | 0,039 | 0,071 | 0 | 0 | 0,01 | 0 | 18,552 | 16,291 | 0,001 | 0 | 64,816 | 0,007 | 0 | 0,003 | 0 | 0,009 | 0,338 | 0 | 0 | 100,377 |
| pal0092-306.90 | 0,224 | 0,071 | 0,041 | 0,04 | 0 | 0,061 | 0,001 | 0 | 18,734 | 15,963 | 0,004 | 0 | 63,247 | 0 | 0 | 0,026 | 0 | 0,033 | 0,002 | 0 | 0 | 98,447 |
| pal0092-306.90 | 0,727 | 0 | 0,036 | 0,036 | 0 | 0 | 0 | 0 | 18,786 | 15,147 | 0,022 | 0 | 63,514 | 0,038 | 0 | 0 | 0 | 0 | 0 | 0 | 0 | 98,306 |
| pal0092-306.90 | 9,596 | 0,029 | 0 | 0 | 0,111 | 0,025 | 0,006 | 0,027 | 19,826 | 0,074 | 0 | 0,022 | 66,552 | 0,474 | 0,006 | 0 | 0 | 1,374 | 0,109 | 0,001 | 0 | 98,227 |
| pal0118-381.35 | 0,253 | 0,042 | 0,116 | 0,039 | 17,21 | 0,108 | 0,042 | 0,003 | 15,937 | 9,663 | 0,089 | 0,028 | 38,088 | 0,067 | 0,097 | 0,048 | 0 | 12,581 | 0,16 | 0 | 1,213 | 95,778 |
| pal0118-381.35 | 0,185 | 0,014 | 0,081 | 0,022 | 17,398 | 0,144 | 0,052 | 0,003 | 15,719 | 9,533 | 0,061 | 0,022 | 38,709 | 0,034 | 0,065 | 0,025 | 0 | 11,781 | 0,142 | 0 | 1,199 | 95,184 |
| pal0118-381.35 | 0,439 | 0,073 | 0 | 0,032 | 27,155 | 0 | 0,045 | 0,017 | 1,509 | 0 | 0,103 | 0,011 | 59,687 | 0,039 | 0 | 0 | 0 | 5,943 | 0 | 0,033 | 0,041 | 95,125 |
| pal0118-381.35 | 0,007 | 0 | 0,022 | 0,076 | 23,274 | 0 | 0,022 | 0,06 | 21,863 | 0 | 0,069 | 0,021 | 27,181 | 0,043 | 0 | 0,006 | 0 | 14,017 | 0,028 | 0,011 | 0,098 | 86,793 |
| pal0092-222.95 | 0,9 | 0,012 | 0,421 | 0,011 | 0 | 0 | 0,006 | 0,146 | 1,941 | 0,014 | 0 | 0,003 | 15,152 | 10,578 | 0 | 0,026 | 0,035 | 0,028 | 0,022 | 0 | 73,281 | 102,575 |
| pal0092-222.95 | 0,117 | 0,034 | 0 | 0,673 | 0,029 | 0 | 0 | 0,012 | 0,227 | 0 | 0 | 0,02 | 2,855 | 52,793 | 0 | 0,015 | 37,305 | 0 | 0 | 0,015 | 3,679 | 97,769 |
| pal0092-222.95 | 8,814 | 0 | 0 | 0 | 0 | 0 | 0 | 0 | 21,505 | 0,25 | 0 | 0 | 64,07 | 2,121 | 0 | 0 | 0 | 0,005 | 0 | 0 | 0 | 96,765 |
| pal0092-222.95 | 8,949 | 0 | 0 | 0 | 0,004 | 0,025 | 0 | 0,031 | 20,924 | 0,286 | 0 | 0,011 | 66,082 | 1,486 | 0,02 | 0,007 | 0 | 0 | 0,004 | 0,007 | 0,021 | 97,855 |
| pal0092-222.95 | 8,354 | 0,07 | 0,029 | 0,044 | 0,089 | 0,12 | 0,079 | 0,062 | 15,435 | 0,088 | 0,229 | 0,023 | 44,961 | 0,948 | 0,152 | 0,084 | 0,056 | 30,506 | 0,25 | 0,079 | 0,077 | 101,73 |
| pal0092-222.95 | 2,199 | 0,064 | 0,205 | 0,02 | 0,042 | 0,079 | 0,05 | 0,096 | 4,649 | 0,098 | 0,045 | 0,021 | 36,709 | 23,598 | 0,081 | 0,049 | 0,329 | 0,144 | 0,202 | 0,165 | 32,254 | 101,094 |
| pal0092-222.95 | 4,272 | 0 | 0,341 | 0 | 0,004 | 0,044 | 0 | 0,159 | 8,449 | 0,13 | 0,036 | 0 | 26,644 | 2,952 | 0,014 | 0,021 | 0 | 0,106 | 0 | 0 | 61,136 | 104,308 |
| pal0092-222.95 | 0,041 | 0 | 0 | 0 | 0 | 0 | 0 | 0 | 0,273 | 0 | 0 | 0 | 98,374 | 0,045 | 0 | 0 | 0 | 0 | 0 | 0 | 0 | 98,733 |
| pal0092-222.95 | 8,945 | 0 | 0 | 0 | 0,013 | 0 | 0 | 0 | 21,114 | 0,024 | 0 | 0 | 65,347 | 2,206 | 0 | 0 | 0 | 0,014 | 0 | 0 | 0 | 97,663 |
| pal0092-222.95 | 0 | 0,091 | 0 | 0,014 | 0,01 | 0,013 | 0 | 0 | 0 | 0,023 | 0 | 0,005 | 99,708 | 0 | 0,015 | 0,022 | 0 | 0,047 | 0 | 0,04 | 0,014 | 100,001 |
| pal0092-222.95 | 8,831 | 0,088 | 0 | 0,005 | 0 | 0 | 0,04 | 0,003 | 21,569 | 0,054 | 0 | 0,007 | 65,254 | 2,447 | 0,034 | 0,008 | 0 | 0,089 | 0 | 0,009 | 0,044 | 98,48 |
| pal0092-222.95 | 8,073 | 0,102 | 0,013 | 0,014 | 2,503 | 0 | 0,047 | 0,014 | 20,982 | 1,404 | 0,015 | 0 | 61,274 | 2,068 | 0 | 0,018 | 0 | 1,976 | 0,042 | 0,022 | 0,247 | 98,814 |
| pal0092-222.95 | 6,55 | 0,058 | 0,016 | 0 | 5,855 | 0 | 0,079 | 0,007 | 19,347 | 2,761 | 0,033 | 0 | 57,044 | 1,459 | 0 | 0 | 0 | 4,126 | 0 | 0,034 | 0,472 | 97,841 |
| pal0092-222.95 | 0,115 | 0,014 | 0,026 | 0 | 14,237 | 0 | 0,046 | 0 | 12,21 | 5,717 | 0,022 | 0,025 | 40,856 | 0,598 | 0 | 0 | 0 | 8,443 | 0 | 0 | 0,988 | 83,291 |
| pal0092-222.95 | 0,08 | 0,083 | 0,124 | 0 | 17,376 | 0 | 0,075 | 0,013 | 15,736 | 9,438 | 0,073 | 0,004 | 37,705 | 0,03 | 0,01 | 0,029 | 0 | 12,425 | 0,023 | 0,022 | 1,661 | 94,906 |
| pal0092-222.95 | 0,013 | 0,028 | 0,105 | 0,026 | 17,53 | 0,036 | 0,04 | 0,036 | 14,714 | 9,311 | 0,038 | 0 | 38,409 | 0,043 | 0 | 0,008 | 0 | 11,207 | 0,013 | 0 | 1,669 | 93,226 |
| pal0092-222.95 | 0,007 | 0,057 | 0,053 | 0,067 | 24,136 | 0,049 | 0,073 | 0,033 | 20,268 | 0,038 | 0,041 | 0 | 28,438 | 0,004 | 0 | 0 | 0 | 13,567 | 0 | 0 | 0,061 | 86,892 |
| pal0092-222.95 | 0 | 0,029 | 0,049 | 0 | 24,776 | 0,049 | 0,084 | 0,05 | 20,66 | 0,068 | 0,014 | 0 | 29,992 | 0,093 | 0 | 0 | 0 | 13,609 | 0 | 0 | 0,302 | 89,775 |
| pal0092-222.95 | 0 | 0 | 0,089 | 0,009 | 18,143 | 0,036 | 0,12 | 0,006 | 15,137 | 9,936 | 0,047 | 0,007 | 40,225 | 0,085 | 0 | 0,001 | 0 | 11,818 | 0 | 0 | 1,526 | 97,183 |
| pal0092-222.95 | 0 | 0,057 | 0,022 | 0,058 | 21,894 | 0,086 | 0,613 | 0 | 1,864 | 0,057 | 0 | 0 | 53,564 | 0,771 | 0 | 0,012 | 0 | 17,395 | 0 | 0 | 0,025 | 96,418 |
| pal0092-222.95 | 0,332 | 0 | 0,014 | 0 | 19,724 | 0 | 0,2 | 0 | 2,533 | 0,047 | 0,004 | 0 | 54,721 | 11,911 | 0,018 | 0 | 0,035 | 7,409 | 0 | 0 | 0,138 | 97,086 |
| pal0092-222.95 | 0,197 | 0,071 | 0,006 | 0 | 22,026 | 0 | 0,139 | 0,007 | 18,372 | 0,017 | 0,019 | 0,001 | 30,351 | 0,959 | 0 | 0,01 | 0 | 15,815 | 0 | 0 | 0,111 | 88,101 |
| pal0092-222.95 | 0,38 | 0 | 0,021 | 0 | 16,587 | 0 | 0,145 | 0,026 | 10,573 | 0,051 | 0,047 | 0,016 | 37,63 | 3,947 | 0,015 | 0,015 | 0 | 20,892 | 0,047 | 0 | 0,137 | 90,525 |
| pal0092-222.95 | 1,218 | 0,056 | 0,009 | 0 | 15,6 | 0 | 0,193 | 0,007 | 10,293 | 0,17 | 0,045 | 0 | 47,886 | 11,326 | 0,04 | 0,013 | 0,06 | 10,41 | 0,038 | 0,01 | 0,347 | 97,721 |
| pal0092-222.95 | 0,366 | 0 | 0,037 | 0 | 20,254 | 0,11 | 0,196 | 0,016 | 2,514 | 0,02 | 0 | 0 | 55,286 | 11,713 | 0,047 | 0,008 | 0 | 8 | 0,044 | 0,001 | 0,127 | 98,739 |
| pal0092-226.85 | 9,809 | 0 | 0 | 0 | 0 | 0,1 | 0 | 0 | 20,032 | 0,049 | 0 | 0,006 | 67,514 | 0,412 | 0 | 0 | 0 | 0,047 | 0 | 0 | 0 | 97,968 |
| pal0092-226.85 | 0 | 0,015 | 0 | 0 | 0 | 0,141 | 0 | 0,01 | 0,019 | 0 | 0 | 0,001 | 98,767 | 0 | 0 | 0 | 0 | 0,08 | 0 | 0 | 0 | 99,033 |

| | | | | | | | | | | | | | | | | | | | | | | | |
|---|---|---|---|---|---|---|---|---|---|---|---|---|---|---|---|---|---|---|---|---|---|---|---|
| pal0092-226.85- | 10,074 | 0,015 | 0 | 0,028 | 0,012 | 0 | 0 | 0 | 20,006 | 0,1 | 0 | 0 | 67,937 | 0,423 | 0 | 0,002 | 0 | 0,023 | 0 | 0 | 0,013 | 98,633 |
| pal0092-226.85- | 0,006 | 0,086 | 0,014 | 0,062 | 25,811 | 0 | 0,055 | 0 | 17,892 | 0,033 | 0,004 | 0,01 | 29,625 | 0,016 | 0 | 0,002 | 0 | 12,046 | 0 | 0 | 0,05 | 85,71 |
| pal0092-226.85- | 8,596 | 0 | 0,006 | 0,083 | 0,004 | 0 | 0,038 | 0,024 | 17,508 | 0,071 | 0 | 0 | 71,105 | 0,56 | 0 | 0,008 | 0 | 0,028 | 0,054 | 0 | 0 | 98,085 |
| pal0092-226.85- | 0,114 | 0 | 0,068 | 0 | 25,68 | 0 | 0,069 | 0,023 | 20,511 | 0,009 | 0,004 | 0,002 | 28,214 | 0,021 | 0 | 0,002 | 0 | 10,91 | 0,017 | 0 | 0,054 | 85,698 |
| pal0092-226.85- | 5,174 | 0,013 | 0,002 | 0,004 | 0 | 0 | 0,109 | 0,015 | 8,841 | 0,046 | 0 | 0,001 | 28,341 | 32,442 | 0 | 0,004 | 0,402 | 0,08 | 0,023 | 0,073 | 0,005 | 75,575 |
| pal0092-226.85- | 0,057 | 0 | 0,049 | 0,045 | 25,991 | 0 | 0,079 | 0,02 | 22,198 | 0,018 | 0,065 | 0 | 27,85 | 0,006 | 0 | 0 | 0 | 11,513 | 0 | 0,009 | 0,075 | 87,975 |
| pal0092-226.85- | 0,086 | 0 | 0,024 | 0 | 24,265 | 0 | 0,058 | 0,02 | 19,199 | 0 | 0,009 | 0,016 | 29,468 | 0,045 | 0,024 | 0 | 0 | 14,78 | 0,021 | 0,008 | 0,009 | 88,028 |
| pal0092-226.85- | 0,051 | 0 | 0,053 | 0 | 25,328 | 0,012 | 0,084 | 0,003 | 21,664 | 0,046 | 0 | 0,012 | 27,788 | 0,035 | 0,049 | 0 | 0 | 11,612 | 0 | 0 | 0,081 | 86,815 |
| pal0092-226.85- | 0,046 | 0 | 0,041 | 0 | 24,255 | 0 | 0,043 | 0,003 | 18,697 | 0,002 | 0,016 | 0,01 | 29,293 | 0,007 | 0 | 0 | 0 | 14,576 | 0,004 | 0 | 0,011 | 87,002 |
| pal0092-226.85- | 0,121 | 0 | 0,108 | 0 | 18,937 | 0,024 | 0,035 | 0,049 | 16,286 | 9,692 | 0,003 | 0 | 39,199 | 0,023 | 0,017 | 0,021 | 0 | 9,367 | 0,045 | 0 | 1,202 | 95,129 |
| pal0092-226.85- | 0,063 | 0 | 0,068 | 0 | 26,413 | 0,061 | 0,009 | 0,013 | 20,143 | 0 | 0 | 0 | 29,162 | 0,013 | 0 | 0 | 0 | 10,783 | 0 | 0 | 0,01 | 86,738 |
| pal0092-226.85- | 0,051 | 0 | 0,085 | 0,013 | 19,019 | 0,012 | 0,028 | 0 | 16,284 | 10,069 | 0,02 | 0,006 | 39,08 | 0 | 0 | 0 | 0 | 9,458 | 0,064 | 0 | 1,348 | 95,536 |
| pal0092-226.85- | 9,222 | 0 | 0,008 | 0 | 0,023 | 0 | 0 | 0,02 | 21,129 | 0,06 | 0 | 0,002 | 65,946 | 2,045 | 0 | 0,002 | 0 | 0,099 | 0 | 0,004 | 0,002 | 98,562 |
| pal0092-226.85- | 0,059 | 0,043 | 0,113 | 0,035 | 22,84 | 0,012 | 0,017 | 0,03 | 17,971 | 1,811 | 0,046 | 0,017 | 30,58 | 0,08 | 0,017 | 0,03 | 0 | 12,999 | 0 | 0 | 0,299 | 86,995 |
| pal0092-226.85- | 10,054 | 0,015 | 0 | 0,009 | 0,025 | 0,038 | 0 | 0,048 | 19,401 | 0,093 | 0 | 0,004 | 67,67 | 0,018 | 0 | 0,007 | 0 | 0,07 | 0 | 0 | 0,008 | 97,459 |
| pal0093-269.9-A | 0,253 | 0 | 0,148 | 0 | 13,736 | 0 | 0,149 | 0 | 17,448 | 9,528 | 0,081 | 0,008 | 37,199 | 0 | 0 | 0,021 | 0 | 14,899 | 0 | 0 | 1,492 | 94,96 |
| pal0093-269.9-A | 0,196 | 0 | 0,008 | 0 | 5,657 | 0 | 0,075 | 0,02 | 29,566 | 7,572 | 0,039 | 0 | 43,47 | 0,082 | 0 | 0,016 | 0 | 6,887 | 0 | 0 | 0,129 | 93,717 |
| pal0093-269.9-A | 0 | 0 | 0,117 | 0,039 | 13,362 | 0,048 | 0,185 | 0 | 18,127 | 9,318 | 0,03 | 0,006 | 36,926 | 0 | 0,008 | 0 | 0 | 15,921 | 0 | 0 | 1,255 | 95,341 |
| pal0093-269.9-A | 0,015 | 0 | 0,04 | 0 | 18,551 | 0 | 0,187 | 0 | 20,707 | 1,343 | 0,009 | 0 | 28,338 | 0 | 0 | 0,007 | 0 | 17,914 | 0,041 | 0 | 0,594 | 87,746 |
| pal0093-269.9-A | 0 | 0,041 | 0,104 | 0 | 14,303 | 0,167 | 0,125 | 0,013 | 17,485 | 8,137 | 0,085 | 0,01 | 34,807 | 0,009 | 0 | 0,039 | 0 | 16,914 | 0 | 0 | 1,361 | 93,598 |
| pal0093-269.9-A | 0,087 | 0,085 | 0 | 0 | 7,242 | 0,049 | 0,065 | 0,046 | 28,926 | 7,895 | 0 | 0,003 | 42,385 | 0 | 0,036 | 0,007 | 0 | 6,281 | 0 | 0 | 0,048 | 93,154 |
| pal0093-269.9-A | 0,216 | 0 | 0,04 | 0,009 | 3,473 | 0 | 0,03 | 0 | 30,779 | 9,755 | 0 | 0,001 | 45,215 | 0,073 | 0 | 0 | 0 | 3,869 | 0,074 | 0 | 0,079 | 93,613 |
| pal0093-269.9-A | 0,057 | 0 | 0,015 | 0,066 | 0,007 | 0 | 0 | 0 | 0 | 0 | 0,037 | 0 | 99,358 | 0,024 | 0,015 | 0,025 | 0 | 0 | 0,019 | 0,008 | 0 | 99,631 |
| pal0093-269.9-A | 10,861 | 0,029 | 0,036 | 0,005 | 0 | 0 | 0,007 | 0,01 | 19,629 | 0,065 | 0 | 0 | 67,946 | 0,376 | 0 | 0,007 | 0 | 0,07 | 0 | 0,001 | 0,03 | 99,072 |
| pal0093-269.9-A | 0,106 | 0 | 0,184 | 0 | 16,403 | 0 | 0,028 | 0,033 | 19,152 | 0 | 0 | 0,003 | 26,654 | 0 | 0,037 | 0,003 | 0 | 23,352 | 0 | 0,019 | 0,079 | 86,052 |
| pal0093-333.45- | 0,032 | 0 | 0,041 | 0 | 0 | 0,038 | 0 | 0 | 0,021 | 0 | 0 | 0 | 99,048 | 0 | 0,018 | 0,004 | 0 | 0 | 0,044 | 0 | 0,007 | 99,253 |
| pal0093-333.45- | 0,39 | 0,099 | 0 | 0,013 | 0 | 0 | 0 | 0 | 18,681 | 15,441 | 0 | 0 | 62,925 | 0,018 | 0 | 0 | 0 | 0 | 0,059 | 0 | 0,053 | 97,679 |
| pal0093-333.45- | 0,299 | 0 | 0 | 0,035 | 1,661 | 0,109 | 0,052 | 0 | 32,179 | 10,879 | 0,049 | 0 | 47,83 | 0 | 0,017 | 0 | 0 | 1,091 | 0 | 0 | 1,012 | 95,213 |
| pal0093-333.45- | 0,362 | 0 | 0,013 | 0 | 1,587 | 0,012 | 0,02 | 0,033 | 32,462 | 10,597 | 0 | 0 | 47,072 | 0,026 | 0 | 0 | 0 | 1,073 | 0 | 0 | 1,052 | 94,309 |
| pal0093-333.45- | 0 | 0,045 | 0,021 | 0 | 0 | 0,051 | 0 | 0 | 0 | 0,005 | 0,012 | 0,008 | 98,962 | 0 | 0,029 | 0 | 0 | 0 | 0,01 | 0 | 0,023 | 99,164 |
| pal0093-333.45- | 0 | 0 | 0,002 | 0 | 17,108 | 0 | 0,23 | 0 | 20,109 | 0,036 | 0,047 | 0 | 26,506 | 0,019 | 0 | 0,017 | 0 | 21,815 | 0,037 | 0,038 | 1,125 | 87,089 |
| pal0093-333.45- | 0,445 | 0 | 0,032 | 0 | 1,493 | 0 | 0,013 | 0 | 32,808 | 10,415 | 0,04 | 0 | 47,185 | 0,017 | 0 | 0,01 | 0 | 0,993 | 0 | 0 | 1,199 | 94,65 |
| pal0093-266.4-1 | 0,076 | 0 | 0,028 | 0 | 19,55 | 0 | 0,046 | 0 | 22,254 | 0,433 | 0 | 0,004 | 27,226 | 0,003 | 0,015 | 0,03 | 0 | 18,973 | 0 | 0 | 0,382 | 89,019 |
| pal0093-266.4-2 | 0 | 0,166 | 0,031 | 0,017 | 14,081 | 0,036 | 0,064 | 0,019 | 19,941 | 7,76 | 0,016 | 0,014 | 34,427 | 0 | 0 | 0,02 | 0 | 15,952 | 0 | 0 | 1,338 | 93,879 |
| pal0093-266.4-3 | 1,014 | 0 | 0,049 | 0,027 | 1,171 | 0,012 | 0,015 | 0,023 | 33,977 | 9,409 | 0,04 | 0,006 | 47,169 | 0 | 0 | 0,009 | 0 | 1,356 | 0 | 0,014 | 0,456 | 94,746 |
| pal0093-266.4-4 | 0 | 0 | 0,07 | 0,04 | 18,634 | 0 | 0,111 | 0,01 | 21,236 | 0,493 | 0,077 | 0 | 26,431 | 0,034 | 0 | 0,027 | 0 | 18,647 | 0 | 0 | 0,378 | 86,188 |
| pal0093-266.4-5 | 9,976 | 0 | 0 | 0,023 | 0 | 0 | 0,013 | 0,01 | 21,711 | 0,061 | 0,036 | 0 | 64,709 | 2,309 | 0 | 0 | 0,023 | 0,154 | 0 | 0,002 | 0 | 99,027 |
| pal0093-266.4-6 | 10,185 | 0 | 0 | 0 | 0 | 0,012 | 0 | 0 | 21,62 | 0,076 | 0 | 0 | 65,838 | 1,826 | 0 | 0 | 0,012 | 0,009 | 0,019 | 0,006 | 0,006 | 99,609 |
| pal0093-266.4-7 | 1,03 | 0 | 0,006 | 0 | 0,833 | 0 | 0 | 0,023 | 35,127 | 9,38 | 0 | 0,009 | 45,985 | 0,003 | 0 | 0 | 0 | 1,258 | 0,07 | 0 | 0,376 | 94,098 |
| pal0093-266.4-8 | 0,046 | 0,056 | 0,084 | 0 | 17,765 | 0 | 0,08 | 0,062 | 20,38 | 1,306 | 0,032 | 0,01 | 26,97 | 0,042 | 0,026 | 0 | 0 | 18,029 | 0,131 | 0,001 | 2,463 | 87,481 |
| pal0093-266.4-9 | 1,089 | 0 | 0,036 | 0 | 0,764 | 0,122 | 0 | 0,007 | 35,355 | 9,188 | 0,03 | 0,004 | 45,763 | 0,09 | 0 | 0,001 | 0 | 1,384 | 0,053 | 0 | 0,378 | 94,263 |
| pal0093-266.4-1 | 0,061 | 0,028 | 0,085 | 0,013 | 16,632 | 0 | 0,094 | 0 | 21,94 | 3,418 | 0,121 | 0,003 | 30,733 | 0,064 | 0 | 0,017 | 0 | 17,426 | 0,105 | 0 | 0,71 | 91,449 |
| pal0097-324.8-1 | 0 | 0,03 | 0 | 0,023 | 0 | 0 | 0 | 0,021 | 0 | 0,01 | 0,043 | 0,002 | 99,251 | 0,009 | 0 | 0 | 0 | 0 | 0,031 | 0,018 | 0,001 | 99,439 |
| pal0097-324.8-2 | 0,25 | 0 | 0,011 | 0 | 0,14 | 0 | 0,022 | 0 | 21,556 | 14,875 | 0,062 | 0,007 | 60,548 | 0,036 | 0,033 | 0,008 | 0 | 0,276 | 0,169 | 0,016 | 0,268 | 98,275 |
| pal0097-324.8-3 | 0,015 | 0,11 | 0,059 | 0,017 | 9,247 | 0,154 | 0,094 | 0,058 | 18,581 | 10,383 | 0,121 | 0,029 | 38,776 | 0,043 | 0,096 | 0,027 | 0 | 17,404 | 0,2 | 0,04 | 2,657 | 98,104 |
| pal0097-324.8-4 | 0,249 | 0 | 0,032 | 0 | 1,058 | 0 | 0 | 0,053 | 33,41 | 10,779 | 0 | 0 | 46,834 | 0,022 | 0,03 | 0,002 | 0 | 1,143 | 0,036 | 0 | 1,058 | 94,706 |
| pal0097-324.8-5 | 0,293 | 0 | 0,015 | 0,022 | 1,218 | 0,049 | 0 | 0,046 | 33,232 | 10,934 | 0,011 | 0,012 | 46,537 | 0 | 0,029 | 0,001 | 0 | 1,091 | 0 | 0 | 0,964 | 94,451 |
| pal0097-324.8-6 | 0,096 | 0 | 0 | 0 | 0,676 | 0,087 | 0 | 0,01 | 16,597 | 5,639 | 0 | 0,003 | 74,66 | 0 | 0 | 0 | 0 | 0,704 | 0,063 | 0 | 0,451 | 98,985 |
| pal0097-324.8-7 | 0,485 | 0 | 0 | 0 | 0 | 0 | 0,001 | 0 | 18,85 | 16,033 | 0 | 0,001 | 64,899 | 0,001 | 0 | 0,007 | 0 | 0,028 | 0 | 0 | 0,018 | 100,323 |
| pal0097-324.8-8 | 0,23 | 0,014 | 0,07 | 0,009 | 1,339 | 0 | 0,02 | 0 | 32,646 | 11,011 | 0 | 0 | 46,643 | 0 | 0 | 0 | 0 | 1,231 | 0 | 0 | 0,982 | 94,195 |
| pal0097-324.8-9 | 0,07 | 0 | 0,073 | 0,06 | 10,075 | 0 | 0,133 | 0 | 18,212 | 9,57 | 0,046 | 0,02 | 35,219 | 0,025 | 0,075 | 0,041 | 0 | 18,639 | 0,082 | 0 | 3,041 | 95,376 |
| pal0097-324.8-1 | 0,128 | 0,028 | 0,028 | 0,013 | 1,401 | 0,097 | 0 | 0 | 32,282 | 11,045 | 0 | 0,003 | 47,38 | 0 | 0 | 0 | 0 | 1,38 | 0,028 | 0 | 0,982 | 94,794 |
| pal0097-272.32- | 11,115 | 0 | 0 | 0 | 0 | 0,063 | 0 | 0 | 19,837 | 0,032 | 0 | 0 | 67,977 | 0,332 | 0 | 0 | 0 | 0,005 | 0,002 | 0 | 0 | 99,363 |
| pal0097-272.32- | 10,446 | 0 | 0 | 0,005 | 0 | 0,063 | 0 | 0 | 20,377 | 0,028 | 0 | 0 | 66,773 | 1,111 | 0 | 0,008 | 0 | 0,047 | 0 | 0 | 0 | 98,858 |
| pal0097-272.32- | 0,118 | 0,055 | 0,018 | 0 | 14,264 | 0 | 0,142 | 0,045 | 18,066 | 9,236 | 0,049 | 0,008 | 36,552 | 0 | 0 | 0 | 0 | 14,568 | 0,038 | 0 | 1,031 | 94,188 |
| pal0097-272.32- | 0,037 | 0,069 | 0,045 | 0 | 14,15 | 0 | 0,119 | 0,055 | 18,724 | 9,447 | 0,059 | 0,01 | 37,093 | 0 | 0 | 0 | 0 | 14,832 | 0,086 | 0 | 1,008 | 95,732 |
| pal0097-272.32- | 0 | 0,07 | 0,008 | 0 | 19,544 | 0 | 0,227 | 0,033 | 22,254 | 0,001 | 0,017 | 0,002 | 26,304 | 0 | 0 | 0 | 0 | 19,952 | 0 | 0 | 0,1 | 88,512 |
| pal0097-272.32- | 0 | 0 | 0,037 | 0,026 | 14,525 | 0,036 | 0,078 | 0,026 | 17,916 | 9,661 | 0,063 | 0 | 37,388 | 0 | 0 | 0,011 | 0 | 14,291 | 0 | 0 | 1,135 | 95,193 |
| pal0097-272.32- | 0 | 0 | 0,035 | 0,069 | 14,332 | 0,048 | 0,076 | 0,013 | 17,904 | 8,672 | 0,061 | 0 | 36,088 | 0 | 0 | 0,003 | 0 | 15,083 | 0 | 0,004 | 1,315 | 93,703 |
| pal0097-338.2-1 | 0 | 0 | 0 | 0 | 0 | 0,064 | 0 | 0 | 0,006 | 0 | 0 | 0 | 98,536 | 0 | 0 | 0 | 0 | 0 | 0 | 0 | 0 | 98,606 |
| pal0097-338.2-2 | 0,191 | 0 | 0,019 | 0 | 1,417 | 0 | 0 | 0,036 | 32,796 | 10,645 | 0 | 0,005 | 46,769 | 0 | 0,026 | 0 | 0 | 0,966 | 0 | 0 | 0,917 | 93,786 |
| pal0097-338.2-3 | 0,371 | 0 | 0 | 0 | 0 | 0,024 | 0 | 0 | 18,609 | 15,962 | 0,026 | 0,009 | 64,1 | 0 | 0,081 | 0,001 | 0 | 0,056 | 0 | 0 | 0 | 99,237 |
| pal0097-338.2-4 | 0,323 | 0 | 0,03 | 0 | 0,962 | 0,012 | 0 | 0 | 34,316 | 10,895 | 0,001 | 0,011 | 45,889 | 0 | 0,015 | 0,007 | 0 | 0,793 | 0,008 | 0 | 1,146 | 94,406 |
| pal0097-338.2-5 | 0,242 | 0,071 | 0 | 0 | 2,069 | 0 | 0 | 0,056 | 31,292 | 10,643 | 0,026 | 0,007 | 48,403 | 0,018 | 0,006 | 0 | 0 | 1,055 | 0,019 | 0 | 0,778 | 94,683 |
| pal0097-338.2-6 | 0,473 | 0,113 | 0 | 0 | 0 | 0,024 | 0,025 | 0,016 | 18,234 | 15,616 | 0,036 | 0,004 | 63,785 | 0,018 | 0,019 | 0 | 0 | 0,014 | 0 | 0 | 0,007 | 98,383 |
| pal0097-338.2-7 | 0,19 | 0 | 0,008 | 0 | 1,58 | 0 | 0,003 | 0,04 | 32,97 | 10,939 | 0,026 | 0,002 | 47,255 | 0 | 0,003 | 0 | 0 | 0,793 | 0 | 0 | 0,938 | 94,747 |
| pal0093-261.05- | 1,179 | 0 | 0 | 0 | 0,915 | 0 | 0,007 | 0 | 34,993 | 9,302 | 0 | 0 | 47,014 | 0,039 | 0,01 | 0 | 0 | 1,002 | 0,065 | 0 | 0,672 | 95,198 |
| pal0093-261.05- | 0 | 0 | 0 | 0 | 17,024 | 0 | 0,053 | 0 | 24,18 | 2,353 | 0,015 | 0,005 | 30,448 | 0,038 | 0,022 | 0,007 | 0 | 11,197 | 0,006 | 0 | 0 | 85,347 |
| pal0093-261.05- | 0 | 0,075 | 0,013 | 0 | 0 | 0 | 0,015 | 0 | 0 | 0,008 | 0 | 0,003 | 98,719 | 0 | 0 | 0 | 0 | 0,09 | 0,04 | 0 | 0 | 98,962 |
| pal0093-261.05- | 0,013 | 0,075 | 0,036 | 0,037 | 0 | 0,051 | 0 | 0 | 0 | 0,008 | 0 | 0,003 | 99,472 | 0,002 | 0,031 | 0 | 0 | 0,042 | 0 | 0 | 0,024 | 99,793 |
| pal0093-261.05- | 0,93 | 0 | 0,044 | 0,053 | 1,59 | 0,024 | 0 | 0 | 32,742 | 9,043 | 0,042 | 0,009 | 48,083 | 0,1 | 0,036 | 0,005 | 0 | 0,98 | 0 | 0 | 0,706 | 94,385 |
| pal0093-261.05- | 1,132 | 0,128 | 0,055 | 0,044 | 1,069 | 0,012 | 0,016 | 0 | 34,011 | 9,478 | 0,044 | 0,018 | 45,82 | 0,032 | 0,007 | 0,003 | 0 | 1,031 | 0,008 | 0,004 | 0,562 | 93,47 |

**Appendix 3. EPMA standards**

Standard used in the silicate-oxide mode

| Element | X-ray | Crystal | CH | Acc.v | Peak | Pos. | BG_L | BG_U |
|---|---|---|---|---|---|---|---|---|
| Na | Ka | TAP | 1) | 15.0 | 129.515 | 1.19101 | 5.000 | 5.000 |
| Zr | La | PETJ | 2) | 15.0 | 194.437 | 0.60705 | 5.000 | 5.000 |
| V | Ka | LIFH | 4) | 15.0 | 174.379 | 0.25036 | 5.000 | 5.000 |
| Au | Ma | PETH | 5) | 15.0 | 187.056 | 0.58400 | 3.000 | 3.000 |
| Mg | Ka | TAP | 1) | 15.0 | 107.249 | 0.98900 | 5.000 | 5.000 |
| Pb | Ma | PETJ | 2) | 15.0 | 169.278 | 0.52860 | 4.000 | 4.000 |
| Mn | Ka | LIFH | 4) | 15.0 | 146.490 | 0.21018 | 5.000 | 5.000 |
| Nb | La | PETH | 5) | 15.0 | 183.337 | 0.57243 | 5.000 | 5.000 |
| Al | Ka | TAP | 1) | 15.0 | 90.347 | 0.83393 | 5.800 | 5.800 |
| K | Ka | PETJ | 2) | 15.0 | 119.816 | 0.37414 | 5.000 | 5.000 |
| Co | Ka | LIFH | 4) | 15.0 | 124.753 | 0.17890 | 5.000 | 5.000 |
| Cl | Ka | PETH | 5) | 15.0 | 151.455 | 0.47278 | 5.000 | 5.000 |
| Si | Ka | TAP | 1) | 15.0 | 77.074 | 0.71254 | 5.000 | 5.000 |
| Ca | Ka | PETJ | 2) | 15.0 | 107.547 | 0.33584 | 5.000 | 4.500 |
| Ni | Ka | LIFH | 4) | 15.0 | 115.636 | 0.16579 | 5.000 | 5.000 |
| Ag | La | PETH | 5) | 15.0 | 133.084 | 0.41544 | 4.000 | 4.000 |
| P | Ka | TAP | 1) | 15.0 | 66.479 | 0.61570 | 4.500 | 5.000 |
| Fe | Ka | LIF | 2) | 15.0 | 134.661 | 0.19360 | 4.000 | 4.000 |
| Zn | Ka | LIFH | 4) | 15.0 | 100.140 | 0.14352 | 5.000 | 5.000 |
| Te | La | PETH | 5) | 15.0 | 105.386 | 0.32892 | 4.000 | 4.000 |
| Ti | Ka | PETH | 5) | 15.0 | 88.130 | 0.27485 | 1.300 | 5.000 |

Standards used in the sulphide mode

| Element | X-ray | Crystal | CH | Acc.v | Peak | Pos. | BG_L | BG_U |
|---|---|---|---|---|---|---|---|---|
| Se | La | TAP | 1) | 15.0 | 97.447 | 0.89900 | 1.900 | 2.500 |
| U | Ma | PETJ | 2) | 15.0 | 125.150 | 0.39100 | 5.000 | 5.000 |
| V | Ka | LIFH | 4) | 15.0 | 174.379 | 0.25036 | 5.000 | 5.000 |
| Au | Ma | PETH | 5) | 15.0 | 187.056 | 0.58400 | 3.000 | 3.000 |
| As | La | TAP | 1) | 15.0 | 104.904 | 0.96709 | 5.000 | 5.000 |
| S | Ka | PETJ | 2) | 15.0 | 172.088 | 0.53722 | 5.000 | 5.000 |
| Co | Ka | LIFH | 4) | 15.0 | 124.757 | 0.17890 | 5.000 | 5.000 |
| Pb | Ma | PETH | 5) | 15.0 | 169.270 | 0.52860 | 2.500 | 3.500 |
| Mo | La | PETJ | 2) | 15.0 | 173.182 | 0.54066 | 5.000 | 5.000 |
| Ni | Ka | LIFH | 4) | 15.0 | 115.618 | 0.16579 | 5.000 | 5.000 |
| Ag | La | PETH | 5) | 15.0 | 133.084 | 0.41544 | 4.000 | 4.000 |
| Fe | Ka | LIF | 2) | 15.0 | 134.673 | 0.19360 | 4.000 | 4.000 |
| Cu | Ka | LIFH | 4) | 15.0 | 107.503 | 0.15406 | 5.000 | 5.000 |
| Sb | La | PETH | 5) | 15.0 | 110.196 | 0.34394 | 3.000 | 3.000 |
| Zn | Ka | LIF | 2) | 15.0 | 99.807 | 0.14352 | 5.000 | 5.000 |
| Bi | Ma | PETH | 4) | 15.0 | 163.879 | 0.51180 | 5.000 | 4.000 |
| Te | La | PETH | 5) | 15.0 | 105.386 | 0.32892 | 4.000 | 4.000 |
| Ti | Ka | PETH | 5) | 15.0 | 88.147 | 0.27485 | 1.300 | 4.000 |

**Appendix 4. Petrographic descriptions of the studied samples**

**Sample PAL0093-244.30**

Sample is from an albitised and chloritised metasedimentary rock. Granoblastic matrix comprises of albite and quartz with accessory chlorite, sericite, biotite and apatite. Albite has recrystallised, but not achieved idiomorphism. Some albite grains show twinning. Chlorite occurs as clusters. Albitisation seem to be early compared to later chloritisation and sulphidation. Pyrrhotite is the main sulphide with pyrite inclusions, cobaltite grains and minor grains of chalcopyrite and sphalerite. Pyrrhotite locally shows Co-pentlandite exsolution lamellae. Rutile and ilmenite are also present and could be part of the original sediment.

Gold content in the sample interval is 0.61ppm.

**Sample PAL0093-248.35**

The sample represents the same rock interval that sample PAL0093-244.30. It is an albitised, chloritised and sulphidised metasediment. Matrix is equigranular granoblastic quartz and albite. Accesory minerals are chlorite, biotite, apatite. Opaque minerals include pyrrhotite, pyrite, chalcopyrite, co-pentlandite as flames in pyrrhotite, molybdenite, sphalerite, galena and uranitite. The large uraninite grains are older than the sulphidation in which pyrrhotite brecciates them and forms mixed grains.

Gold content: 0.96ppm

**Sample PAL0093-256**

Sample represents a K-altered metasedimentary rock. Main minerals are granoblastic quartz and albite matrix, quartz being the dominant one with lepidoblastic sericite. The sericitisation is very intense and occurs as layers. Accessory biotite, rutile and apatite. Albitisation is early and sulphidation and sericitisation are later in roughly the same event. Sulphides include pyrrhotite, pyrite, cobaltite, chalcopyrite, molybdenite, sphalerite and co-pentlandite in pyrrhotite as exsolution lamellae. Quartz grains around the sulphides are bigger than in the matrix indicating recrystallisation.

Gold content: 6.39ppm

**Sample PAL0093-258.95**

Sample represents same rock unit than previous sample (PAL0093-256). Granoblastic quartz matrix have been recrystallised in the sulphidisation, this is indicated by the larger grains only around the sulphide veins, no albite detected. Sericitisation is pervasive and intense and some microfolding can be seen from it. Accessory minerals include zircons and rutile. Main sulphides are pyrrhotite, pyrite, chalcopyrite, co-pentlandite and cobaltite. Cobaltite occurs as fine-grained idiomorphic grains.

Gold content: 115 ppm

**Sample PAL0093-261.05**

Sample represents the sme rock interval than PAL0093-256 and PAL0093-258.95. Granoblastic quartz in abundant sericite and some chlorite.

Layered structure is obvious, with somewhat oriented quartz grains are layered with the oriented sericite around them. Accessory minerals include biotite and rutile. Opaque minerals include pyrrhotite, pyrite chalcopyrite and disintegrated uraninite with small grains of galena. Pyrrhotite has also partly disintegrated.

Gold content: 2.65 ppm

**Sample PAL0093-266.40**

The sample represents a K-altered metasedimentary rock. Very similar to samples PAL0093-261.05 and PAL0093-258.95 except with more albitisation. Main minerals are equigranular albite and quartz, more albite than quartz, and sericite. Accessory minerals include biotite, cordierite with slight chloritisation, rutile and apatite. Originally an albitised metasediment, which has later on sericitised and sulphidised in the same event. Grainsize and shapes of sericite varies. Fine grained sericite is occurs only next to intense pinitisation of cordierite. There is some unaltered biotite, but, partly chloritised, biotite also occurs. Sulphidation is contemporary with mineralisation. Cordierite is poikiloblastic and pinitised. Cobaltite occurs as fine-grained semi-idiomorphic dissemination. Some tiny Au grains among quartz grains. Biotite is turning to some Al-rich chlorite.

Gold content: 5.67 ppm

**Sample PAL0093-269.90**

Sample is from an albitised metasedimentary rock taken from a hydrothermal breccia. Main minerals include granoblastic albite, quartz and lepidoblastic biotite, chlorite and muscovite. Early albitisation is followed by metamorphic biotitisation and minor chloritisation. Metamorphisis also causes amphibolisation, indicated by amphibole porphyroblasts. These pophyroblasts have since altered totally and very intensively into chlorite, biotite and in places rutile. Chlorite and biotite are a in fine-grained mess, but the shape of amphibole porphyroblasts have survived, some muscovite in there as well. In this alteration process sulphides were formed, but also coarse-grained later sulphides exist. Cobaltite exists typically as fine-grained almost idiomorphic grains, earlier than the late coarse grained pyrrhotite.

Gold content: 0.57

**Sample PAL0093-274.05**

Sample represents K-altered metasedimentary rock. Main minerals include, albite/oligoclase (based on EPMA results), sericite, quartz and biotite. Accessory minerals include chlorite, cordierite, tourmaline, rutile and apatite. Early albitisation is followed by intense sericitisation together with sulphidation with minor chloritisation. Tourmaline comes in with the same process and cordierite is chloritised and pinitised. Sulphides include pyrrhotite, cobaltite, pyrite, chalcopyrite, molybdenite, co-pentlandite, and galena which occurs with uraninite. Precursor of the rock is albitised metasediment, which has later sericitised, biotitised with minor chloritised and sulphidised roughly in the same event. This event is also associated with tourmalisation. Some of the sulphides (entirely pyrrhotite) are within the cleavages and among the micas. Cordierite is poikiloblastic and variously pinitised. Layered structure can be seen from the rock.

Gold content: 6.43ppm

**Sample PAL0093-276.70**

Sample is from Mg-Fe rich amphibole metasedimentary rock. Main minerals are cordierite and amphiboles with accessory quartz, biotite, sericite, chlorite, tourmaline, rutile, magnetite, zircon and apatite. Sulphides include pyrrhotite and chalcopyrite. Precursor of the rock has most probably been very Mg-rich sedimentary rock as suggested by granoblastic texture and remnants of quartz within cordierite.

**Sample PAL0097-260.73**

Sample is from a hydrothermally altered Mg-Fe amphibole metasedimentary rock. Granoblastic albite matrix with oriented amphiboles and biotite. Amphiboles and biotite look hydrothermal. Accessory minerals include quartz, chlorite, zircon, uraninite and rutile. Some of the zircons seem to be hydrothermal due to lack of zonation in the alteration halo and very clear edges.

Gold content: 4.1ppm

**Sample PAL0097-261.35**

Sample is from a hydrothermally altered Mg-Fe amphibole metasedimentary rock. Main minerals include albite, amphiboles and biotite. Originally a silty sediment that got albitised and later amphibolised, biotitised and sulphidised in the same event. Sulphides include pyrrhotite, gersdorffite (EMPA), pyrite and cobaltite. Some of the cobaltite could be part of the original sediment due to rounded edges and the even sporadic distribution.

Gold content: 0.1 ppm

**Sample PAL0097-272.32**

Sample is from a hydrothermally altered albitised siltstone. Fine-grained granoblastic albite matrix with accessory sillimanite and rutile. Main minerals are albite and later biotite and chlorite. Sillimanite occurs as few bigger grain clusters and then as sporadic grains. Chlorite is partly eating away the sillimanite. Sulphidation has happened together with biotite/chlorite. Sulphides include pyrrhotite, pyrite, and chalcopyrite in veinlets. Biotite and chlorite form mixed grains, indicating a temperature change.

Gold content: 0.1 ppm

**Sample PAL0118-381.35**

Sample is from a chlorite rich pelitic rock. Abundant mica with only few qtz grains visible. Main minerals include biotite, chlorite, carbonate, cordierite. Texture of the micas is lepidoblastic. Main opaque minerals are pyrrhotite, pyrite, chalcopyrite, ilmenite. Chlorite around sulphide veins. Pyrrhotite in big veins with pyrite and other sulphides inside as smaller grains. Abundant carbonates together with the big pyrrhotite veins.

Gold content: 3.84 ppm

**Sample PAL0119-109.5**

Sample is from a talc altered rock. Main minerals include quartz, biotite, talc, chlorite and cordierite. Accessory include allanite, zoisite. Original rock is very Mg-rich, probably rich in clay minerals with quartz rich parts. Medium to coarse grained quartz and some cordierite. Mixed grains of talc and chlorite surround the quartz grains and move between the grains together with some biotite. Quartz is recrystallised and unusually sharp edged, looks like shattered glass. Talc/chlorite/biotite mix takes over entirely leaving only gaps where some quartz and deformed feldspar can be seen.

Sulphides seem to be related to the talc/chlorite/biotite. Some cobolt-pentlandite flames and clumps in pyrrhotite

**Sample PAL0093-263.35**

Sample represents intermediate rock, most likely a dyke. Intermediary nature is interpreted from the moderate amount of quartz and the presence of andesine (based on EPMA results). The sample does not contain any gold grade, but it is in located in the middle of the gold grade bearing zone. Main minerals include actinolite, biotite, albite, andesine and quartz. Accessory minerals are zircon and apatite. Sulphides include pyrite, pyrrhotite and regular pentlandite as lamellae in pyrrhotite.

Gold content: < 0.05ppm

**Sample PAL0083-40.85**

Sample is from a hydrothermally altered calcsilicate albite rock. Main minerals include albite, biotite, chlorite, actinolite with accessory quartz and uraninite and carbonates. Carbonates have produced amphiboles (actinolite) in veinlets, some of these reactions are only part way done and visible in the thin section. Some carbonates remain in the albitised matrix as single grains. Some of the amphiboles are turning into chlorite and biotite. Sulphides occurs together with biotite and chlorite in veins. Sulphides and the hydrothermal alteration are most likely the same age. Sulphides include pyrrhotite pyrite and chalcopyrite. Some opaques (probably ilmenite) looks rounded on the edges, suggesting it could be part of the original sediment.

**Sample PAL0092-222.95**

Sample is from Ca-rich metasedimentary rock. Mostly fine-grained albite matrix, cross cut by sulphide veins that are surrounded by micas and amphiboles. Main minerals include albite, biotite and anthophyllite and actinolite. Albite is coarser grained around the veins indicating recrystallisation. Micas around the vein are probably altered amphiboles. Anthophyllite occurs as clumps, together with biotite, in the end of the sulphide vein. Pyrite and pyrrhotite occur in the veins. Ilmenite occurs as small sporadic grains. Co-pentlandite occurs together with pyrite as separate grains.

**Sample PAL0092-226.85**

The sample is from a slightly chlorititzed albitite. Albitised and chloritised sediment with some amount of sulphides. Some carbonates left in the albite matrix. Chlorite is colourless in the thin section. Sulphides include pyrrhotite and one small grain of chalcopyrite. Ilmenite occurs as sporadic grains.

**Sample PAL0092-306.90**

Sample is from a muscovite bearing quarzite and includes a quartz vein. Quartz vein is visible as larger grains. Main minerals include granoblastic quartz and feldspar with accessory muscovite-sericite. Muscovite-sericite occurs as few grains in and around the pyrrhotite-pyrite vein. Some carbonates as very thin veinlets.

**PAL0097-324.8**

Original host rock is barely visible due to the intense hydrothermal sericitisation. Locally granoblastic quartzitic layers are visible that might represent the original texture. The sericitisation goes around some bigger microcline grains - that are probably product of an earlier k-alteration - but it has eaten them a bit as well. Overall the rock consists of sericite mica layers that goes around the bigger feldspar grains and layers with different orientation indicating an possibly a second sericitzation event. Biotite is abundant in the sericite/muscovite mix. Opaque minerals are mostly small rounded pyrrhotite grains and some of them have cobalt pentlandite exsolution lamellae.

**Sample PAL0097-333.45**

Sample represents a granoblastic quartzite. The sericite alteration comes in as a strong overprint and fades to less intense and the mica grains go between the quartz grains. Abundant rutile occurs together with chlorite. Some mixed grains of pyrrhotite and pyrite. Few uraninite grains were found with pyrite and galena on the rims.

**Sample PAL0097-338.2**

Sample represents Quartz vein with k-feldspar pieces on both sides of the thinsection. The k-feldspar is from the host rock and not part of the later quartz vein that is brecciating the rock. Quartz on the host rock is fine grained. Rock heavily sericitised. Chlorite seems to be the same age as the sericite. Hematite occurs mostly inside chlorite as single grains.

**Sample PAL0100-239.15**

Sample is representing a differentiated mafic rock. Main minerals include plagioclase, biotite chlorite with accessory talc, zircon, uraninite, apatite and scheelite. Plagioclase is equigranular and medium grained, micas are lepidoblastic. Sulphides include pyrrhotite, chalcopyrite, and co-pentlandite. Sulphides are coarse grained and might be formed in multiple stages before and after the biotitisation. Micas seems to have been crystallised at the same time along with each other and scheelite forming mixtured grains.

**PAL0100-283.3**

Sample represents intensively hydrothermally altered rock. Chlorite in small pockets and randomly with the later coarse-grained lepidoblastic biotite. Macroscopically looks like talc alteration. After biotite comes fine grained tourmaline, some grains visible but mostly just mush. Aphanitic cordierite and saussuritised granoblastic plagioclase have some coarser grained rutile. Plenty of zircons in coarser grained biotite. Zircons look like hydrothermal in nature due to lack of zonation and very clear edges. Ilmenite as fine dissemination. Later albite veins not saussuritised. Plagioclase rich rock - tuffitic mafic or differentiated part of plagioclase rich rock (sill).

**Sample PAL0107-253.6**

The sample represents a sericitised sediment. Main minerals include quartz, sericite, biotite. Quartz matrix is granoblastic and mica occurs as lepidoblastic and diablastic. Sericite comes in strongly and overprints the matrix or in places goes between the quartz grains, this is where it has probably eaten away the microcline that occurs in sample PAL0107-263.2 which is taken from the same rock. Sericite is lepidoblastic and diablastic. Remnants of old quartz vein are visible as some

bigger quartz grains and some folding is visible in the vein. Some pyrite grains sporadically.

**Sample PAL0107-263.20**

Sample represents a secitised sediment and is taken from the same rock as PAL0107-253.6. Main minerals include quartz and microcline with plenty of small sericitised biotite as dissemination with accessory chlorite. Amount of sericite is less than in the previous sample and more of the microcline is still intact. Some biotite is turning to chlorite. Rutile occurs as fine-grained dissemination.

**Sample PAL0111-9.20**

Sample represents albitised equigranular sediment with small to medium sized albite and quartz grains and in some places very small qtz-plg mush, probably indicating original matrix. Carbonates in the original sediment are turned to amphiboles (actinolite). Very small euhedral pyrite grains are spread sporadically. Rutile occurs with mixed grains with carbonate - rutile in the middle and carbonate crystallised on the edges.

**Sample PAL0111-23.75**

Sample represents albite rich sandstone. Grain size varies, and clasts are rather rounded. Rutile occurs as mixed grains with titanite. Pyrite as single rare tiny grains. In relation to PAL0111/9.20 this seems to be in lower temperature, based on the carbonate not producing amphiboles as much if at all. Clastic structure is more clearly visible.

**Sample PAL0111-139.9**

Sample represent a propyliticly altered rock. Main minerals include microcline, biotite, chlorite, epidote, rutile, quartz with accessory carbonate, actinolite, tourmaline, allanite. Underneath and between the biotite/amphibole/epidote and rutile mush, some clusters of different sized quartz and microcline grains can be seen. Pleochroism of biotite is green, indicating higher iron content. Some of the green is also chlorite which occurs as mixed grains with biotite. Hematite is crystallised in the cleavages of biotite and together with rutile as mush on top of biotite and chlorite. Some epidotes are scattered around and some of them are partly crystallised as allanite.

**Sample PAL0116-112.84**

Aphanitic basalt with later quartz/carbonate veinlets. Could be interpreted as a tuff but few coarser grained quartz/feldspar grains look like filling in cavities which would indicate a lava. Rutile is abundant, very fine grained, pervasive dissemination.

**Sample PAL0116-116.83**

Sample represents a mafic lava with some talc alteration. Aphanitic to coarser grained albite matrix with light amphibole, some of it turning to biotite and mostly talc. Main minerals include albite, amphibole, carbonate, talc with accessory biotite and ilmenite. Ilmenite occurs as grain clusters in a vein like pattern. Seems like there has been an increase in carbonate. Could be an ultramafic magma but has a volcanogenic feel to it due to the grainsize variations. Carbonates occur as big blobs, could be altered from something else. Chlorite is zonally altering the plagioclase and an earlier alteration has completely altered some grains in the matrix.